Funded by the European Union

DIM ESEE-2 innovative workshop

DIM ESEE 2021: Innovation in exploration

Inversion-based modeling for the interpretation of gravity, magnetic and geoelectric datasets

Endre Nádasi
gfne@uni-miskolc.hu

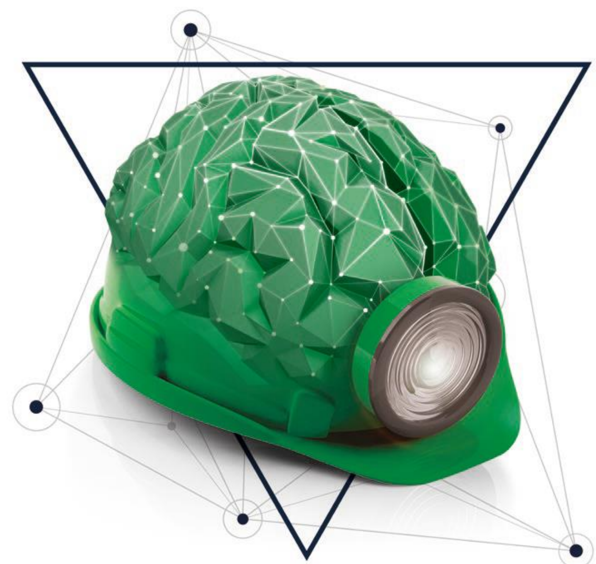

October 20^{th} – 22^{nd}, 2021
IUC Dubrovnik, Croatia / online

Supported by

RawMaterials ACADEMY

Funded by the European Union

SHORT HISTORY OF GRAVITY EXPLORATION

The history of gravity exploration is based on the studies of Galilei, Kepler, and Newton (16^{th}-17^{th} centuries).

Galilei found that objects fall at similar acceleration independent of their mass (in 1589).

The gravity method was the first geophysical technique to be used in oil and gas exploration. In the first third of the 20^{th} century, the torsion balance was the standard instrument for gravity exploration. The torsion balance, invented by Eötvös, was one of the first geophysical instrument and it was used in the exploration of anticline structures and salt domes. He called this instrument the *horizontal variometer*.

First measurements: on Ság Hill (1891) and
on the ice of Lake Balaton (1901-1903).

Gravimeters have been adapted on moving ships and aircraft since the 1950s. Since the 1980s spring gravimeters have incorporated electrostatic feedback that considerably improves their drift performance and linearity.

At the beginning of this century gravity satellites were also launched and promising results were achieved.

Supported by

Funded by the European Union

Gravitational Force

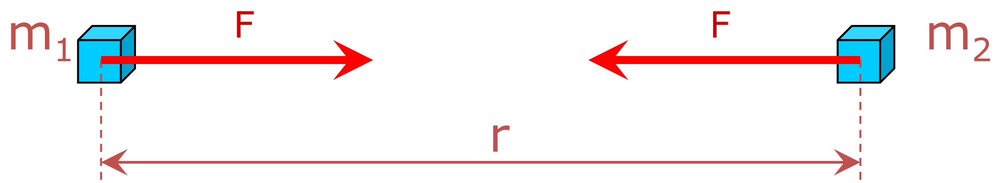

The basis of the gravity survey method is Newton's Law of Gravitation, which states that the force of attraction *F*
between two masses m_1 and m_2, whose dimensions are small with respect to the distance *r* between them, is given by

$$F = G\frac{m_1 m_2}{r^2}$$

where *G* is the Gravitational Constant $G = 6.67384 \pm 0.0008 \cdot 10^{-11}\ \mathrm{Nm^2\ kg^{-1} s^{-2}}$

CODATA (Committee on Data for Science and Technology) 2010

Supported by

RawMaterials ACADEMY

Funded by the European Union

Funded by the European Union

The Earth's Gravitational Field

Consider the gravitational attraction of a spherical, non-rotating, homogeneous Earth of mass *M* and radius *R* on a small mass *m* on its surface. It is relatively simple to show that the mass of a sphere acts as though it were concentrated at the centre of the sphere and by substitution in equation

$$F = \frac{GM}{R^2} m = mg$$

Force is related to mass by an acceleration and the term $g = GM/R^2$ is known as the gravitational acceleration or, simply, *gravity*. The weight of the mass is given by *mg*. On such an Earth, gravity would be constant. However, the Earth's ellipsoidal shape, rotation, irregular surface relief and internal mass distribution cause gravity to vary over its surface.

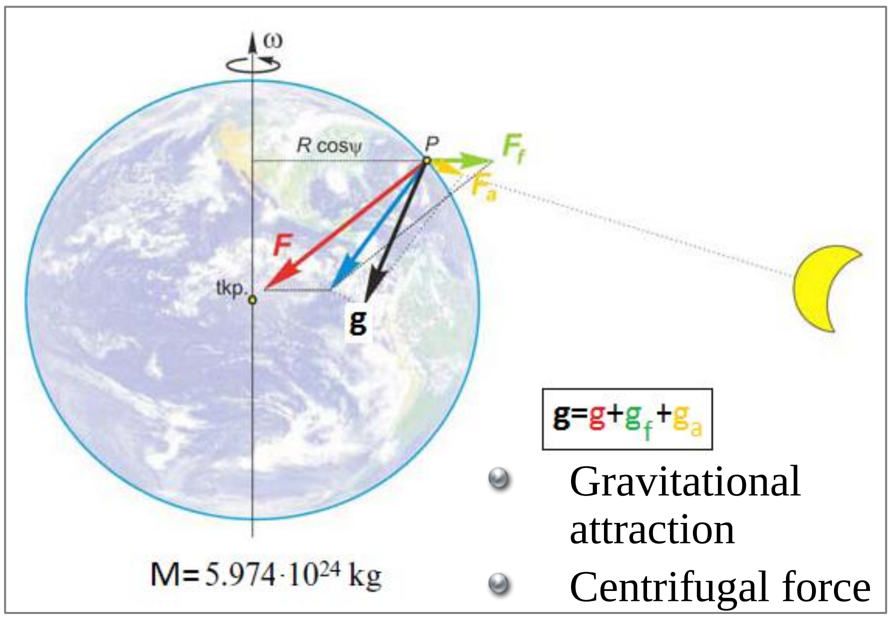

- Gravitational attraction
- Centrifugal force
- Tidal force

Supported by

Funded by the European Union

RawMaterials Connecting matters
Funded by the European Union
2021 ESEE

The Earth's Gravitational Field

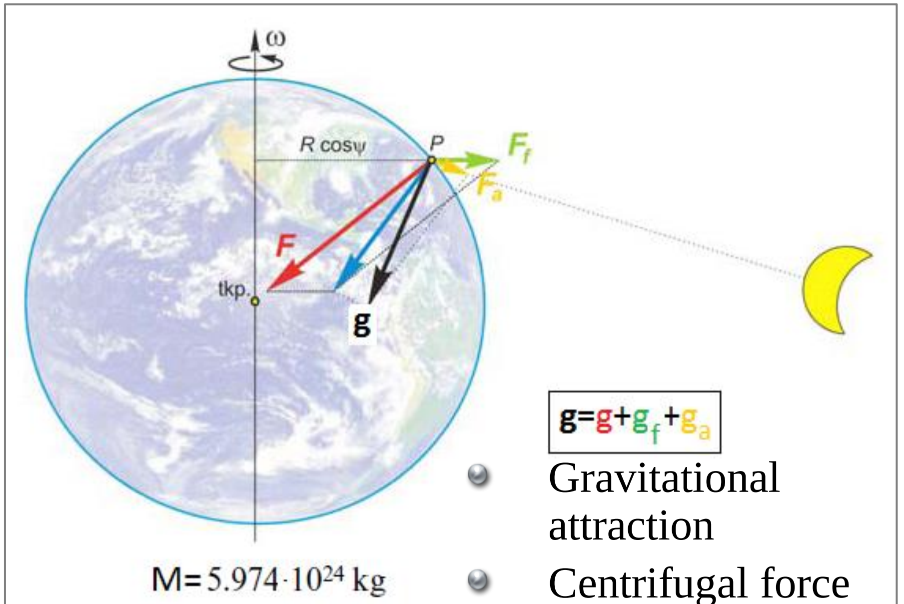

- Gravitational attraction
- Centrifugal force
- Tidal force

The gravitational field is most usefully defined in terms of the *gravitational potential U*:

$$\mathbf{g} = \text{-grad}U \quad \text{where} \quad U = G\frac{M}{R}$$

Whereas the gravitational acceleration *g* is a vector quantity, having both magnitude and direction (vertically downwards), the gravitational potential *U* is a scalar, having magnitude only.
The first derivative of *U* in any direction gives the component of gravity in that direction.

Supported by
RawMaterials ACADEMY
Funded by the European Union

Measurement Units

The mean value of gravity at the Earth's surface is about 9.8 ms^{-2}.
Variations in gravity caused by density variations in the subsurface are of the order of 100 μms^{-2}.

$$[g] = m / sec^2$$

$$1 \text{ Gal} = 10^{-2} \text{ m} / sec^2$$

$$1 \text{ mGal} = 10^{-3} \text{ Gal} = 10^{-5} \text{ m} / sec^2$$

$$1 \text{ gu} = 10^{-1} \text{ mGal} = 10^{-4} \text{ Gal} = 1 \ \mu m / sec^2$$

$$1 \text{ E} = 10^{-9} \ 1/sec^2$$

Supported by

Funded by the European Union

Gravity Survey

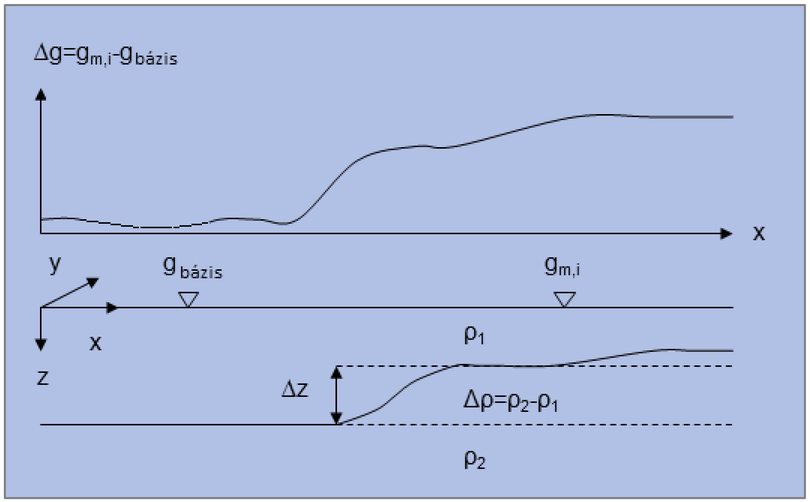

If $g_{m,i} > g_{base}$ then $\Delta\rho > 0 \rightarrow \rho_2 > \rho_1$
If $g_{m,i} < g_{base}$ then $\Delta\rho < 0 \rightarrow \rho_2 < \rho_1$

- Measured quantity is

  $\Delta g_z(x,y,z)$ [mGal]

- Gravity anomaly responds to the horizontal density contrast ($\Delta\rho$)
- Main application is mapping subsurface density variation

Supported by
eit RawMaterials ACADEMY
Funded by the European Union

Geological Background

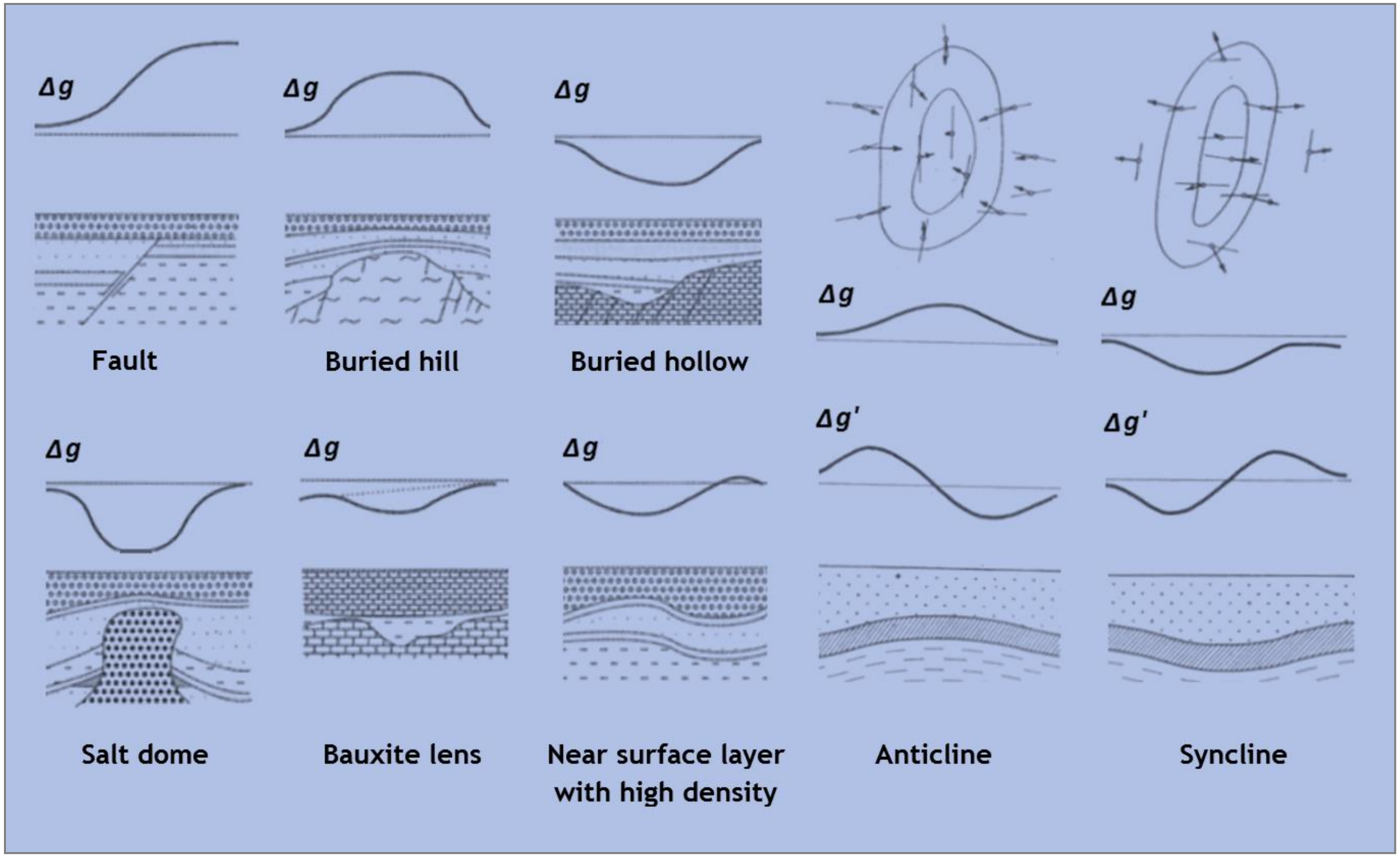

Density of Rocks

Material type	Density Range	Approximate average density (Mg/m3)
Sedimentary rocks		
Alluvium	1.96-2.00	1.98
Clay	1.63-2.60	2.21
Gravel	1.70-2.40	2.00
Silt	1.80-2.20	1.93
Soil	1.20-2.40	1.92
Sand	1.70-2.30	2.00
Sandstone	1.61-2.76	2.35
Shale	1.77-3.20	2.40
Limestone	1.93-2.90	2.55
Dolomite	2.28-2.90	2.70
Chalk	1.53-2.60	2.01
Halite	2.10-2.60	2.22

Coal	1.2–1.5
Salt	2.1–2.4

Material type	Density Range	Approximate average density (Mg/m3)
Metamorphic rocks		
Schist	2.39-2.90	2.64
Gneiss	2.59-3.00	2.80
Phylite	2.68-2.80	2.74
Slate	2.70-2.90	2.79
Granulite	2.52-2.73	2.65
Amphibolite	2.90-3.04	2.96
Igneous rocks		
Rhyolite	2.35-2.70	2.52
Granite	2.50-2.81	2.64
Andesite	2.40-2.80	2.61
Basalt	2.70-3.30	2.99
Gabbro	2.70-3.50	3.03

Ore minerals	
Sphalerite	3.8–4.2
Galena	7.3–7.7
Chalcopyrite	4.1–4.3
Chromite	4.5–4.8
Pyrrhotite	4.4–4.7
Hematite	5.0–5.2
Pyrite	4.9–5.2
Magnetite	5.1–5.3

Funded by the European Union
Supported by
eit RawMaterials ACADEMY
Funded by the European Union

Funded by the European Union

INSTRUMENTS OF GRAVIMETRY

Gravity measurements can be either absolute or relative.

It is called absolute gravity measurement when the absolute acceleration of the Earth's gravity field is determined. More frequently the difference between the gravity field at two points is measured in the course of a gravity survey, and in this case relative measurement is carried out.

The absolute measurement of gravity is based on the accurate timing of a swinging pendulum (there is an inverse relationship between g and the period square of the pendulum) or of a free-falling weight.

Supported by

Funded by the European Union

Torsion Balance

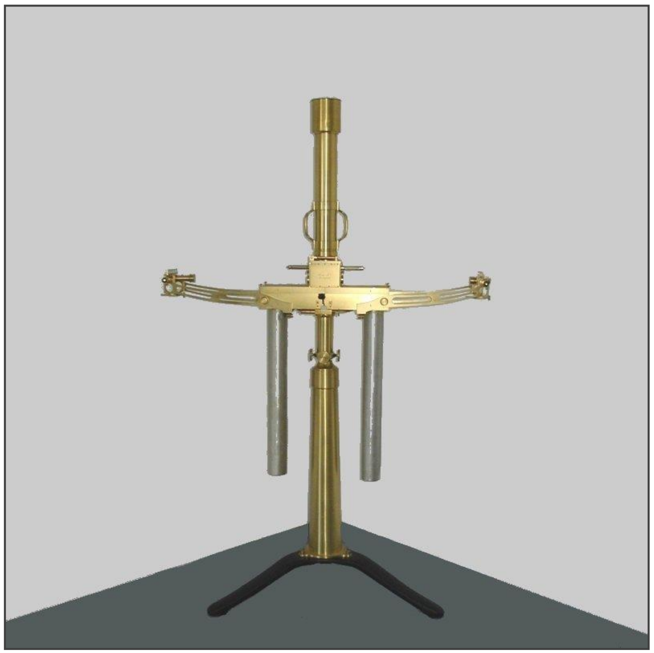

University of Miskolc, Department of Geophysics

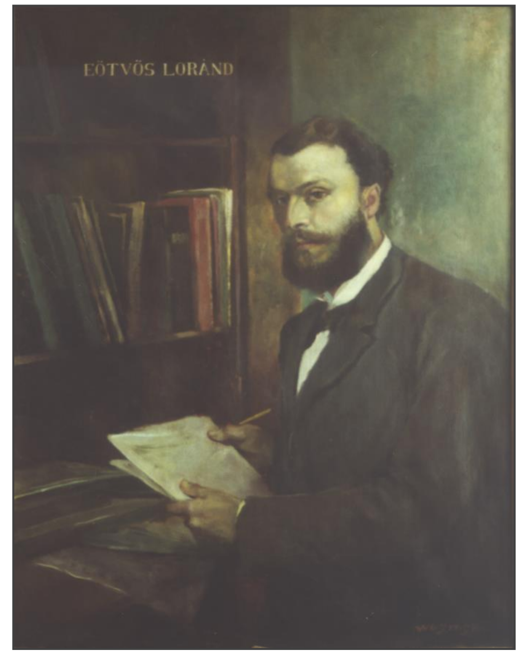

Baron Loránd Eötvös (1848-1919)

Supported by
Funded by the European Union

Torsion Balance

Eötvös developed two types of torsion balance.

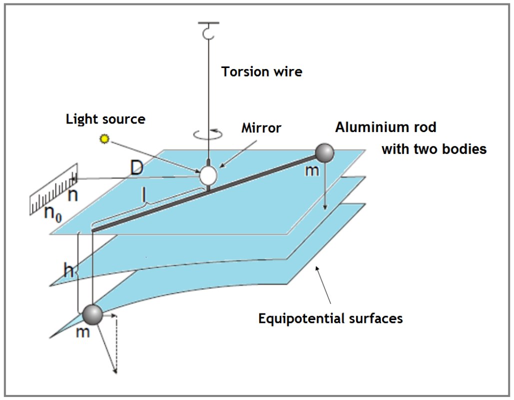

The first one was a light horizontal bar suspended on a torsion wire with platinum masses attached to either end, so that the masses were at the same level. This was the curvature variometer, very similar to that used by Coulomb and Cavendish.

The second torsion balance had a vertical torsion wire carrying a horizontal light bar. A platinum mass was attached to one end of the horizontal bar, while the other end carried a weight of equal mass suspended by a wire. This was named the horizontal variometer by its inventor.

The main feature of this instrument was that the two weights were not at the same level.

The horizontal bar revolves around the torsion wire on a horizontal plane and is deflected from the torsionless position of the wire by the horizontal components of the gravity forces. The bar will come to rest if the resistance of the torsion wire to torsion is equivalent to the torque of rotation exerted by gravity. This second type of torsion balance is known as the Eötvös torsion balance.

Supported by

Torsion Balance

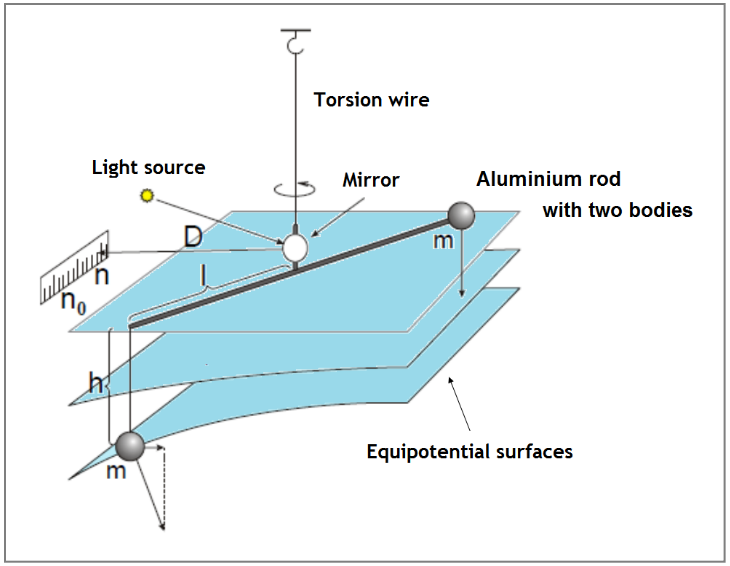

- Gravitational angular force
- Measure the first derivative of g

- Applications:
  - Earlier oil prospecting,
  - Structural directions,
  - Curvature and geoid undulation,

- Disadvantage: time-consuming (~20-30 min/1 datum)

Supported by

Early Measurements

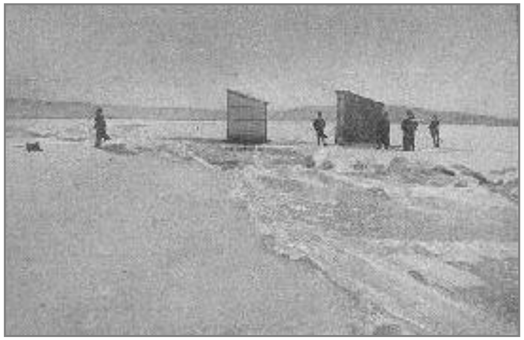

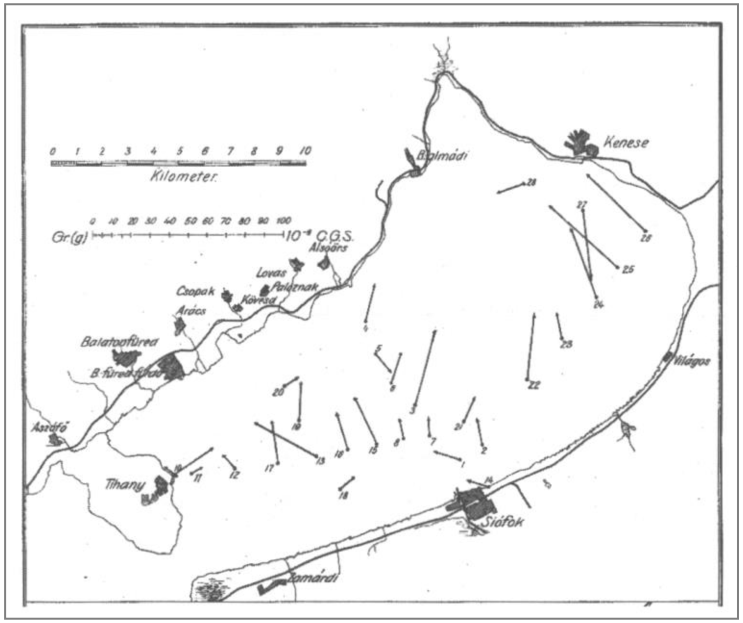

The first gravity horizontal gradient map based upon measurements between 1901-1903 on the frozen Lake Balaton. They discovered a buried mountain range.

Supported by
EIT RawMaterials Academy
Funded by the European Union

Early Measurements

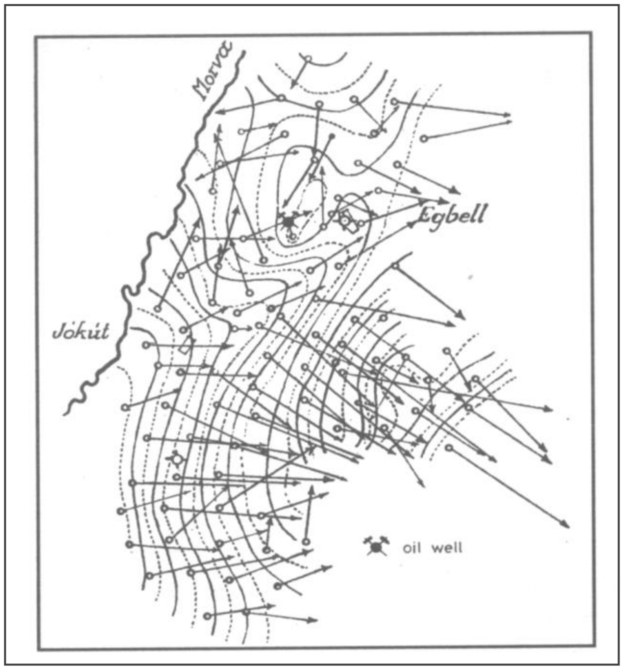

The horizontal gradient map of the first successful oil exploration made by Eötvös torsion balance in the region of Egbell (Slovakia) in 1916.

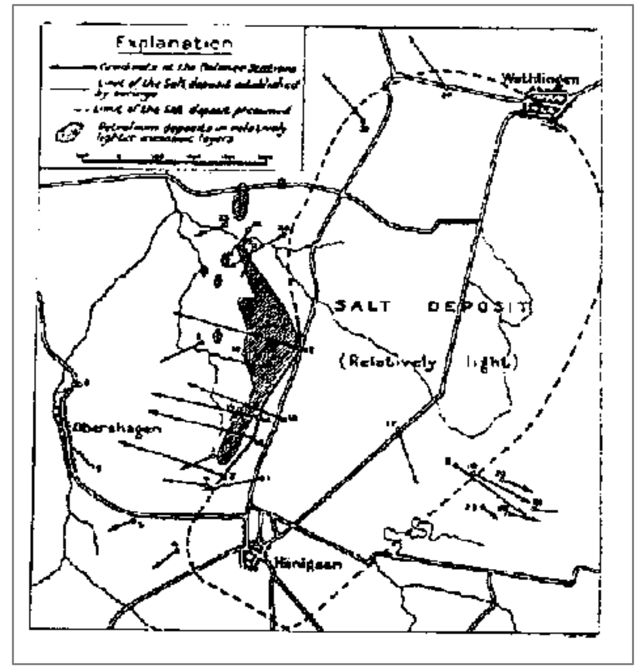

The horizontal gradient map of a salt dome in the region of Hänigsen in 1917.

EIT RawMaterials Connecting matters
Funded by the European Union
DIM ESEE 2021

Measurements Worldwide

The first salt dome and oil-bearing structure that was discovered by the torsion balance was the Nash dome (Texas, USA) in 1924.

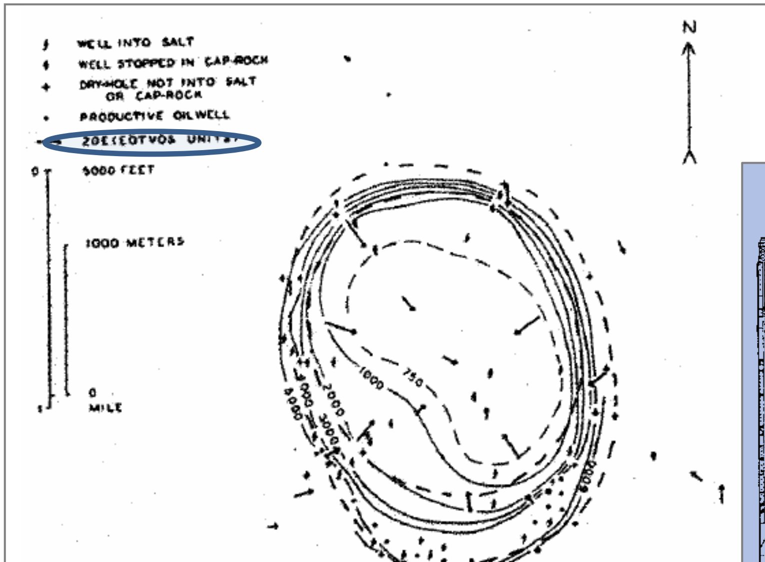

(1E=10^{-9} 1/s^2)

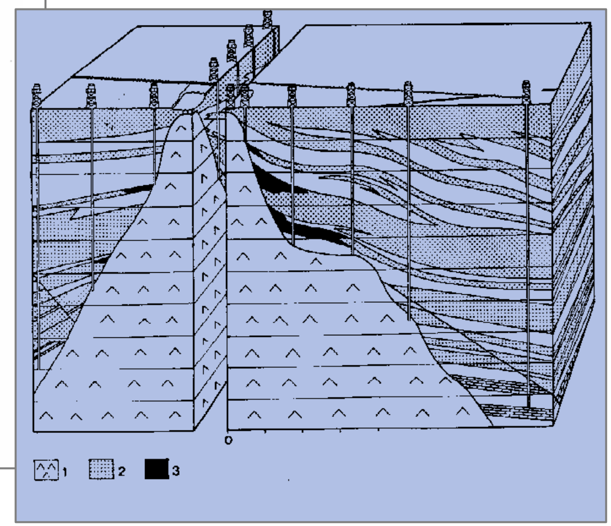

One Eötvös is the unit of gradient of gravity acceleration, which is defined as a 10^{-6} mGal change of gravity over a horizontal distance of 1 centimetre.

Supported by
EIT RawMaterials ACADEMY
Funded by the European Union

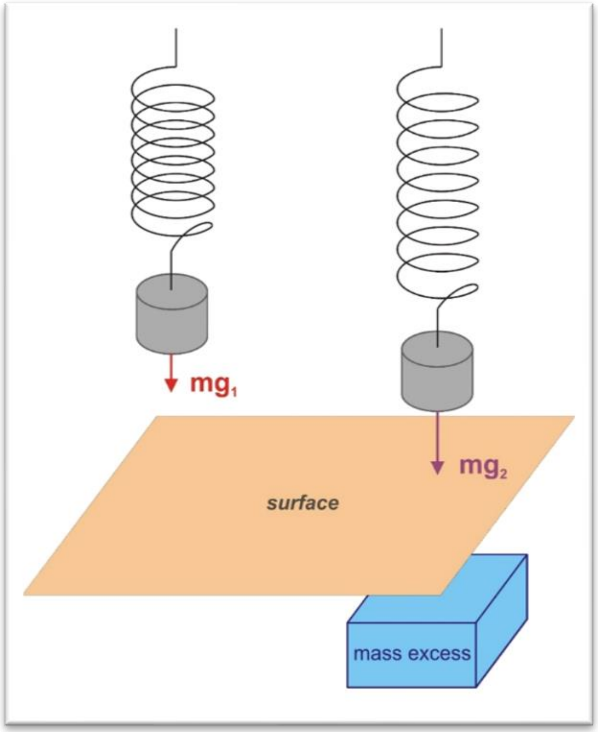

Gravimeters

The simplest way to present the physical principle of a (relative) gravimeter is
a mass is suspended from a vertical spring
the extension of the spring is expressed in function of gravity changes.
For the two stations $mg_1=kl_1$ and $mg_2=kl_2$,
where k is the elastic constant of spring and denotes the length of the spring.

$$\Delta g = g_2 - g_1 = k(l_2 - l_1)/m = c\Delta l$$

It follows that the change in gravity force between the two stations is linearly proportional to the change in the length of the spring.
This stable type of gravimeter is based on Hooke's law.

Supported by

Measurement with mass and spring

- <u>Hooke's law:</u>

  $\Delta F = F_2 - F_1 = k\Delta s$

  (k is elastic constant)

- Principle of gravity measurement:

  $m\Delta g = k\Delta s \rightarrow \Delta g = k\Delta s / m$

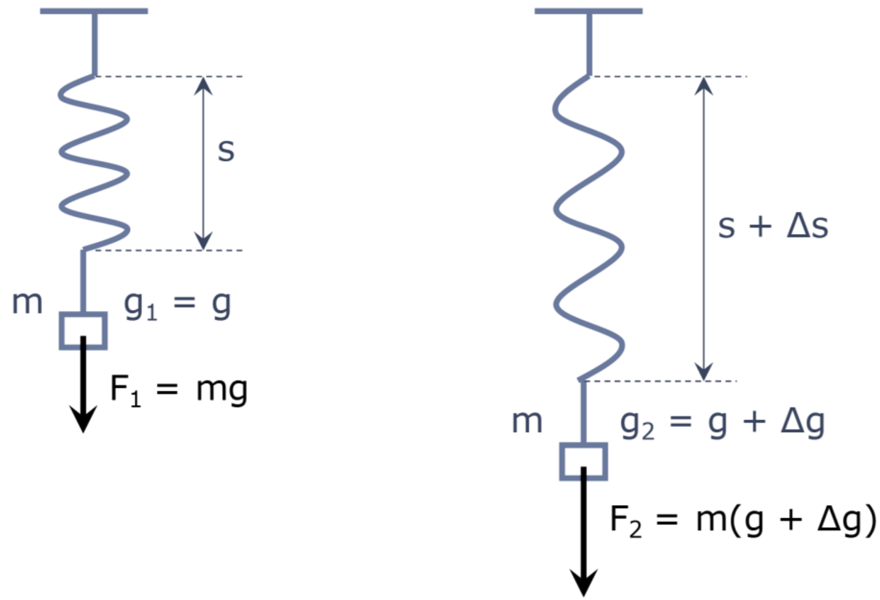

Supported by
EIT RawMaterials Academy
Funded by the European Union

EIT RawMaterials Connecting matters

Funded by the European Union

DIM 2021 ESEE

Gravimeter

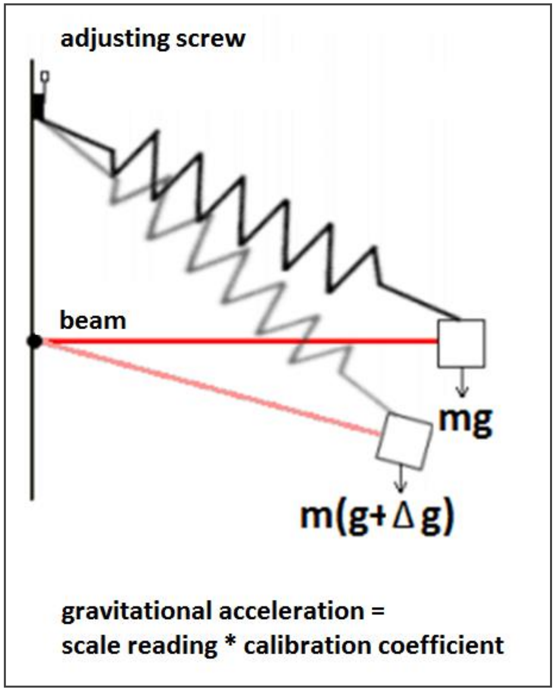

- Weight is attached to a beam and a spring
- Gravity increases, the weight is forced downwards and it forces the beam to rotate, the spring is stretching
- Adjusting the screw to rotate the beam back to horizontal
- Amount the beam moves is proportional to the gravitational force
- Advantage: rapid measurement
- Accuracy ~ 0,1 mGal

Supported by

EIT RawMaterials ACADEMY

Funded by the European Union

SCINTREX Autograv CG-5

-Quartz spring
-Variable capacitor

Accuracy: 1μGal

Supported by
eit RawMaterials ACADEMY
Funded by the European Union

Superconducting Gravimeter

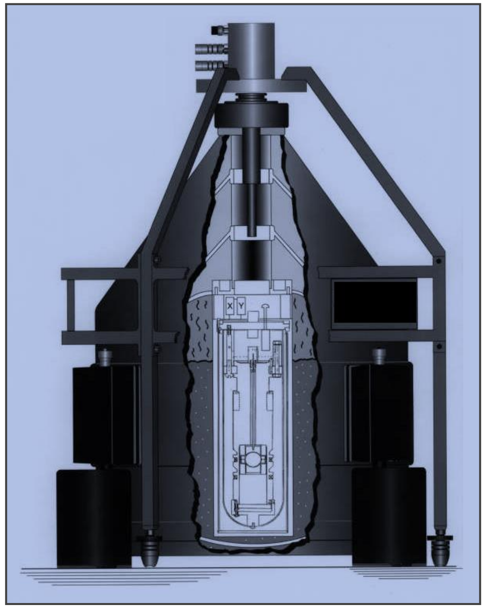

The ***superconducting gravimeter*** has an ultra-low drift of less than 0.5 μGal/month and a virtually constant scale factor.

In its cryogenic environment, the ***superconducting gravimeter*** sensor is totally insensitive to local changes in temperature, relative humidity, or pressure.

With these properties, provides a precise and continuous record of gravity variations that occur over periods of days, months, years, or even decades with a stability and precision that sets the highest industry standard.

- ***Super* stable:** Drift less than 0.5 μGal/month
- ***Super* precise:** 1 nanoGal (10^{-3} μGal) in frequency domain 0.05 μGal in the time domain for 1 minute averaging
- ***Super* low noise:** 0.3 μGal/(Hz)½

Supported by

Corrections of Gravity Data

- Linear correction of instrumental drift
- Tidal correction (neglected)
- Latitude (normal) correction
- Elevation correction (free-air and Bouger)
- Topographic correction
- Eötvös correction for moving instruments (shipborne surveys)

Supported by
eit RawMaterials ACADEMY
Funded by the
European Union

eit RawMaterials Connecting matters
Funded by the European Union
DIM ESEE 2021

Gravity anomalies

The **Faye anomaly** is defined by applying only normal, free-air, terrain (sometimes terrain correction is not applied) and tidal corrections to the measured gravity value.

The **Bouguer anomaly** is defined by applying normal, free-air, terrain and tidal corrections to the measured gravity value. The difference between the Bouguer and the Faye anomaly arises from the Bouguer plate correction (i.e., the density of the rock between the station and the datum elevations is also taken into account for preparing Bouguer anomaly map). For practical exploration it is usually the Bouguer gravity anomaly map that is applied.

Isostatic gravity anomaly is defined by applying isostatic correction to the Bouguer anomaly. The isostatic correction is made from elevation and seawater depth data with the assumption of isostatic balance for all gravity stations. If this **isostatic correction** is also applied to the observed gravity data, besides the corrections applied to Bouguer anomaly, we obtain the isostatic anomaly.

Supported by
eit RawMaterials ACADEMY
Funded by the European Union

Regional Gravity Surveys

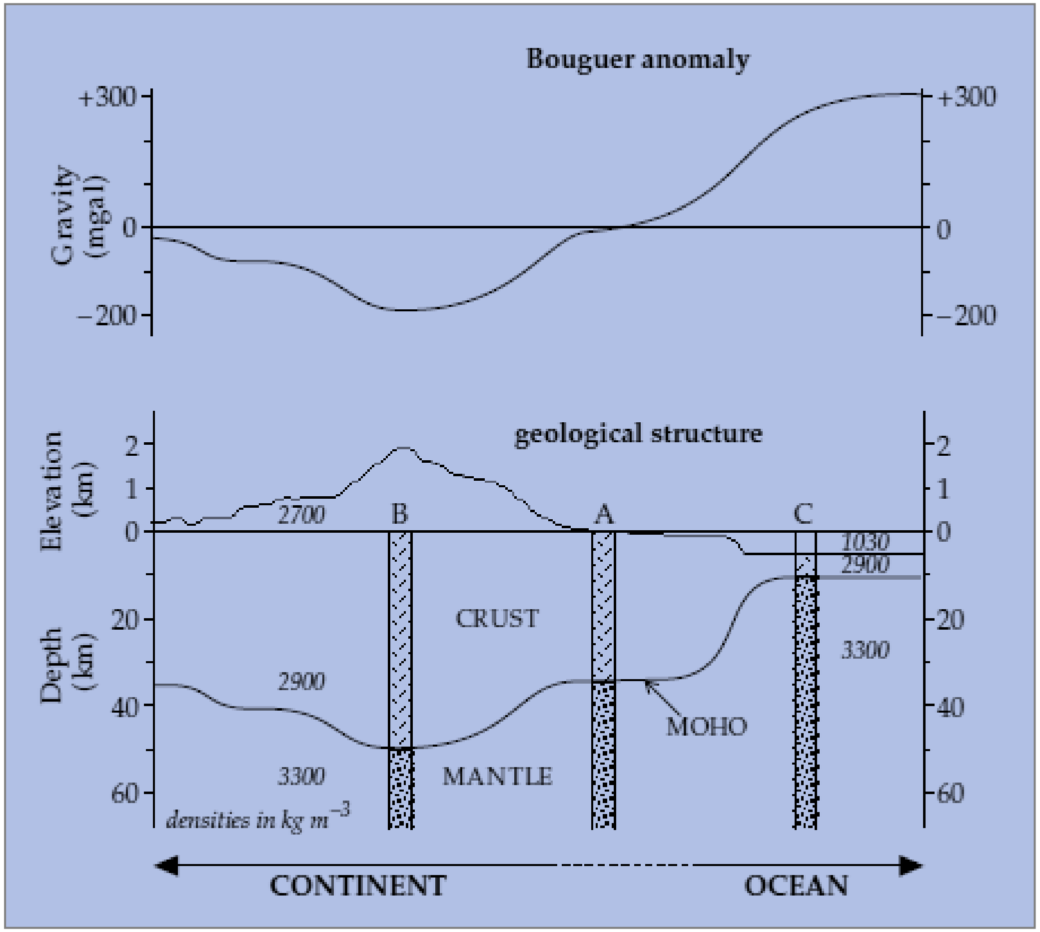

Supported by

Transformations of Bouguer anomaly maps

Separation of regional trends / local anomalies

- Large scale (long wavelength) features generally arise from deep crustal or upper mantle sources
- Shallower density variations have more rapidly varying, short wavelength signatues

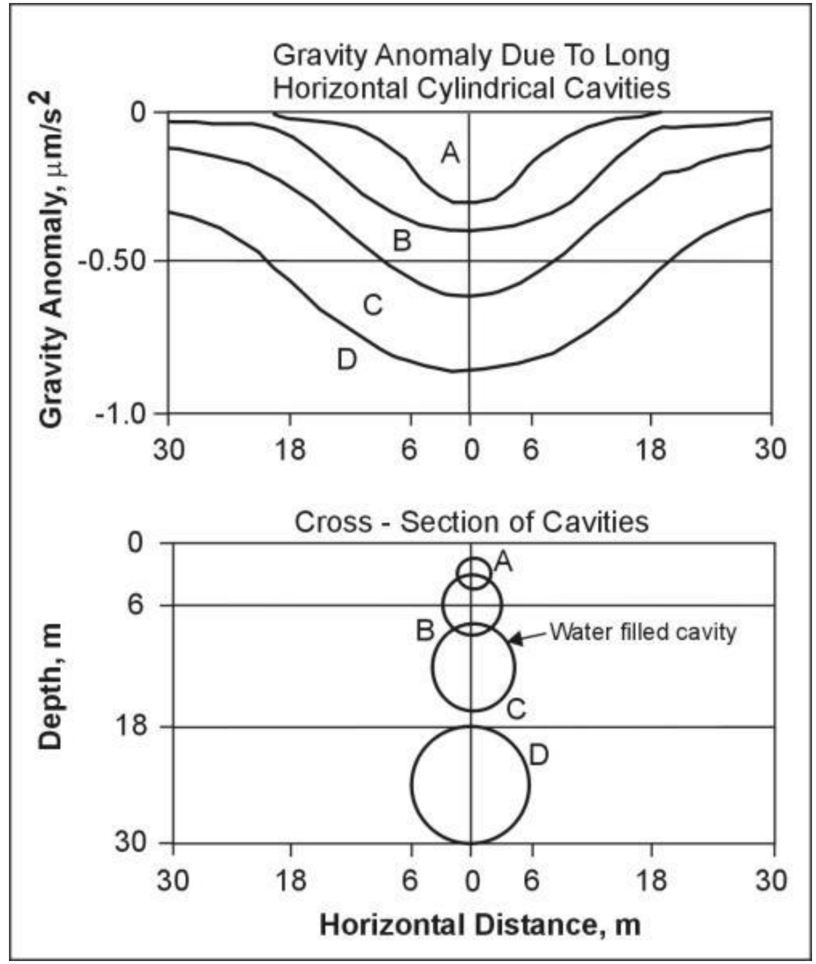

Supported by
RawMaterials Academy
Funded by the European Union

eit RawMaterials
Connecting matters

Funded by the European Union

DIM 2021 ESEE

Applied transformations

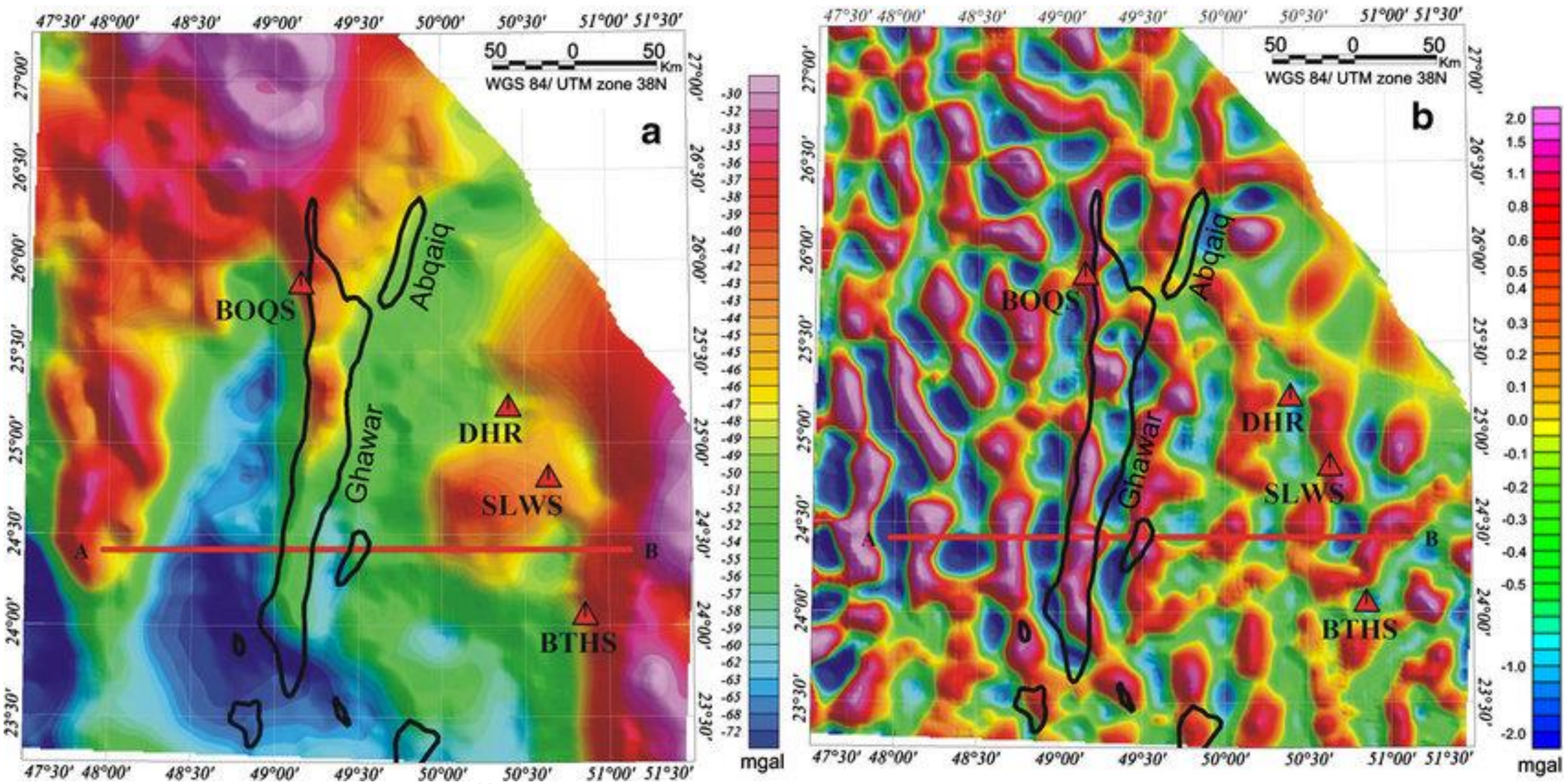

Supported by

eit RawMaterials ACADEMY

Funded by the European Union

- Geophysical model: simplification of Earth, quantitative rock property information
- Geometrical parameters (1D (homogenous, isotropic half space), 2D (inhomogenous half space with a dyke or fault), 3D (half space with sincline), 4D (space + time dimension) model) and petrophysical parameters
- Geophysical data: observations in the field
- Response functions: mathematical connection between the model and data
- Direct problem: different models >calculation> theoretical data
- Inverse problem: field data >calculation> model
- Inversion (optimization) procedure: fitting the theoretical data to measured data

RawMaterials
Connecting matters

Funded by the European Union

DIM 2021 ESEE

Workflow of Inverse Modeling

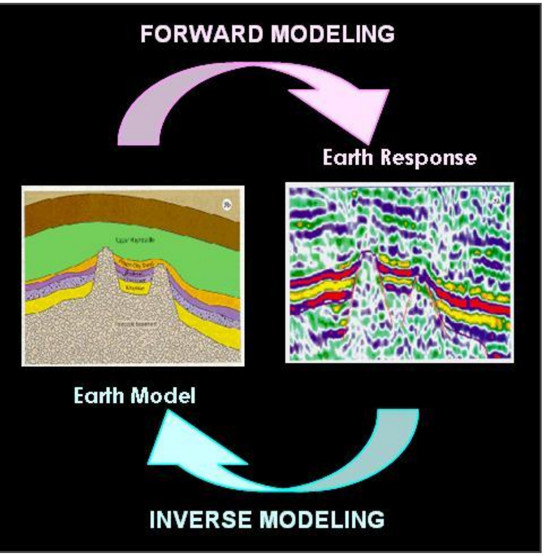

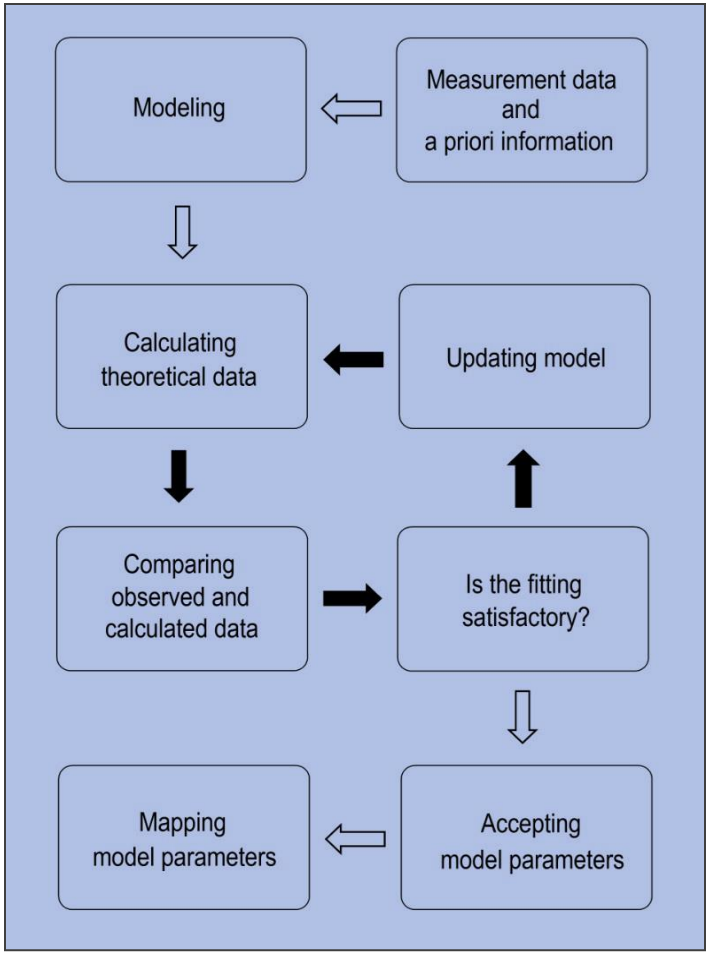

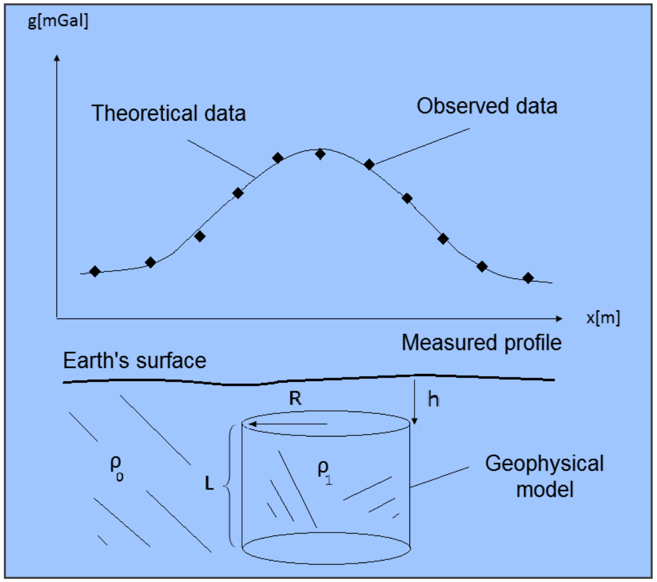

Supported by

RawMaterials ACADEMY

Funded by the European Union

Calculation of Gravity Data

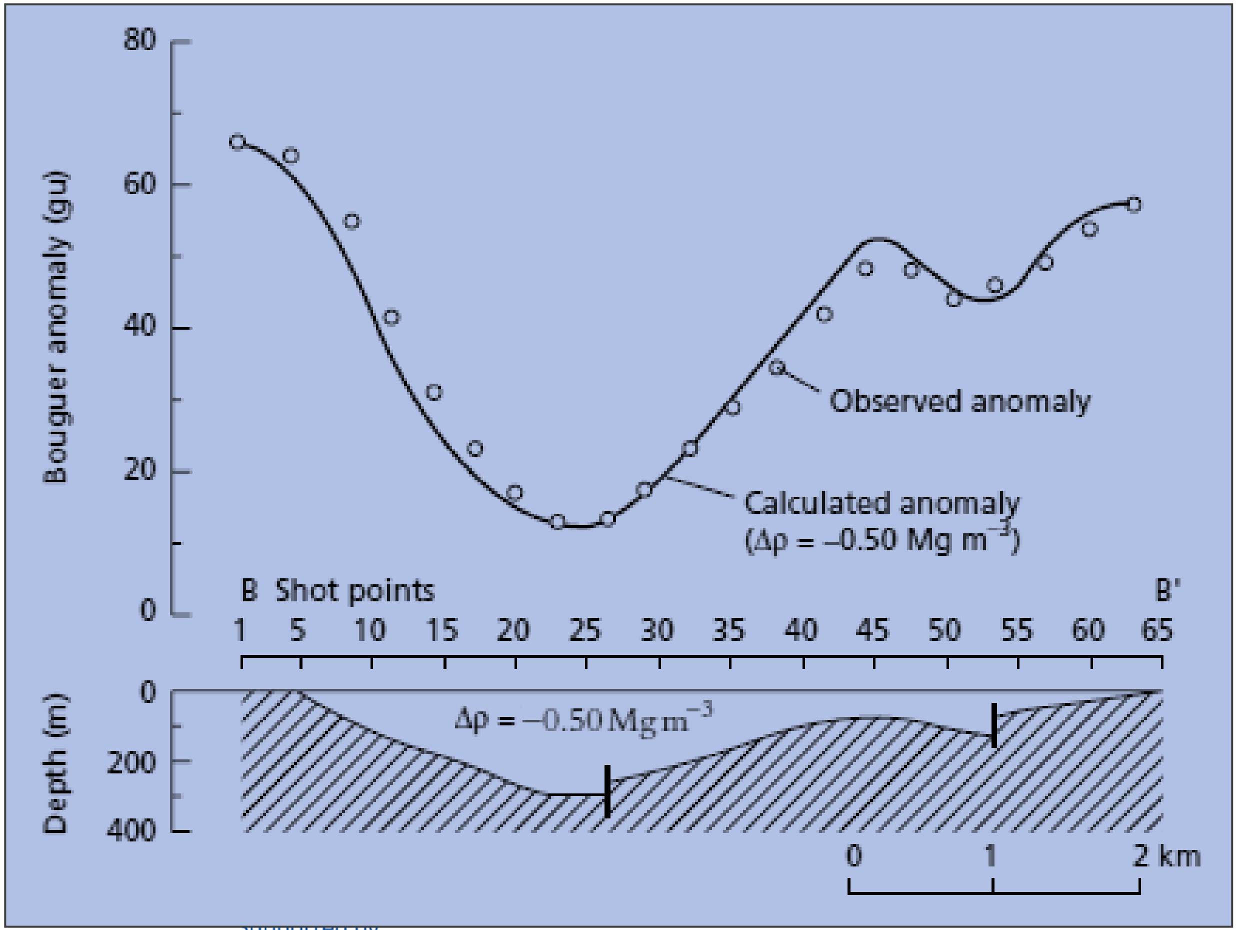

Approximation by Simple Geometry

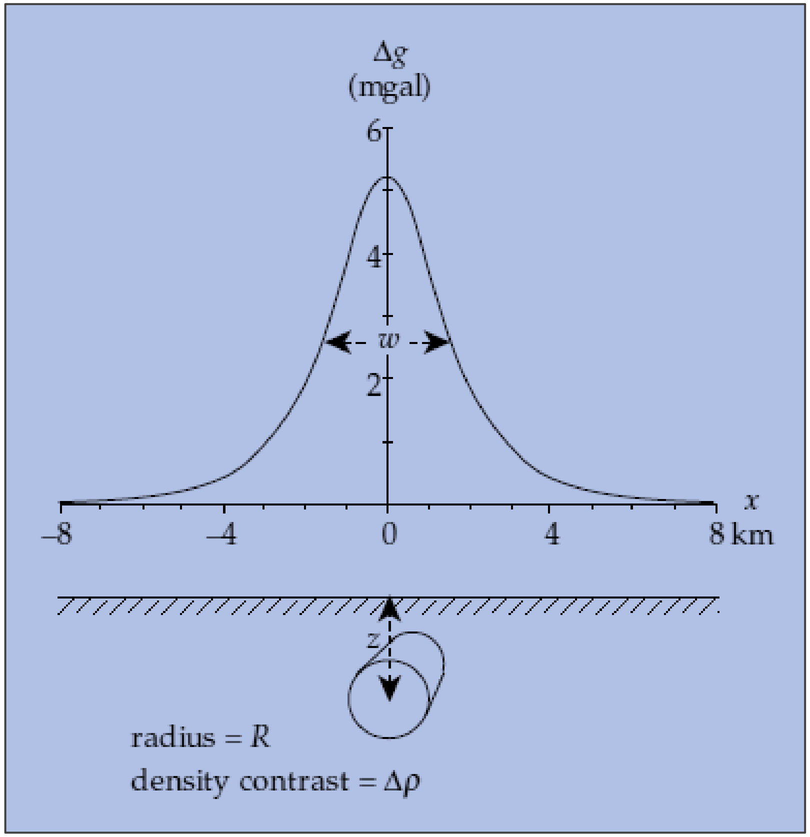

Horizontal cylinder model

- One horizontal dimension is longer than the other two dimensions
- For instance: mine openings, tunnel, river channel, rift valley, anticlinal etc.
- Gravity effect of the cylinder with radius R

$$\Delta g_z = 2\pi G\left(\frac{\Delta\rho R^2}{z}\right)\left[\frac{1}{1+(x/z)^2}\right]$$

- The depth z of the body

$$\Delta g_0 = 2\pi G\left(\frac{\Delta\rho R^2}{z}\right)$$

$$z = 0.5w$$

w: half of the maximum value

Approximation by Simple Geometry

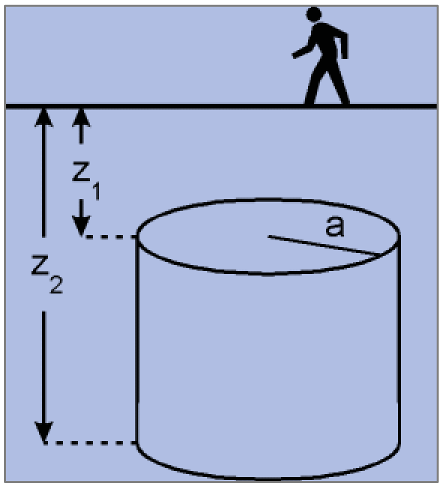

Vertical cylinder model

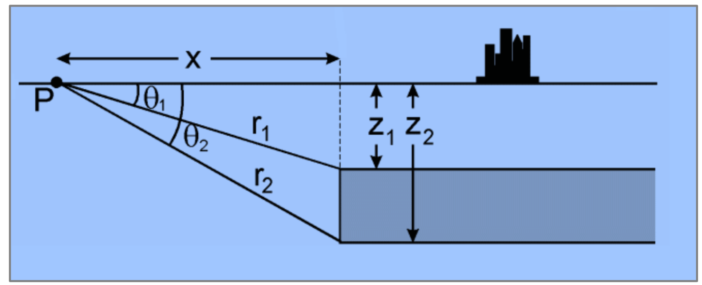

Fault model

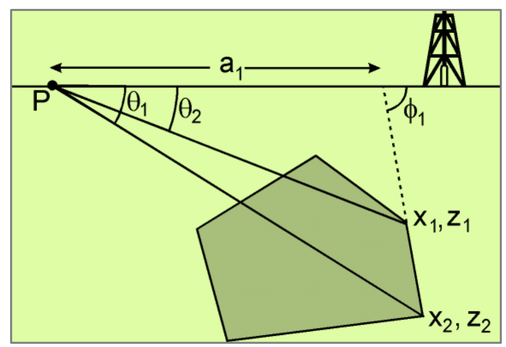

Polygonal model

Supported by

eit RawMaterials Connecting matters

Funded by the European Union

DIM ESEE 2021

Gravity of Rectangular Prism

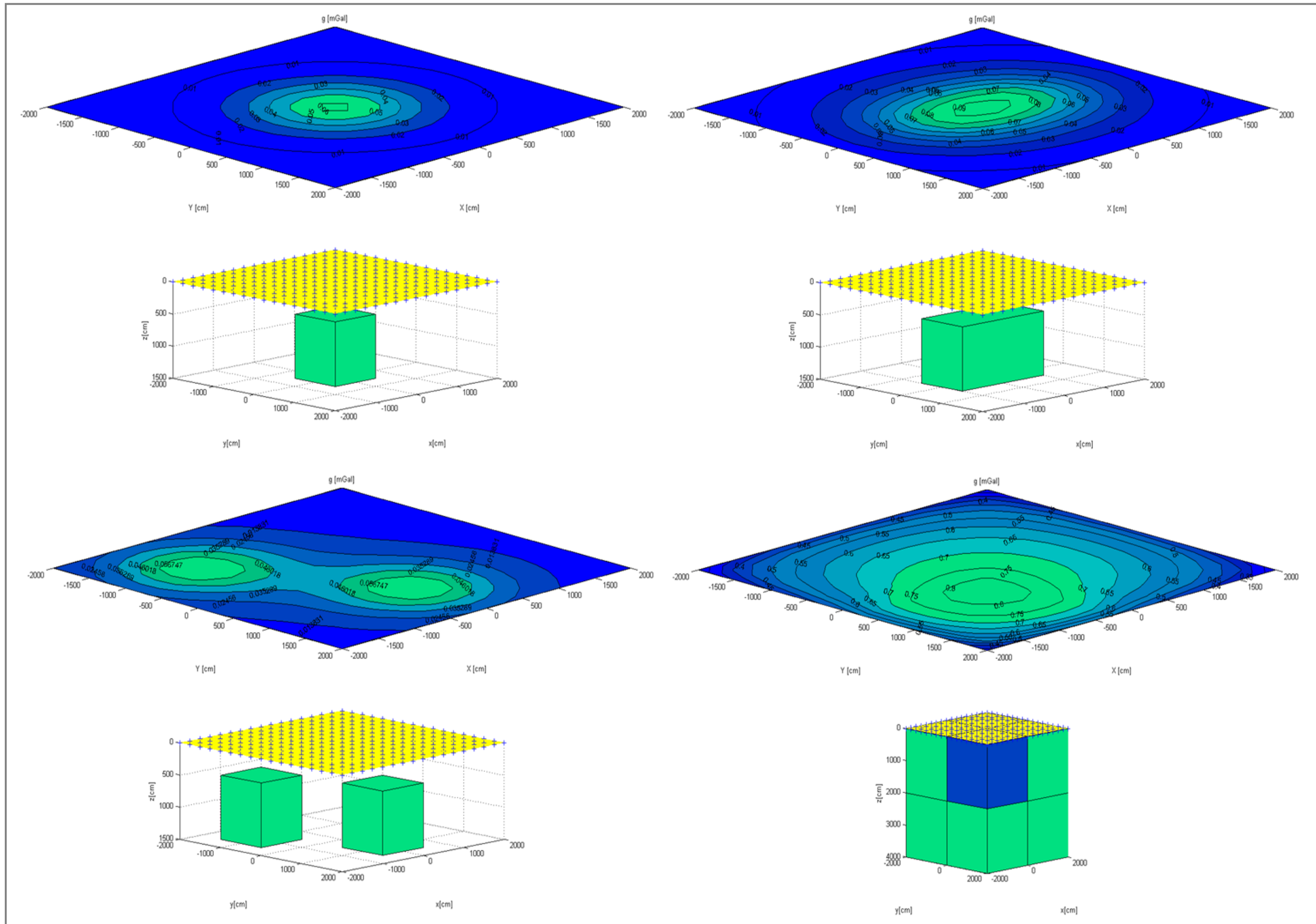

Supported by

eit RawMaterials ACADEMY

Funded by the European Union

Problem of Ambiguity

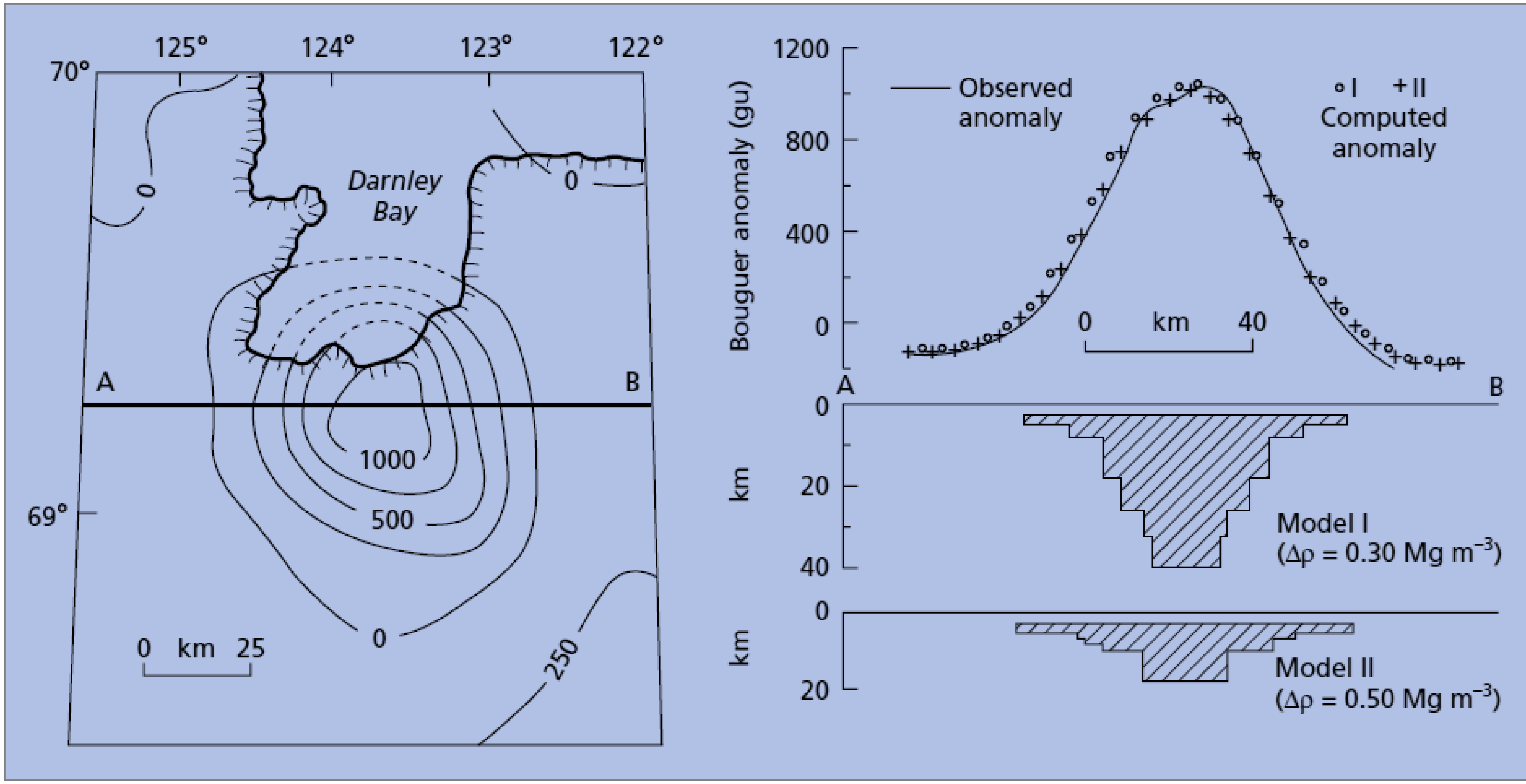

Kearey et al. (2002)

Supported by
RawMaterials ACADEMY
Funded by the European Union

Funded by the European Union

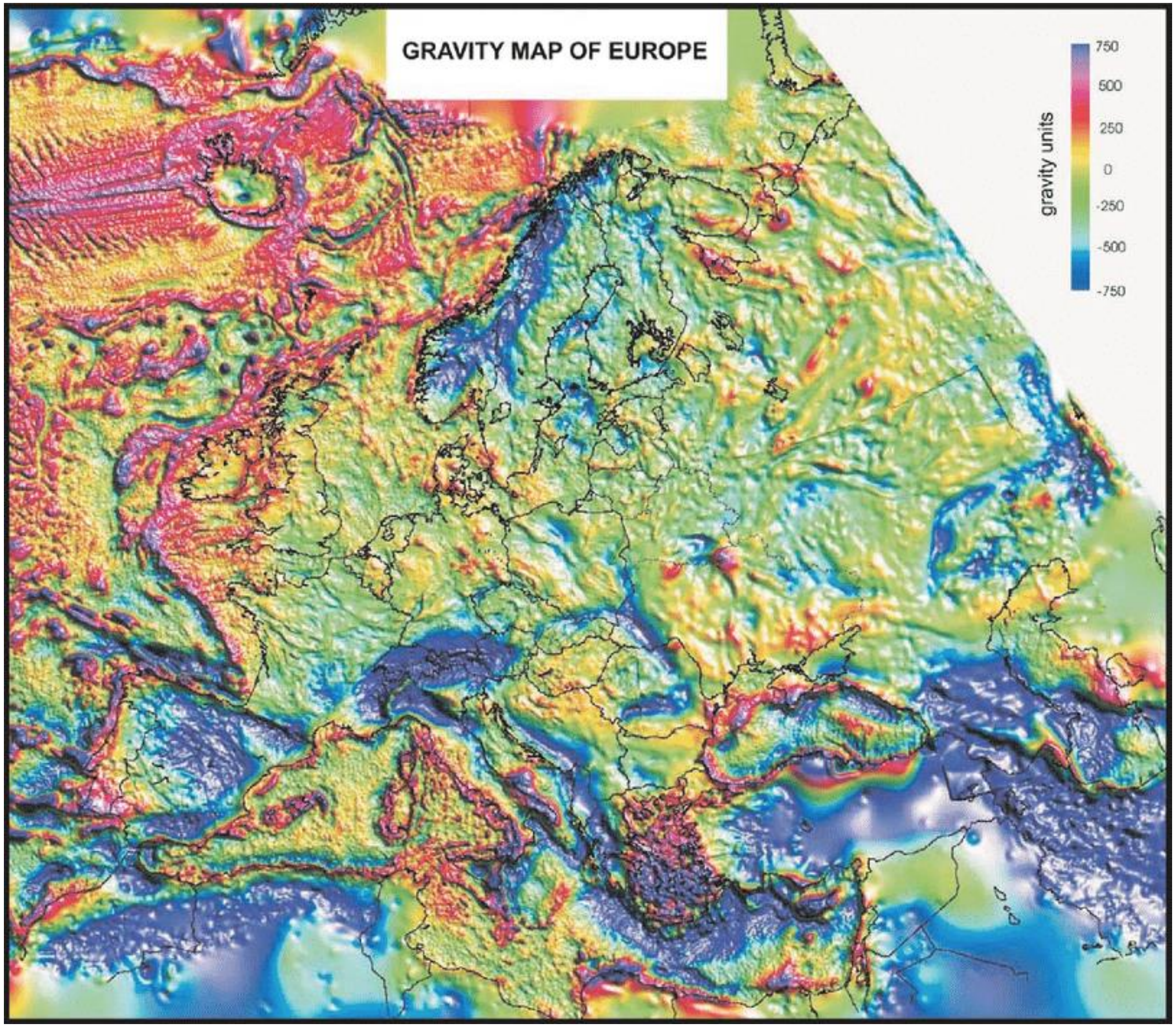

Supported by

Funded by the European Union

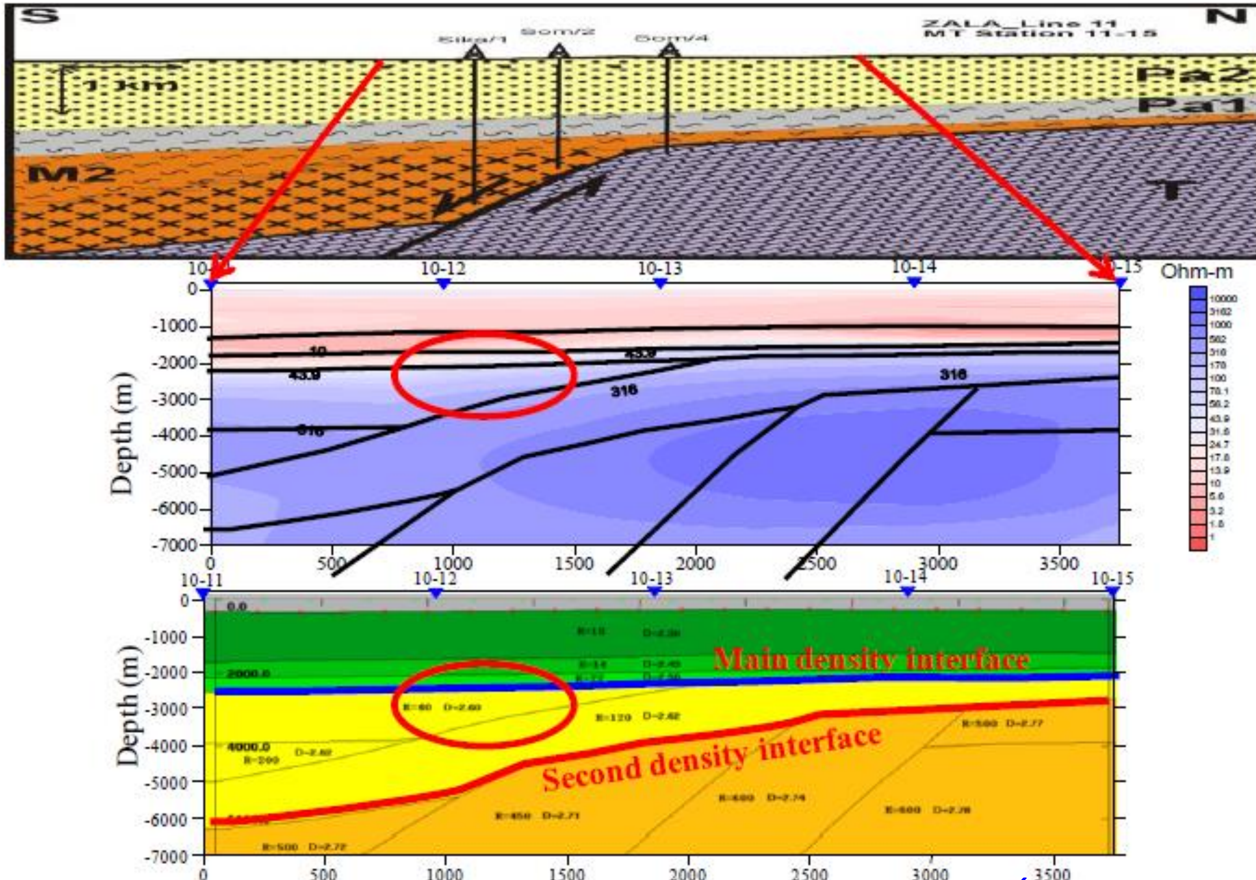

[Kurt Martin Strack](), [Norman C. Allegar](), [Gang Yu](), [Helga Tulinius](), [László Ádám](), [Adrian Gunnarsson](), [Ling Feng He](), [Zhi El Segundo He](): **Exploring for geothermal reservoirs using broadband 2-D MT and gravity in Hungary.** [SEG Technical Program Extended Abstracts]() 27(1) · June 2008

Supported by

RawMaterials
Connecting matters
Funded by the European Union
2021 ESEE

Magnetic Force

Attraction $p_1<0$ és $p_2>0$
$p_1>0$ és $p_2<0$

Repulsion $p_1<0$ és $p_2<0$
$p_1>0$ és $p_2>0$

$$F = k\frac{p_1 p_2}{r^2}$$

where p: magnetic pole strength
k: proportionality factor
$k=1/(4\pi+\mu_0)$ ha $[p]=Wb=Vs$
$k=\mu_0/4\pi$ ha $[p]=Am$
μ_0: magnetic permeability
$\mu_0= 4\pi\cdot10^{-7}$ Vs/Am

Supported by
RawMaterials ACADEMY
Funded by the European Union

eit RawMaterials
Connecting matters
Funded by the European Union
DIM 2021 ESEE

Magnetization

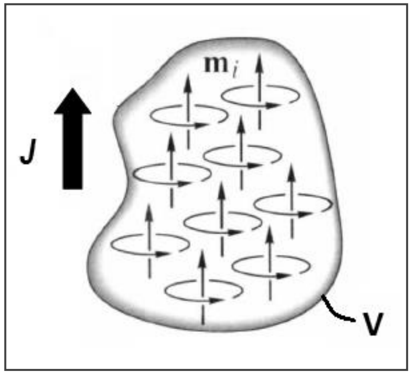

$$m = pl$$

$$m = \int J dV$$

$$B = \mu_0 H$$

$$J = \kappa H + (J_0)$$

where m: magnetic dipole moment
J: vector of magnetization
J_0: vector of remanent magnetization
H: magnetic field strength (H=F/p)
B: magnetic induction
μ: magnetic permeability of the medium
κ: magnetic susceptibility

$$B = \mu_0 (H + J) = \mu_0 (1 + \kappa) H = \mu_0 \mu H$$

Supported by
eit RawMaterials ACADEMY
Funded by the European Union

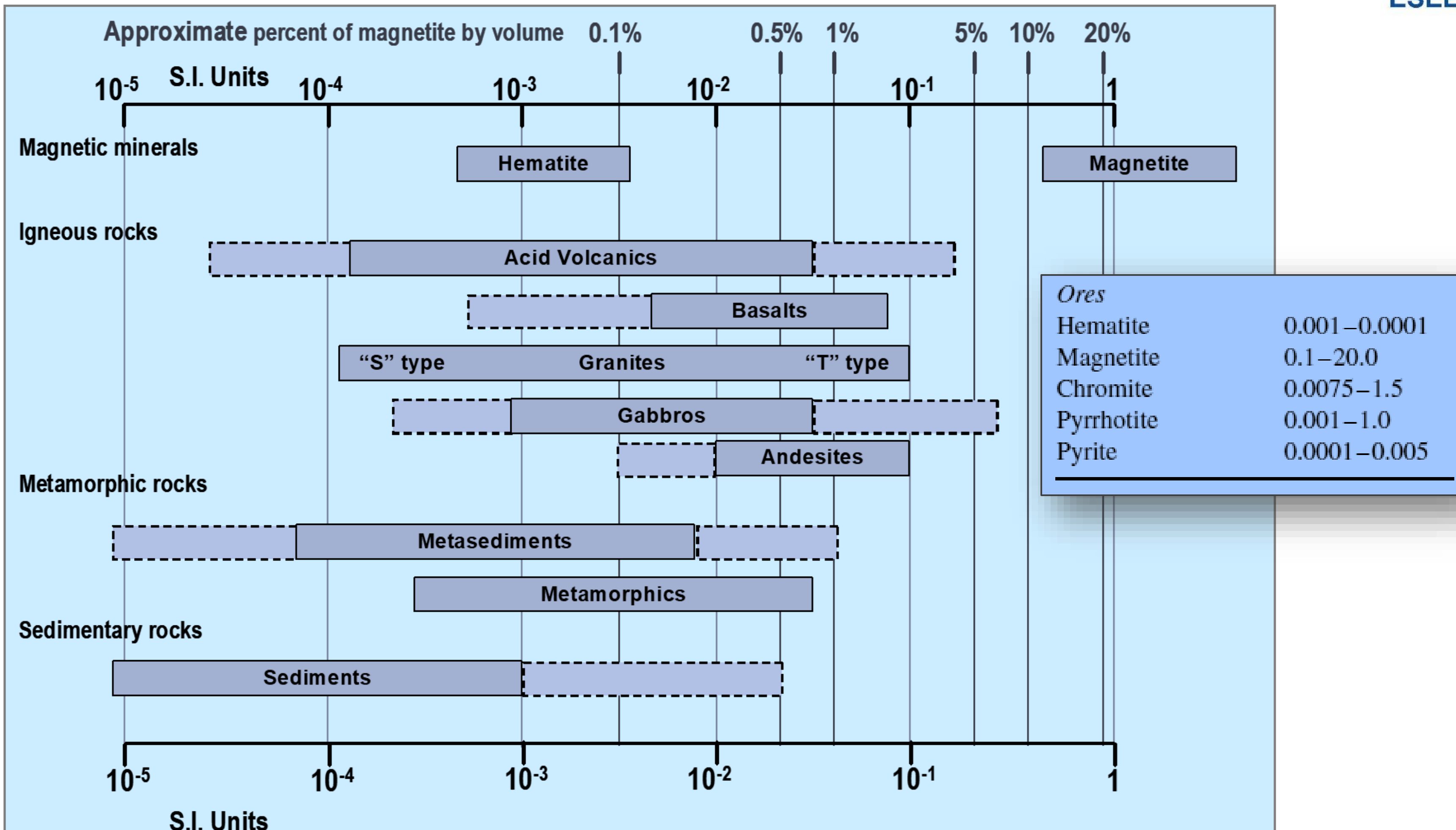

Adapted from Clark and Emerson, Exploration Geophysics, 1991.

The Earth's Magnetic Field

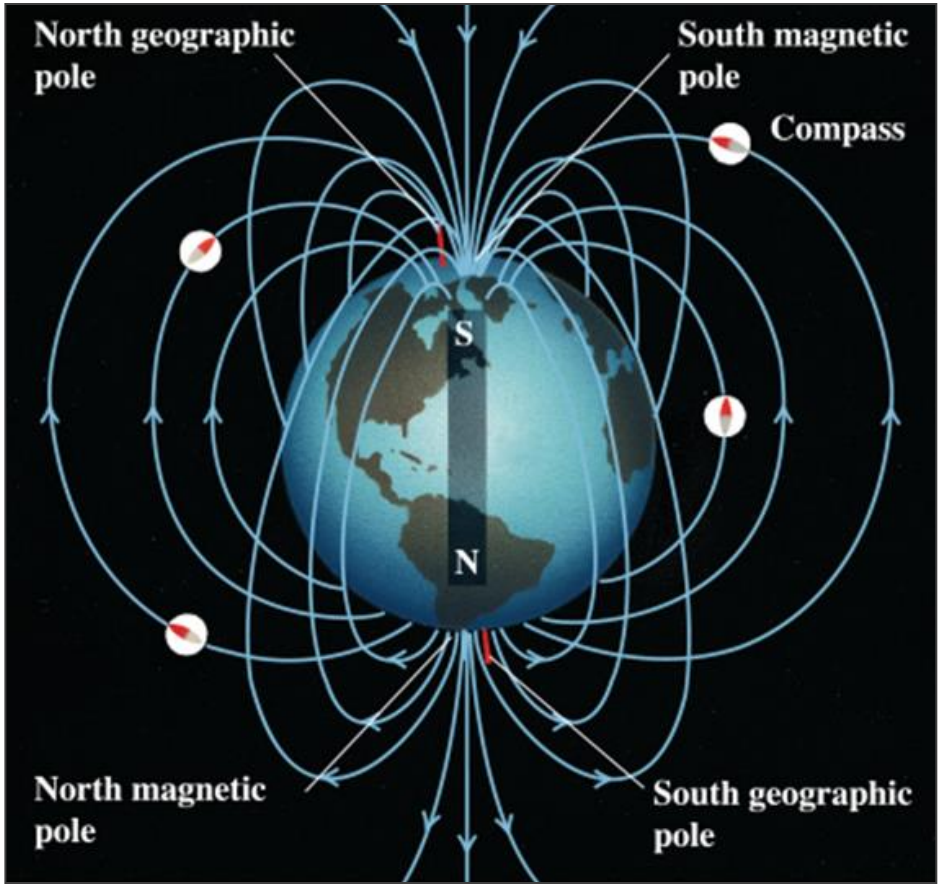

- Outer core: dynamo theory and magneto-hidrodinamics, 95% of the magnetic field, secular variation
- Crust: invarying in time
- Cosmic radiation: interaction with the ionosphere, diurnal effect, magnetic storms

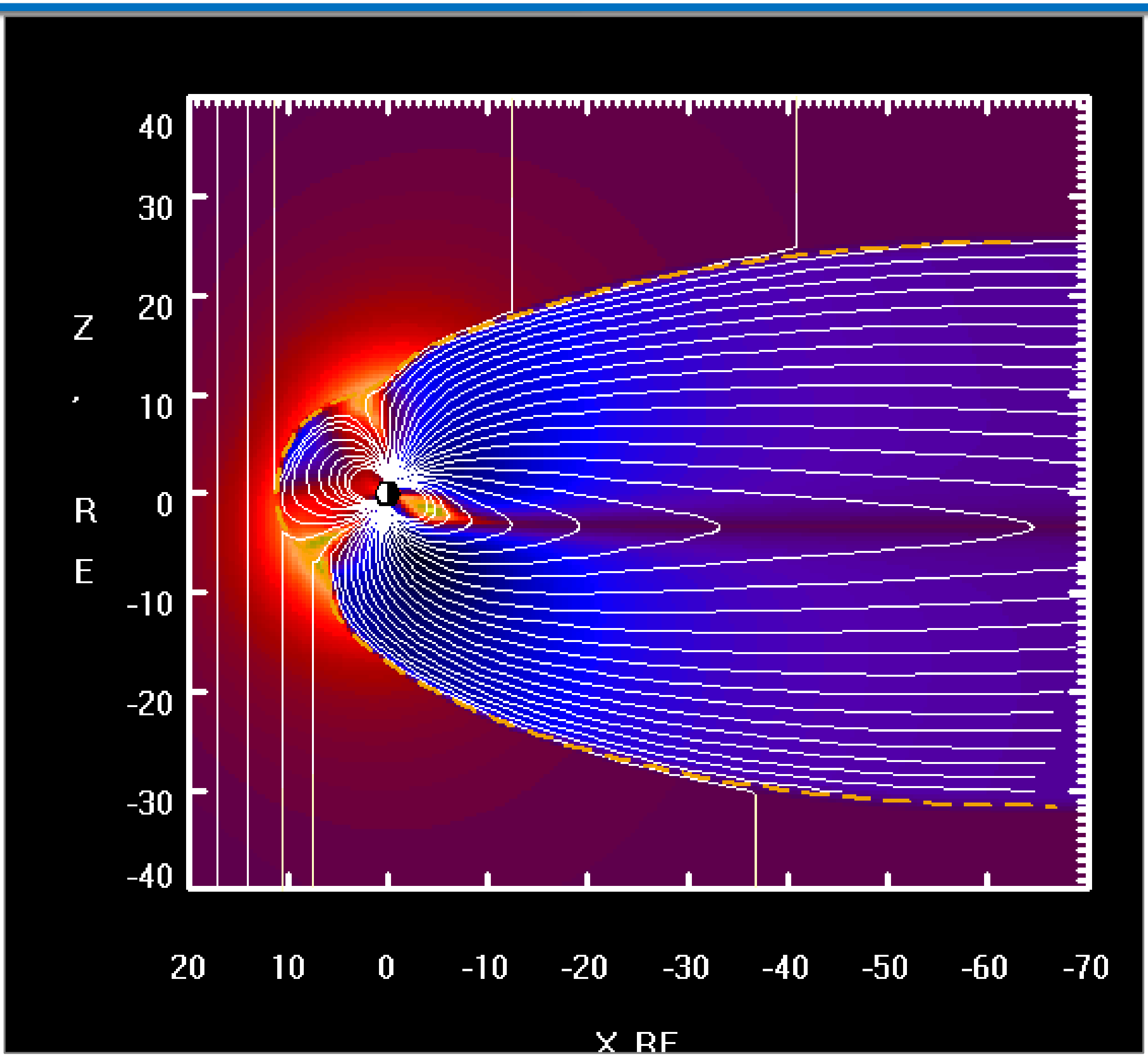
Z , R E
40
30
20
10
0
-10
-20
-30
-40
20 10 0 -10 -20 -30 -40 -50 -60 -70
X RE

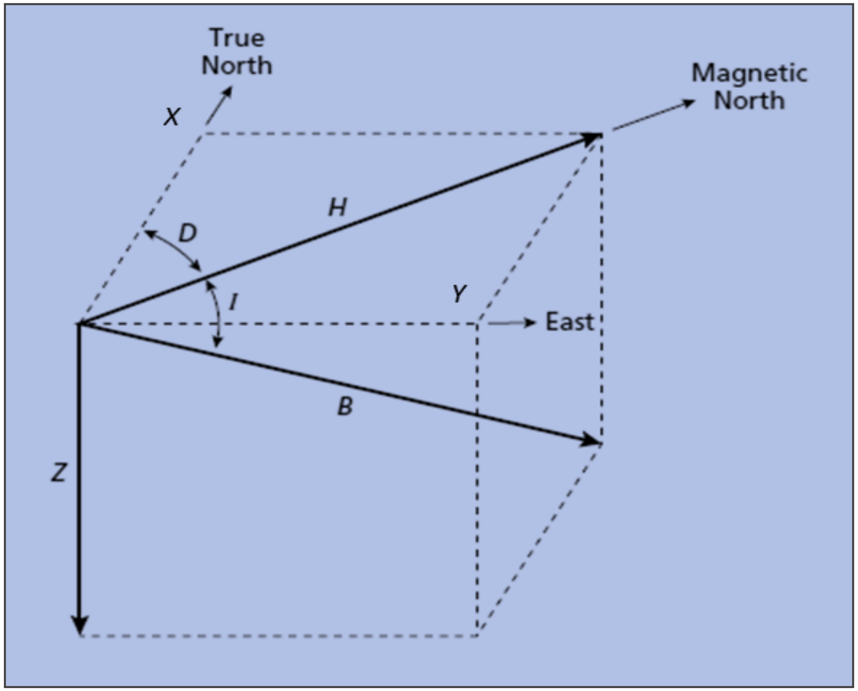

- Total component (B or T)
- Horizontal component (H)
- Vertical component (Z)
- Inclination (I)
- Declination (D)

$$H = B\cos I \qquad Z = B\sin I \qquad D = \mathrm{arctg}\left(\frac{Y}{X}\right)$$

$$X = B\cos I\cos D \quad Y = B\cos I\sin D \quad I = \mathrm{arctg}\left(\frac{Z}{\sqrt{X^2+Y^2}}\right)$$

Supported by
RawMaterials ACADEMY
Funded by the European Union

Magnetic Anomaly

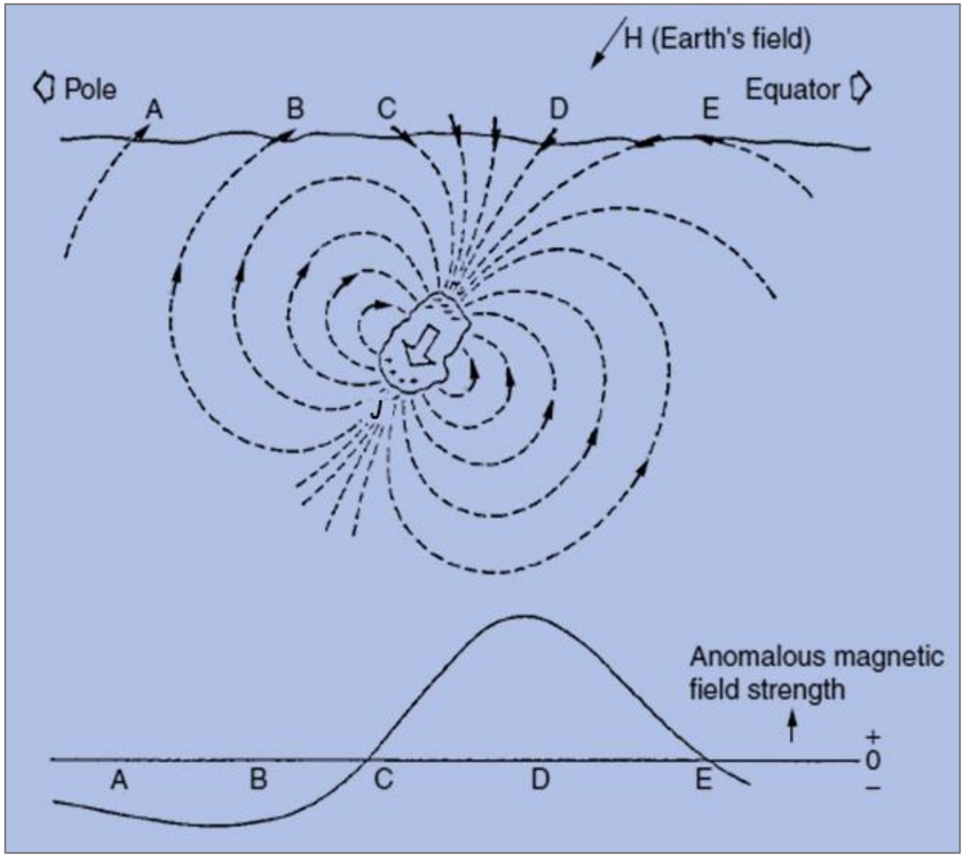

- Earth's magnetic field:
  - Magnetic dipole approximation
  - Homogeneous magnetic field locally (small area)
- Local anomaly:
  - Different rocks have different susceptibilities
  - Different magnetization
- We measure the superposition of the global and local field

$$\mathbf{B}^{(\text{Measured})} = \mathbf{B}^{(\text{Earth})} + \mathbf{B}^{(\text{Body})}$$

Supported by
RawMaterials ACADEMY
Funded by the European Union

Funded by the
European Union

Magnetic Anomaly and Inclination

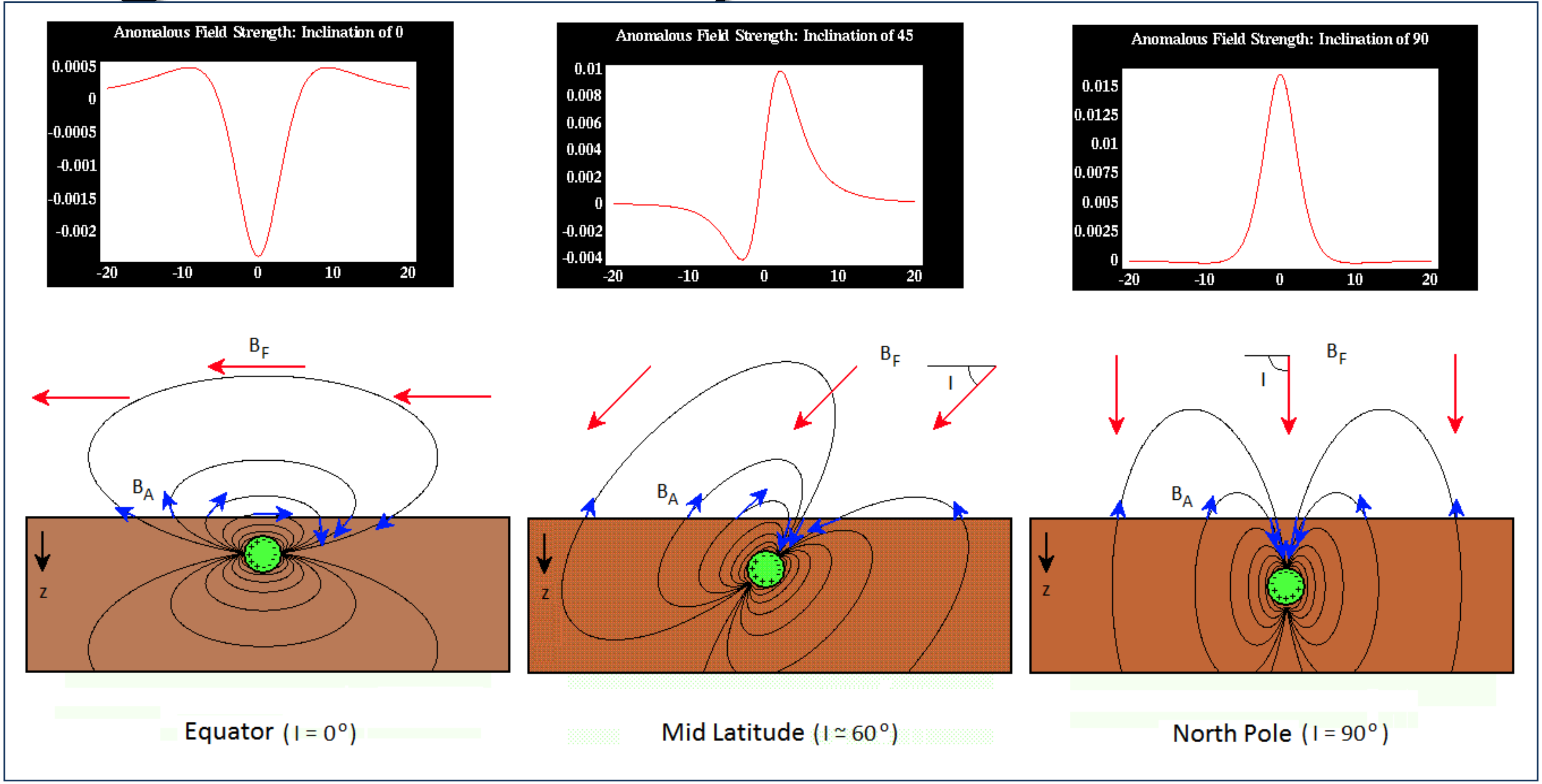

Supported by

Funded by the
European Union

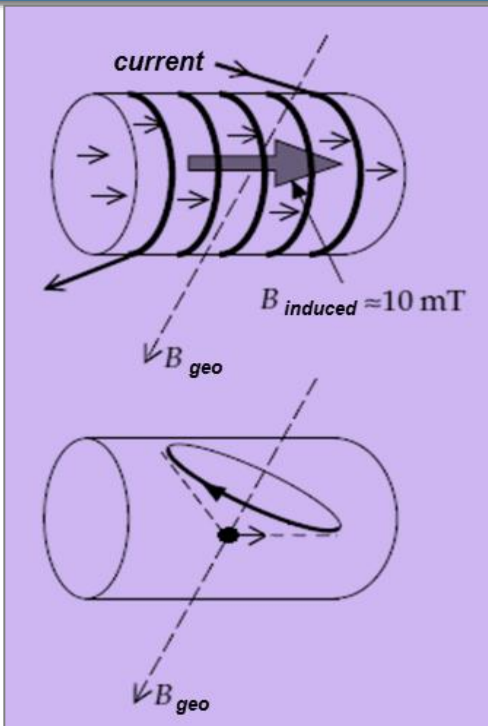

- Elements: water tank (protons), coil (induction and measurement), lifting rod, electronics
- Operation: current supply, induced magnetic field, angular force and protons align to the field, current cut off, precession motion of protons around the Earth's magnetic field
- Observed quantity: precession frequency

$$f = \frac{\gamma}{2\pi}\left|\mathbf{B}\right|$$

where γ=0.042576Hz/nT is the proton's gyro-magnetic ratio and f ~ 2kHz

- Absolute accuracy ~ 0.1 nT
- Rapid measurement: 3sec / reading

RawMaterials Connecting matters
Funded by the European Union
2021 ESEE

Magnetic Gradiometry

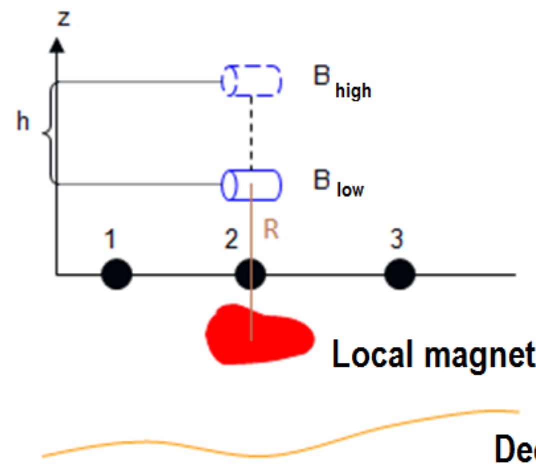

$$\left|\frac{\Delta B}{\Delta z}\right|_1 < \left|\frac{\Delta B}{\Delta z}\right|_2 > \left|\frac{\Delta B}{\Delta z}\right|_3$$

$$\frac{\Delta B}{\Delta z} = \frac{B_{low} - B_{high}}{h}$$

- Vertical (or horizontal) gradient of total magnetic field
- Enhancement of near-surface effects
- Automatic cancellation of diurnal effect
- Field strength: $B = C\frac{m}{h^3}$

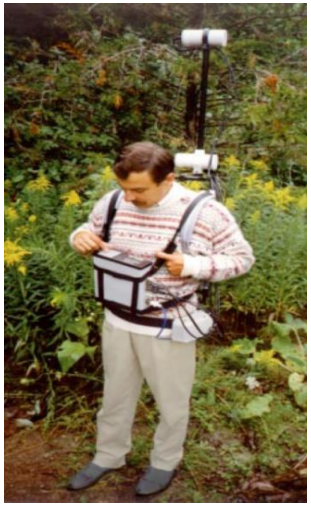

Supported by
RawMaterials ACADEMY
Funded by the European Union

Magnetic Data Processing

- Normal correction (or removing regional trend)
- Diurnal correction
- Topographic correction
- Reduction to magnetic pole
- Analitic continuation

Supported by
RawMaterials ACADEMY
Funded by the European Union

Analytic Continuations

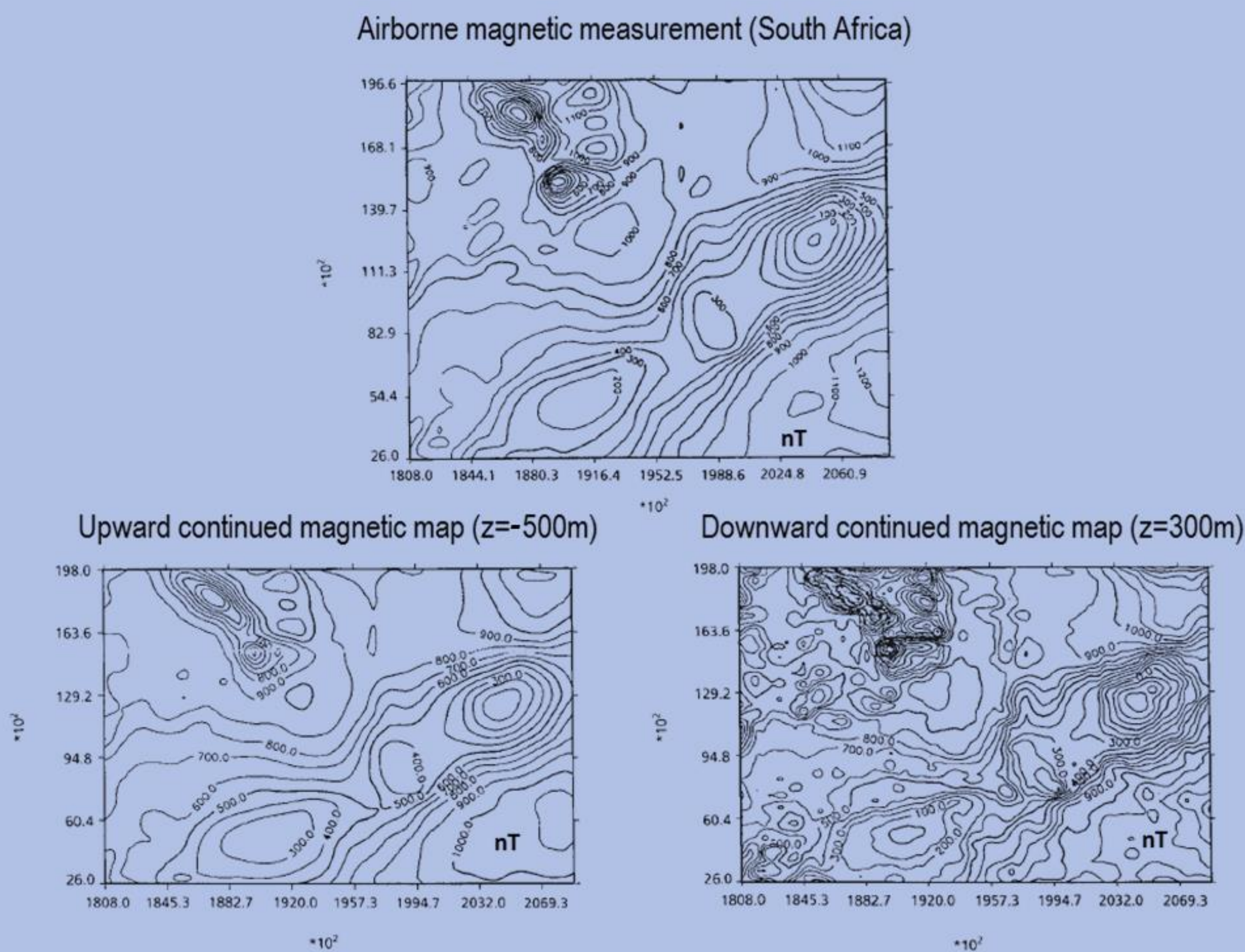

Inverse modeling

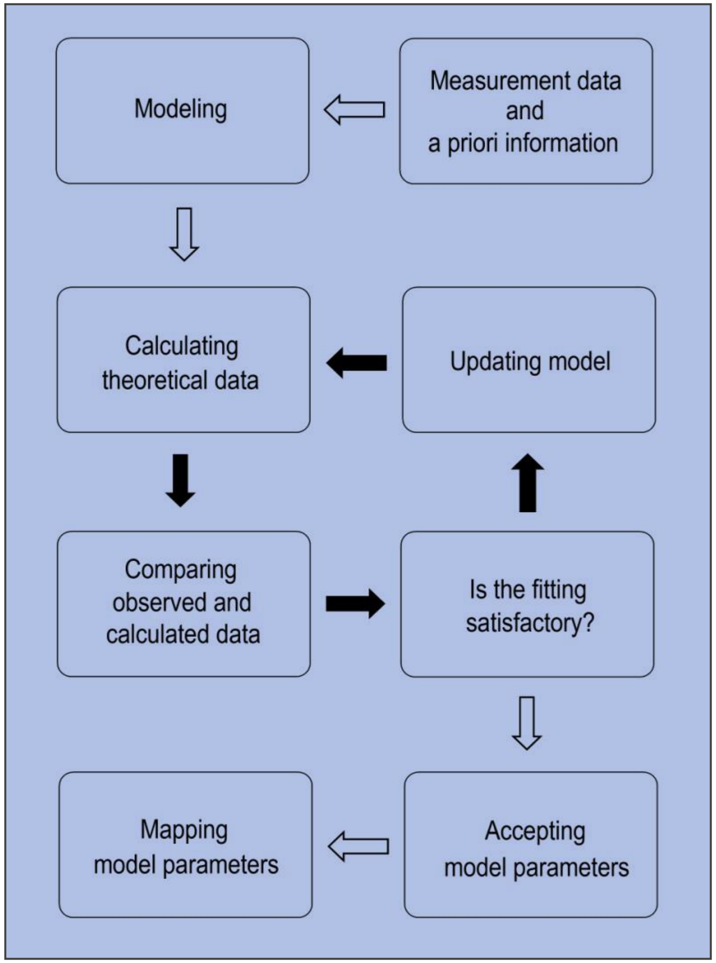

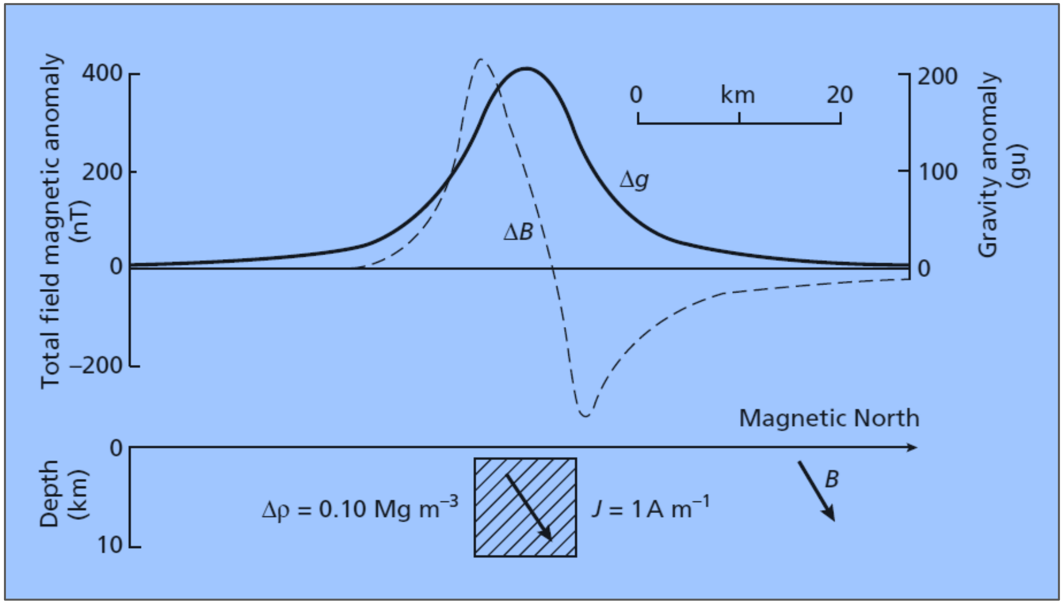

Supported by
RawMaterials ACADEMY
Funded by the European Union

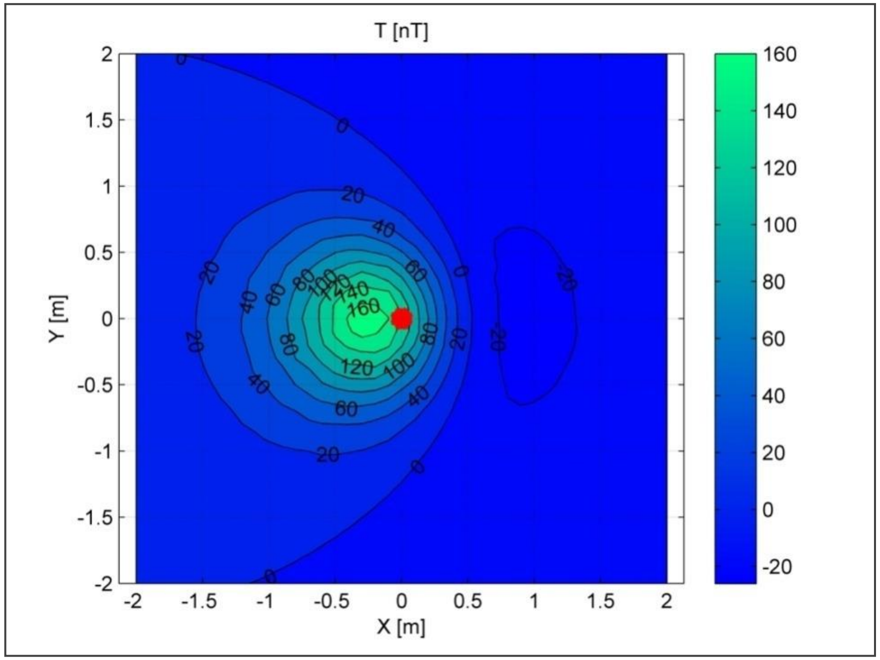

Reduction to pole

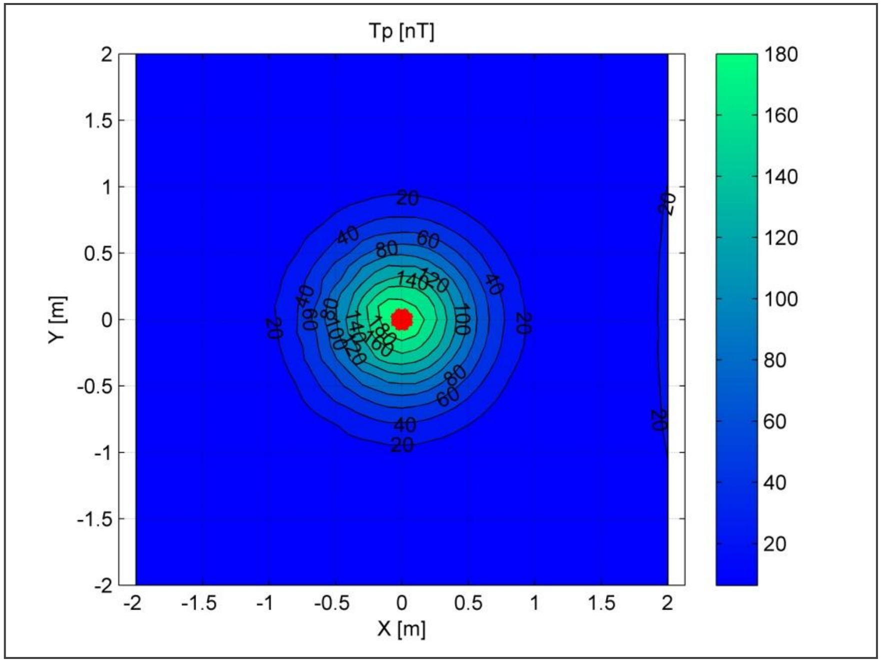

z = 1 km

x = 0 km, y = 0 km

$m_d = 10^9$ Am^2

D = 2.5^0 , I = 63^0

Noise level = 2% Gaussian

Supported by
EIT RawMaterials Academy
Funded by the European Union

Funded by the European Union

Rectangular Prism

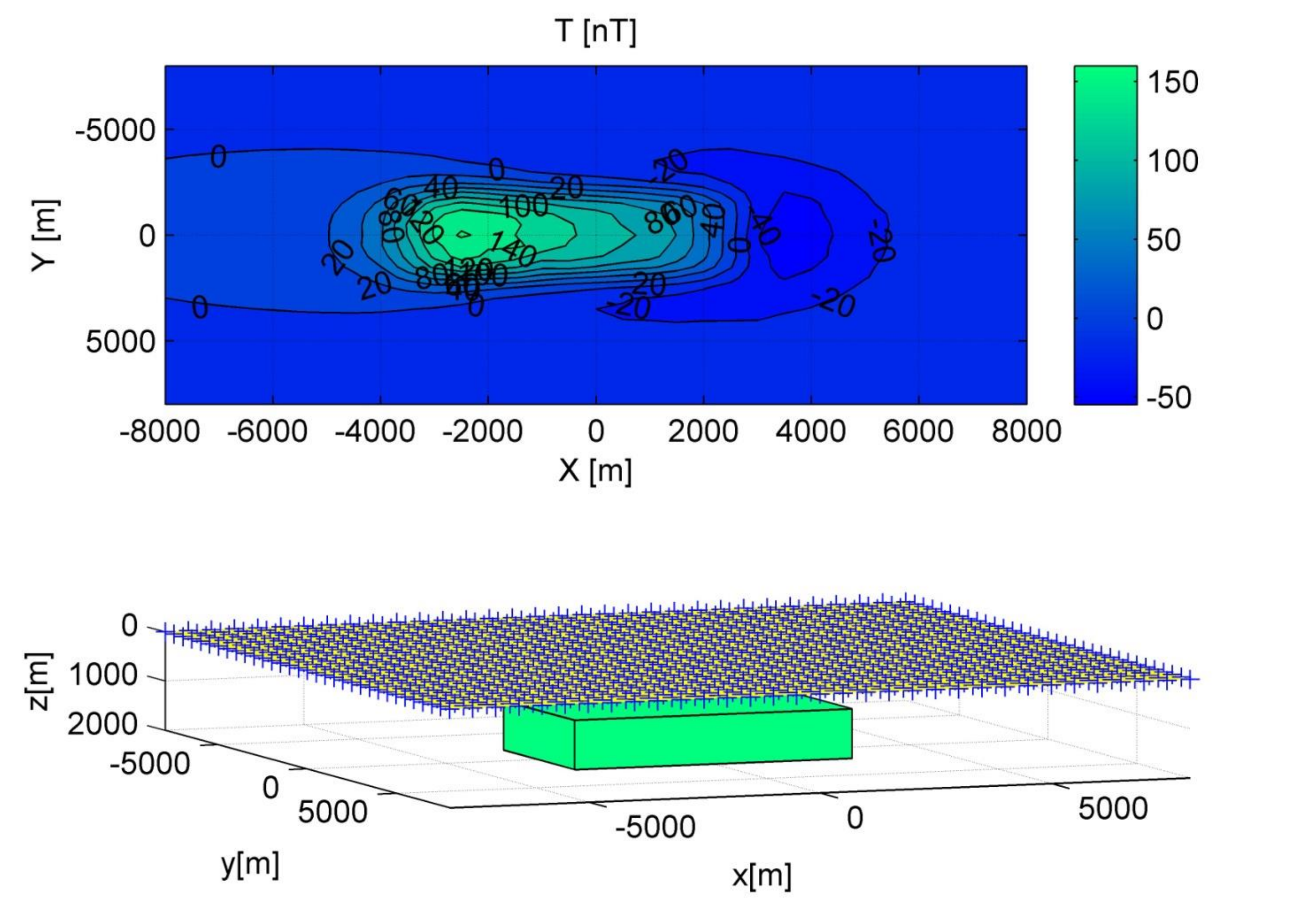

x_1=-4 km, x_2=4 km

y_1=-2 km, y_2=2 km

z_1=1 km, z_2=2 km

J=1 A/m

D=2.5^0 , I=63^0

Noise = 3% Gaussian

Supported by

Funded by the European Union

RawMaterials Connecting matters

Funded by the European Union

DIM 2021 ESEE

Pole Reducted Prism Field

x_1=-3 km, x_2=3 km

y_1=-2 km, y_2=2 km

z_1=1 km, z_2=2 km

J=1 A/m

D=2.5^0 , I=63^0

Noise = 3% Gaussian

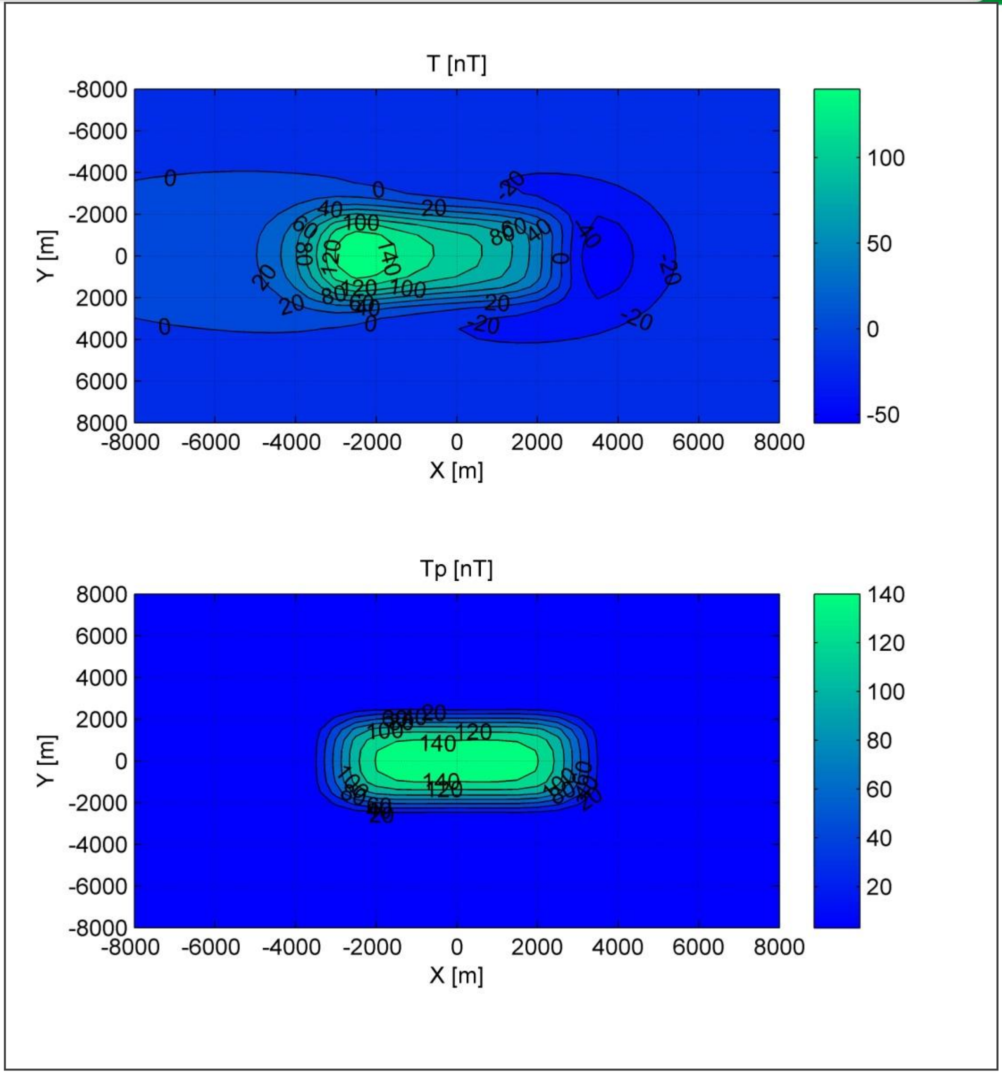

Supported by

RawMaterials ACADEMY

Funded by the European Union

Problem of Ambiguity

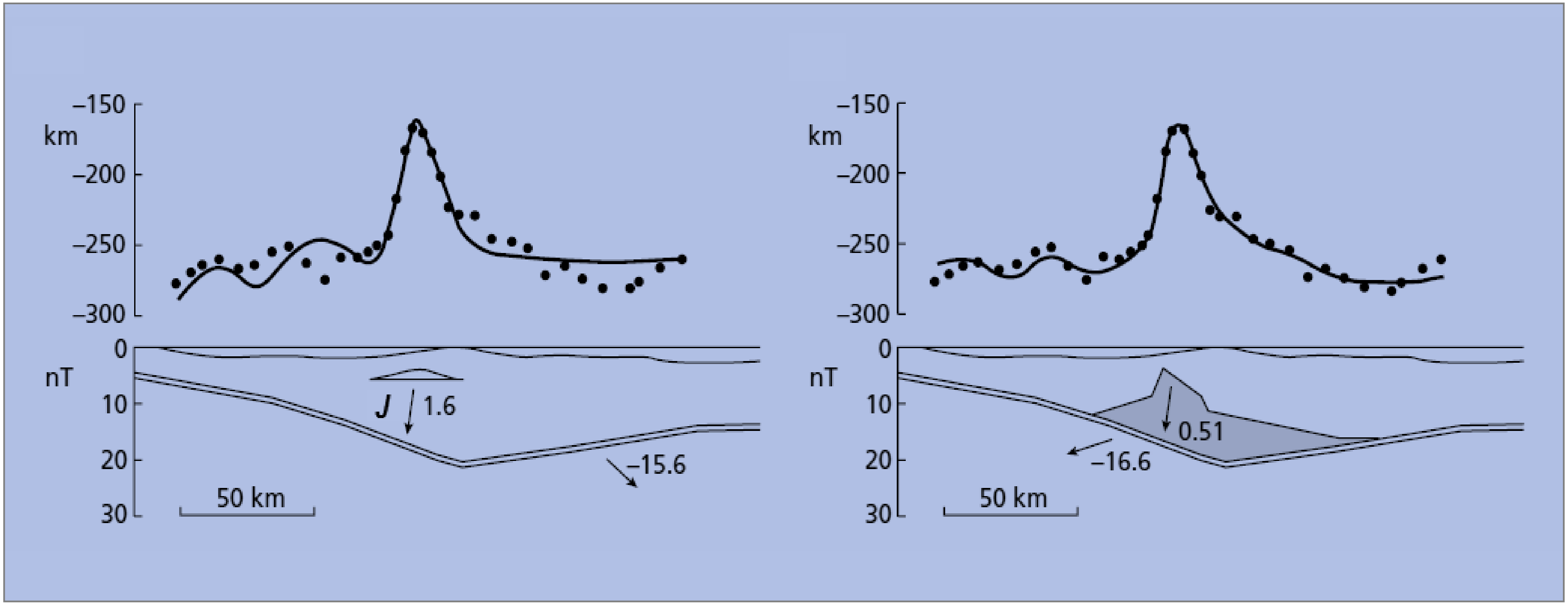

APPLICATIONS

- Finding buried steel tanks and waste drums
- Detecting iron and steel obstructions
- Locating unmarked mineshafts
- Accurately mapping archaeological features
- Mapping basic igneous intrusives & faults
- Evaluating the size and shape of ore bodies

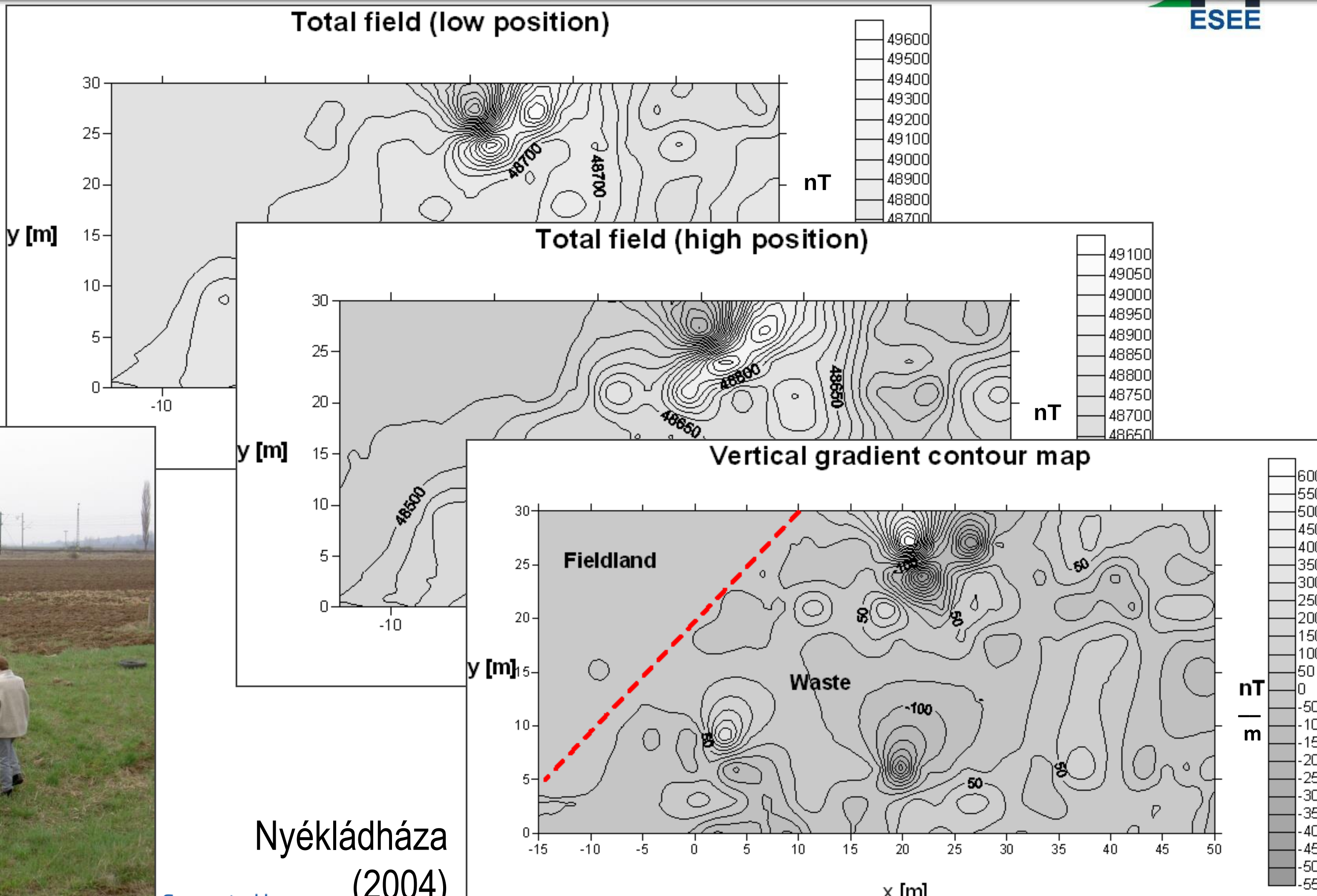

Nyékládháza
(2004)

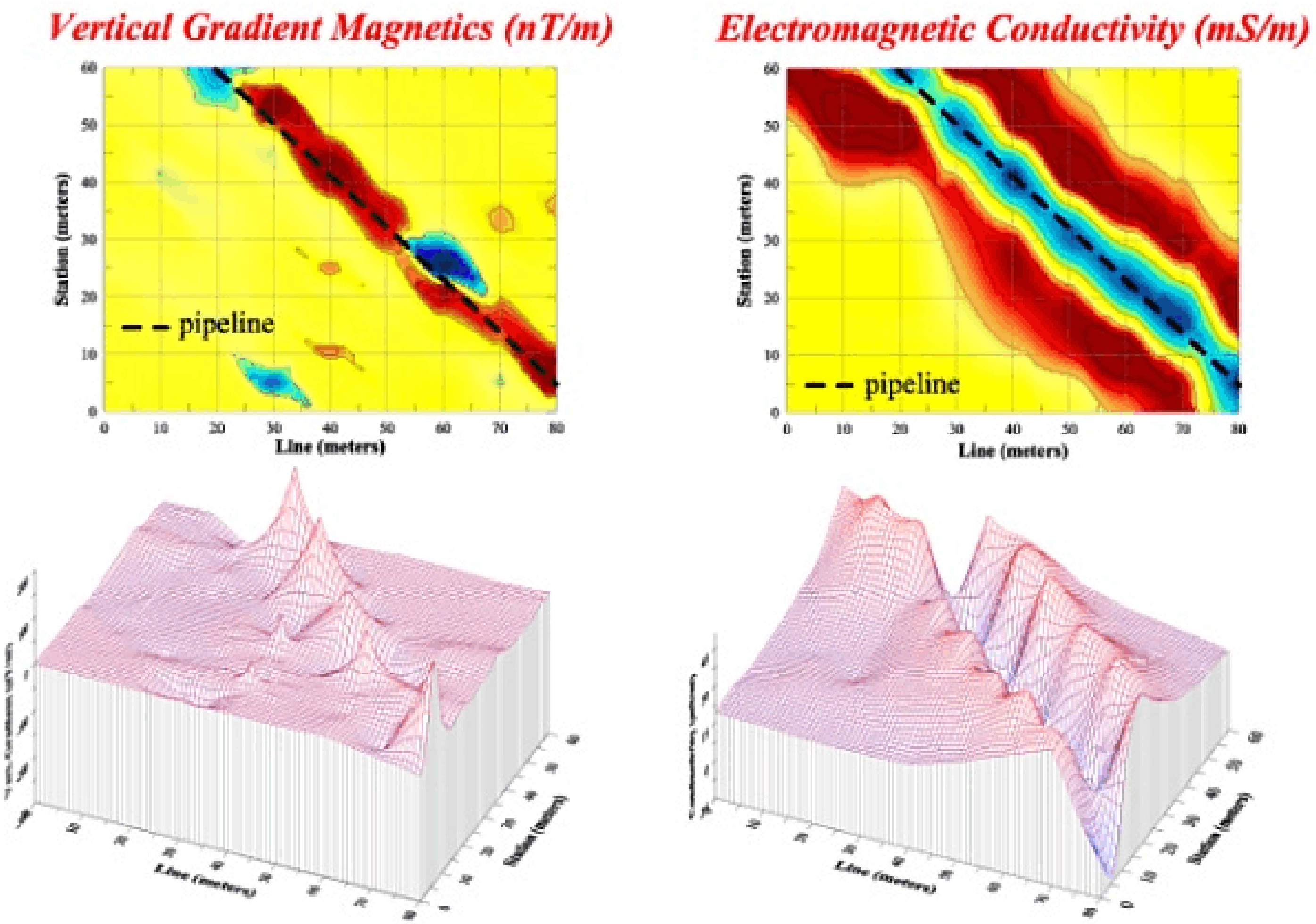
Vertical Gradient Magnetics (nT/m)
Electromagnetic Conductivity (mS/m)
Station (meters)
Line (meters)
pipeline
0
10
20
30
40
50
60
70
80

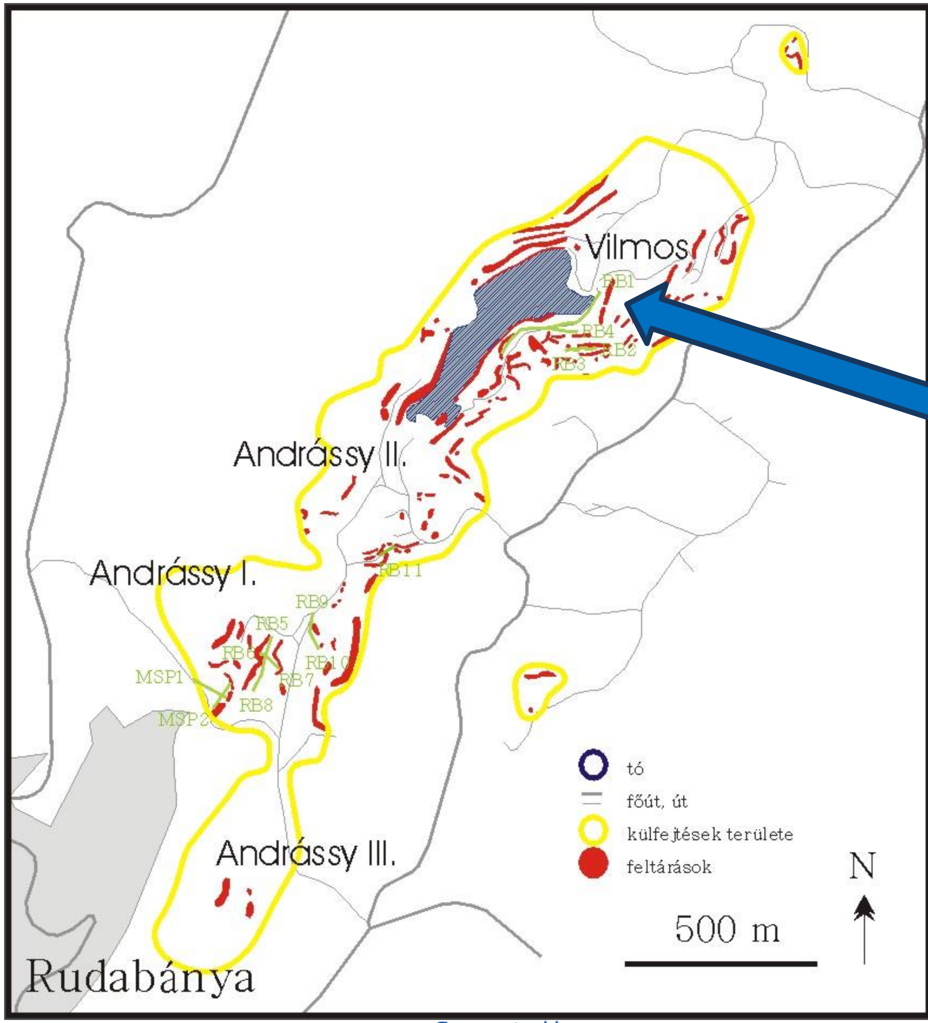

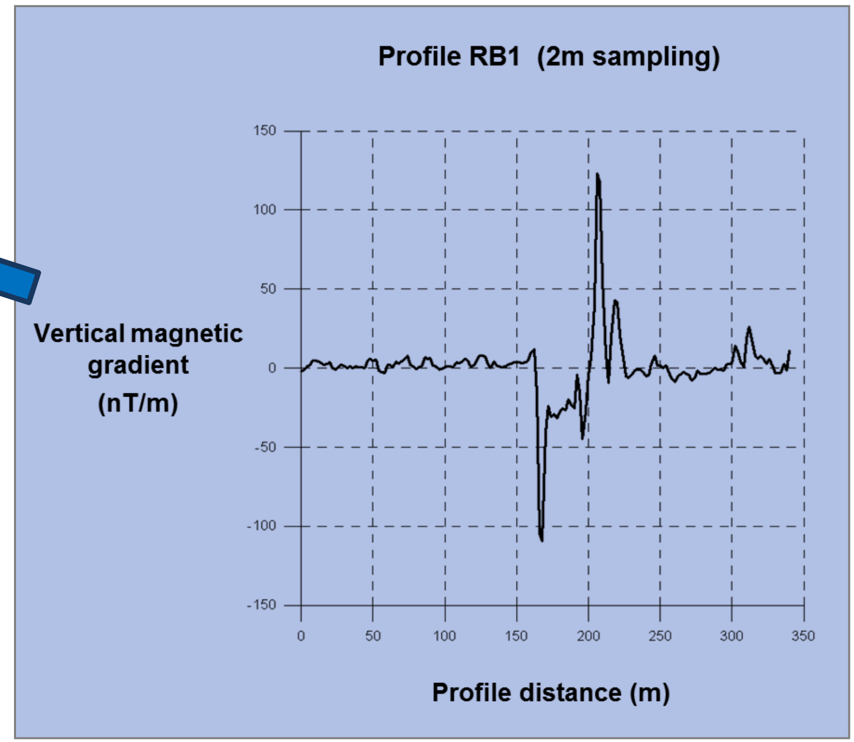

Rudabánya (2007)

RawMaterials
Connecting matters

Funded by the European Union

DIM 2021 ESEE

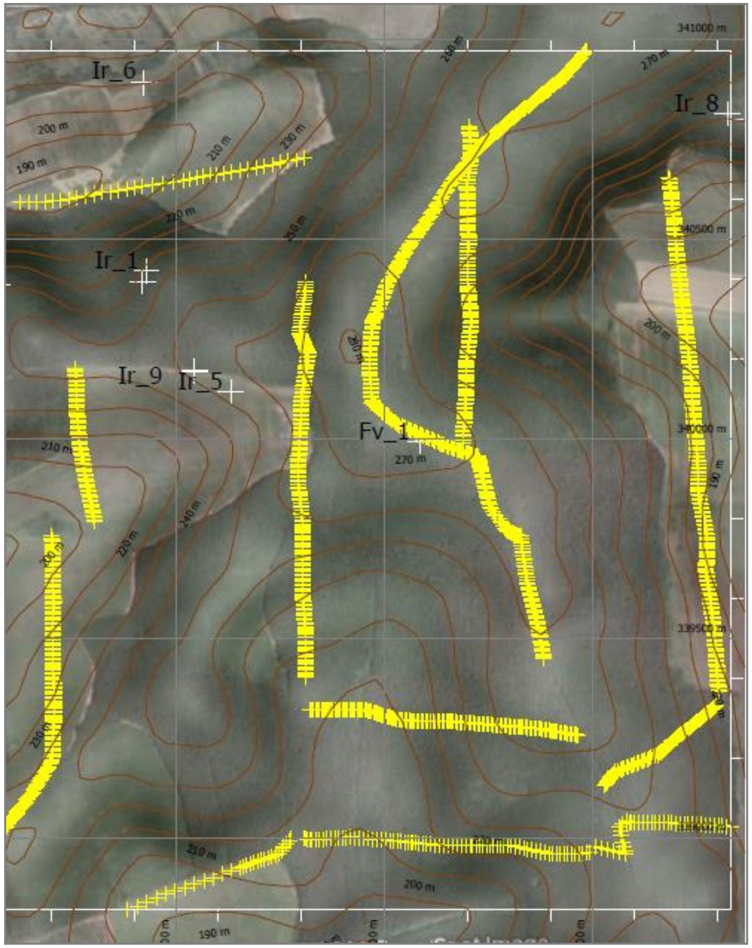

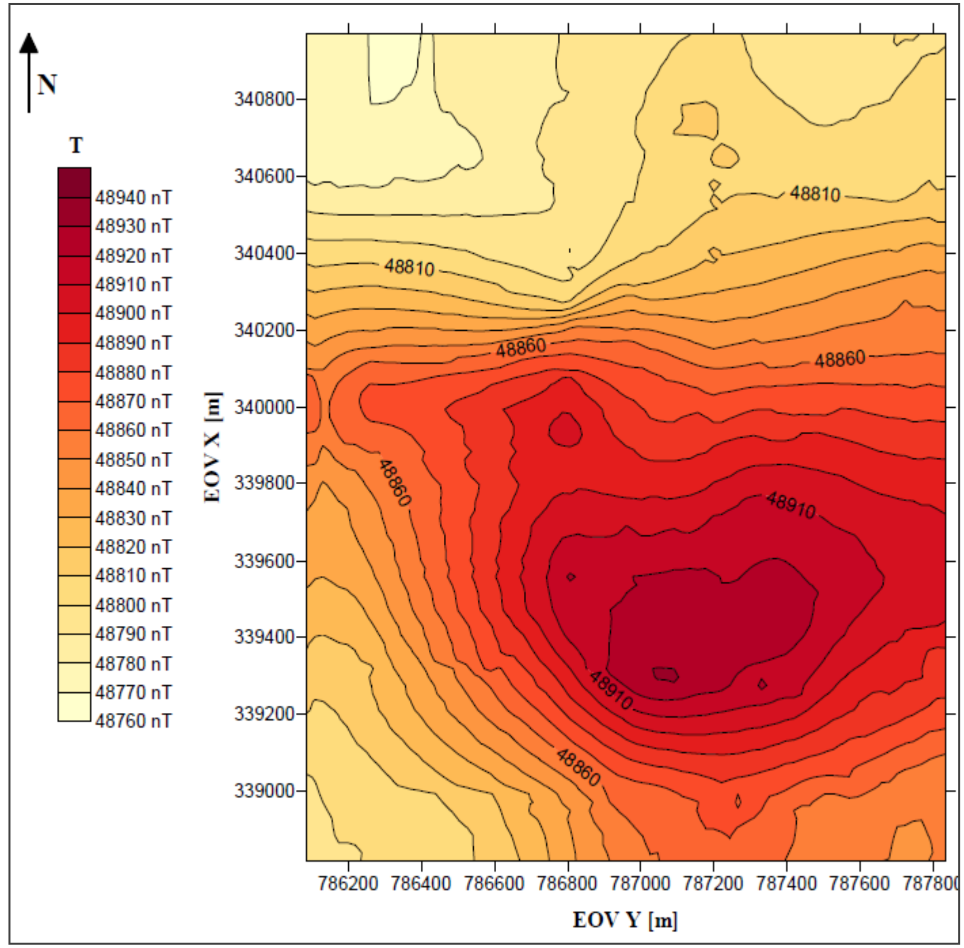

Irota (2011)

Supported by

RawMaterials ACADEMY

Funded by the European Union

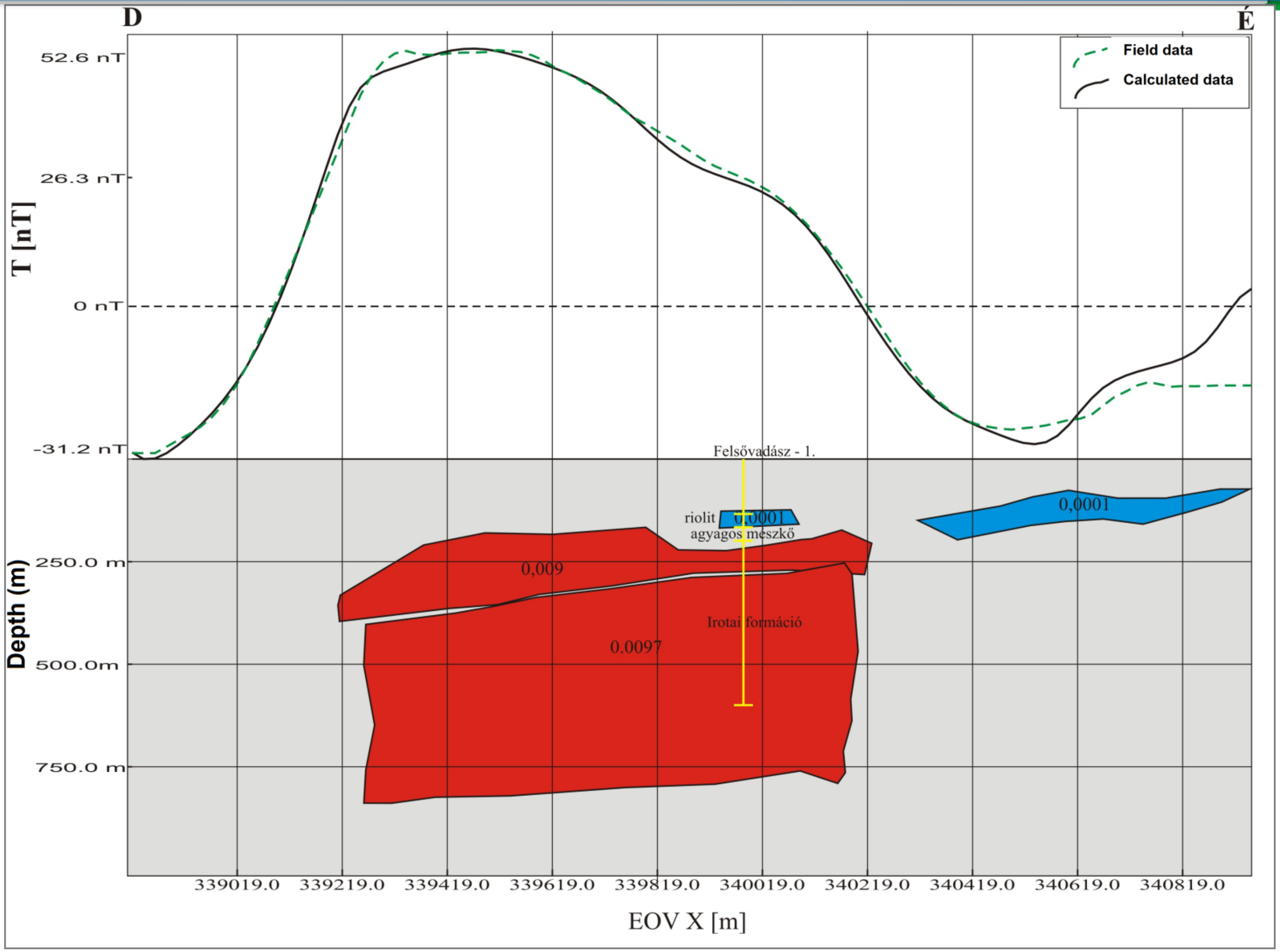
D
É
Field data
Calculated data
52.6 nT
26.3 nT
0 nT
-31.2 nT
T [nT]
Felsővadász - 1.
riolit
0,0001
agyagos meszkő
0,009
Irotai formáció
0.0097
0,0001
250.0 m
500.0m
750.0 m
Depth (m)
339019.0
339219.0
339419.0
339619.0
339819.0
340019.0
340219.0
340419.0
340619.0
340819.0
EOV X [m]

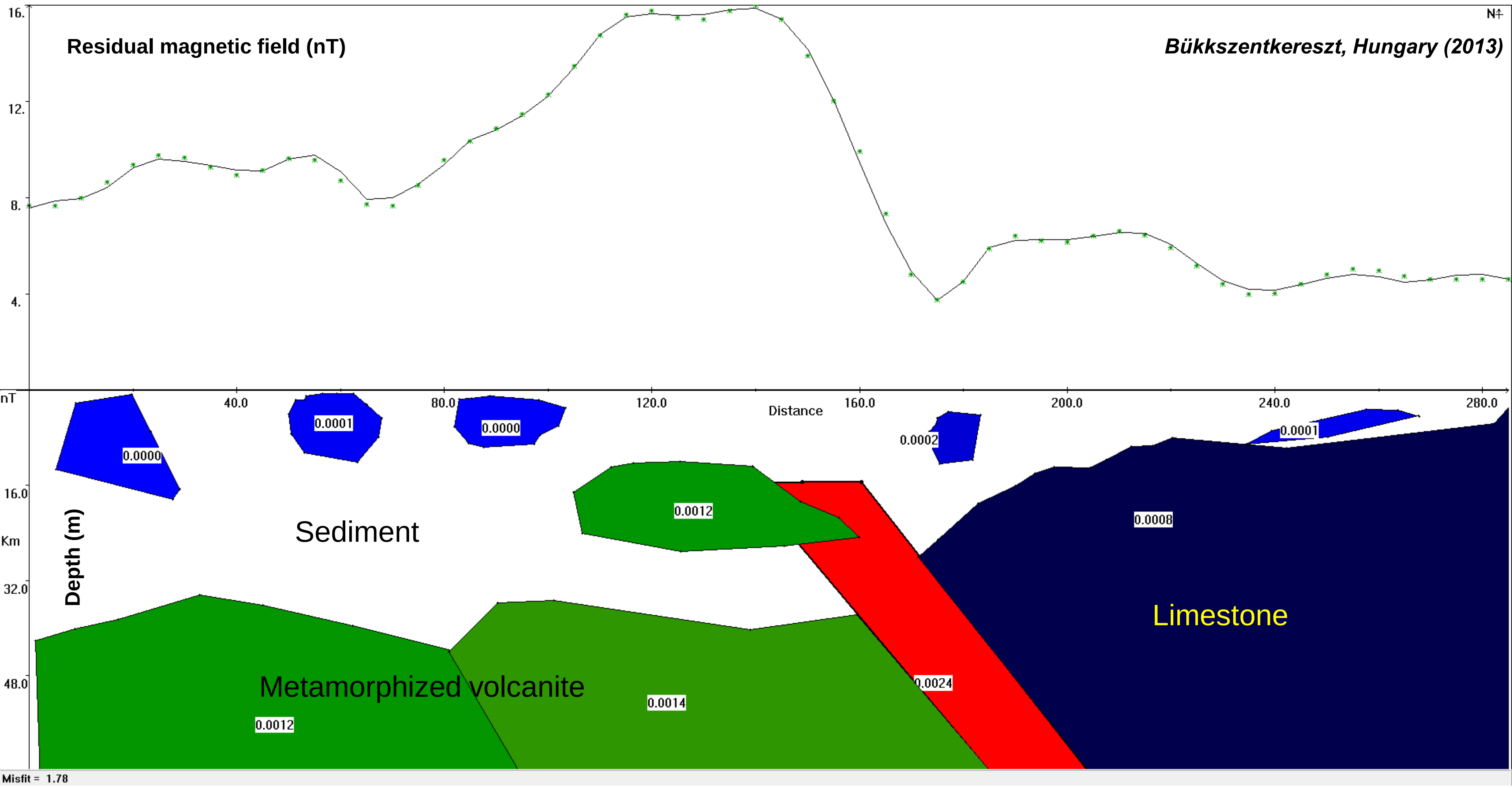

Supported by
RawMaterials ACADEMY
Funded by the European Union

Funded by the European Union

Vertical Gradient Magnetics (nT/m)

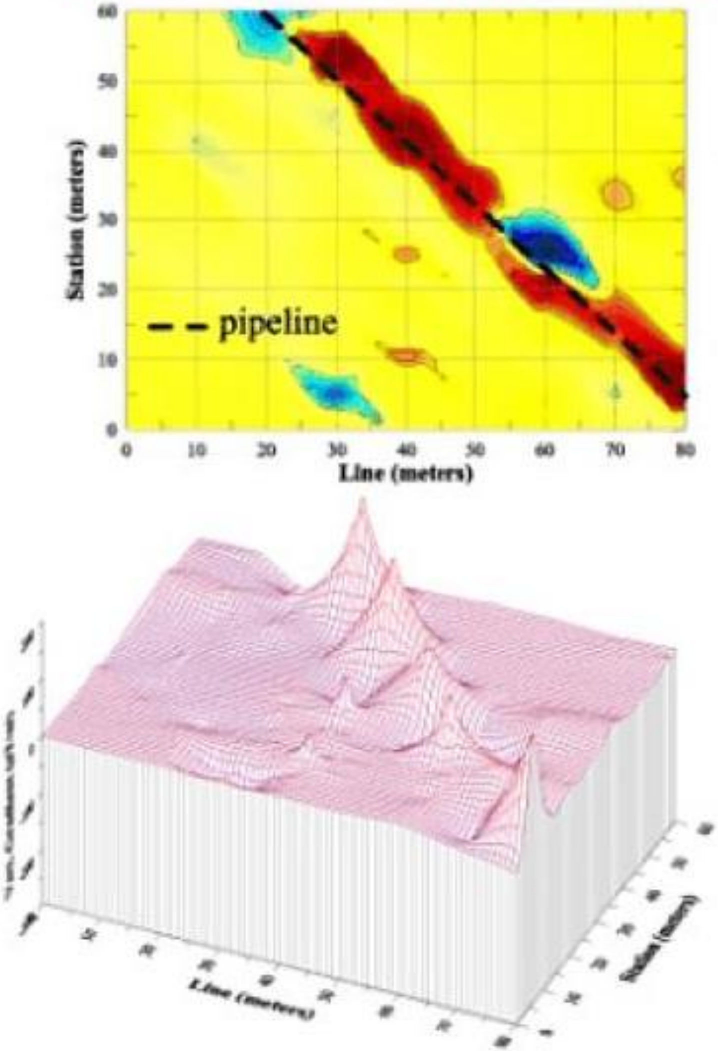

Electromagnetic Conductivity (mS/m)

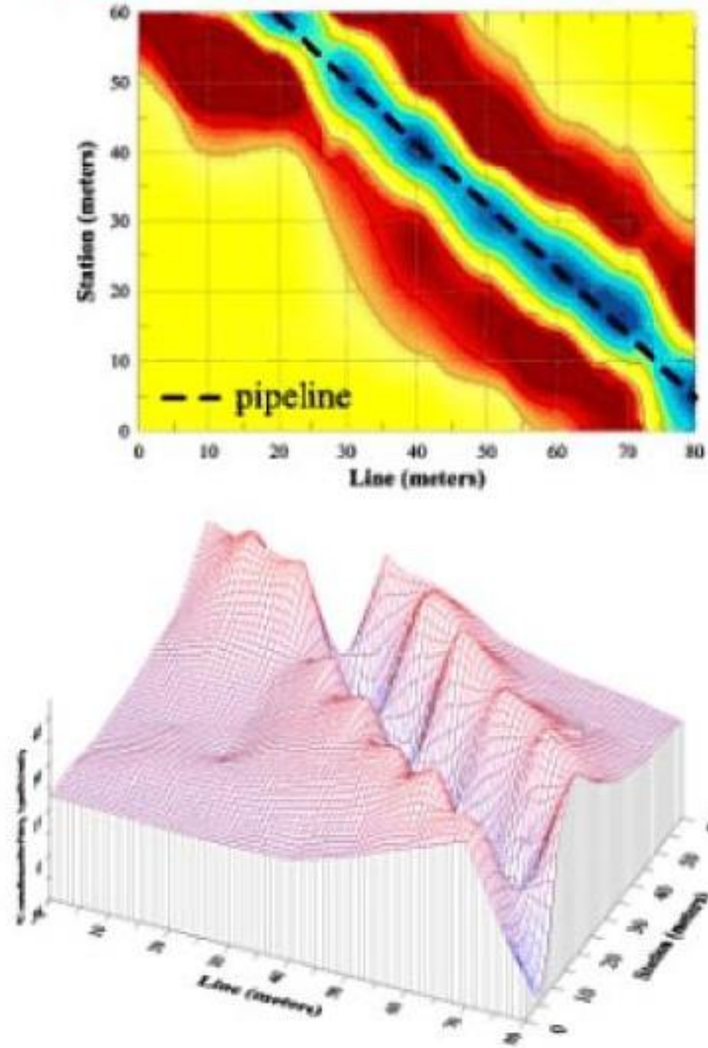

Funded by the European Union

Archeology

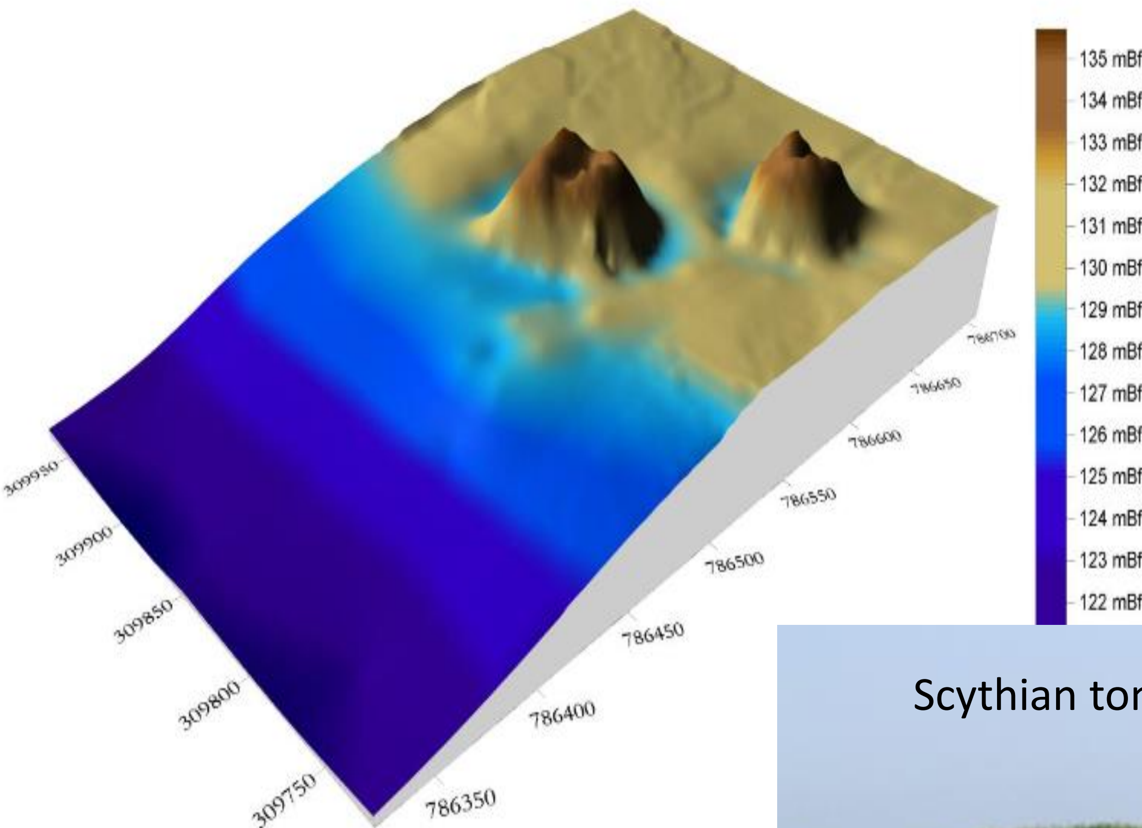

Scythian tombs (Onga) B.C. 5-6 th century

Supported by

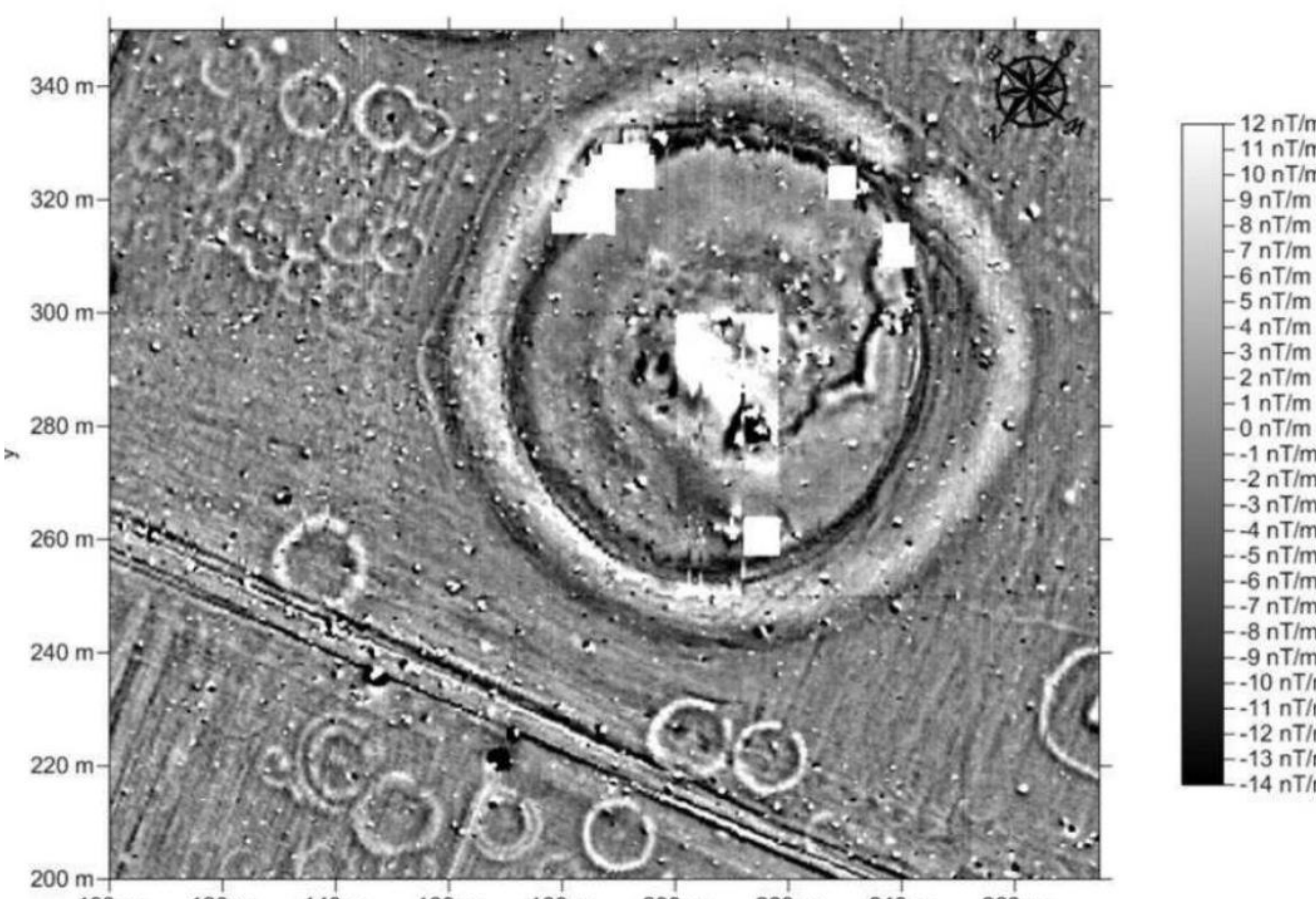

(Finta P. 2012.)

eit RawMaterials ACADEMY

Funded by the European Union

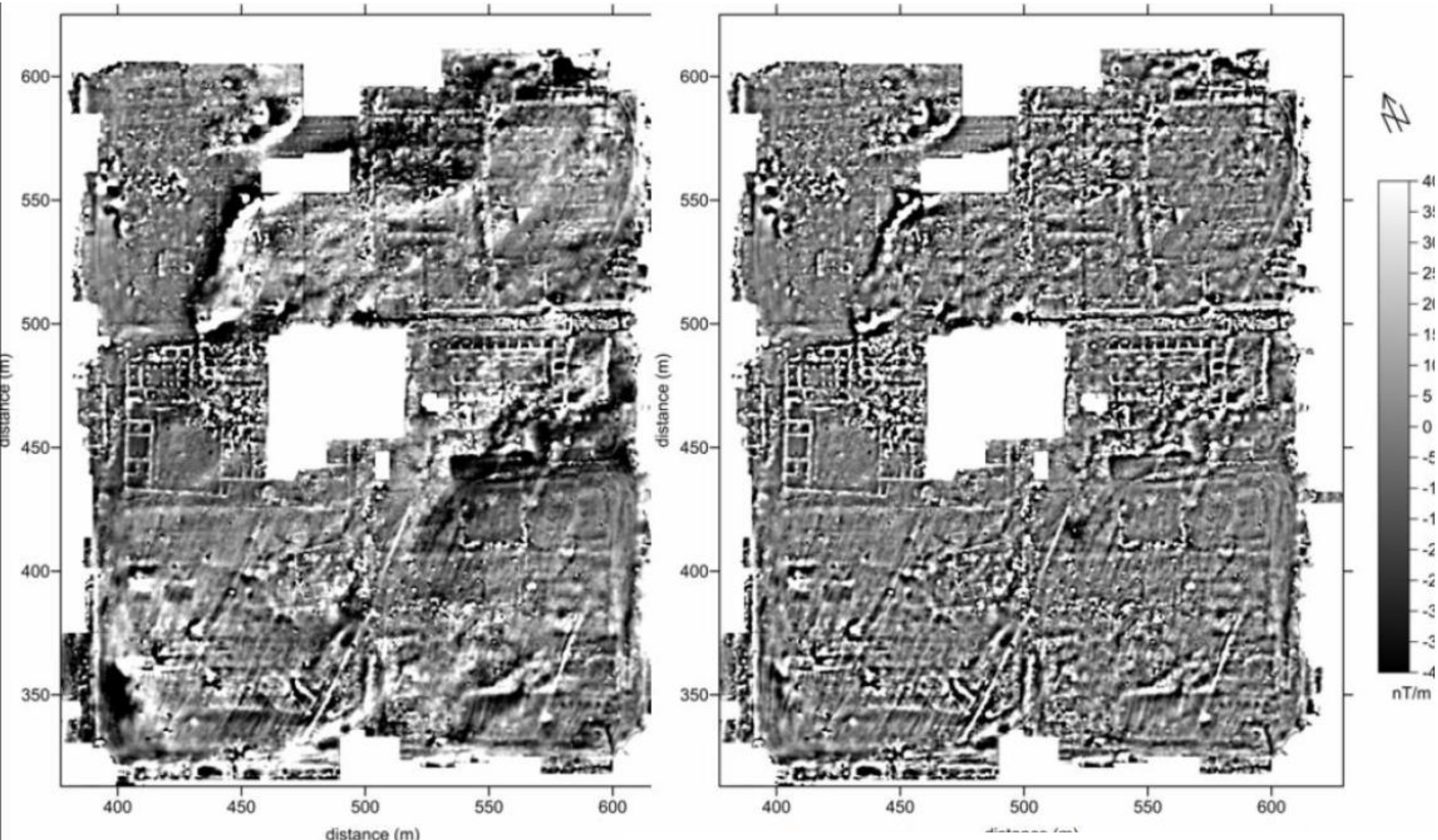

Porolissum Military Camp

Porolissum was an ancient [Roman](#) city in [Dacia](#). Established as a military camp in 106 A.D. during [Trajan's Dacian Wars](#).

Supported by

RawMaterials ACADEMY

Funded by the European Union

The magnetotelluric (MT) method

- Passive EM geophysical exploration method
- Tikhonov (1950), Cagniard (1953)

Magnetosphere + solar wind: 0,001 – 1 Hz
Thunderstorms: 1 Hz <

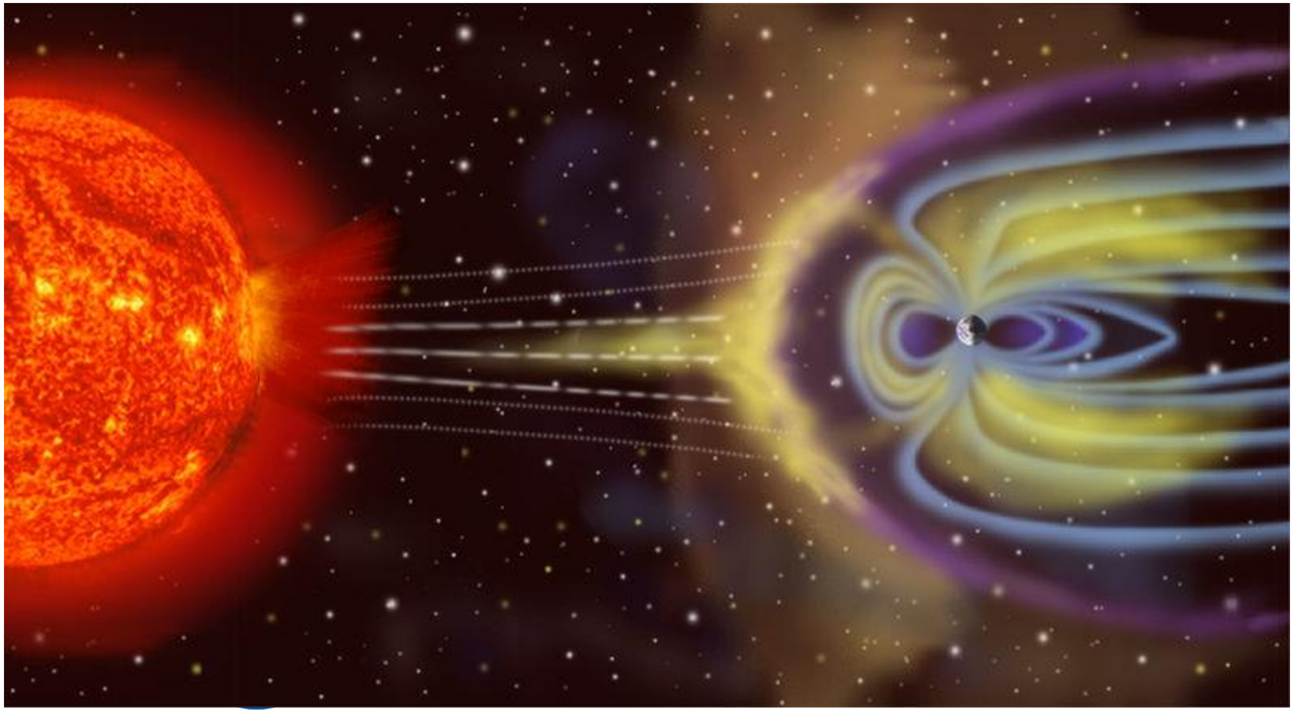

MT in context with EM techniques

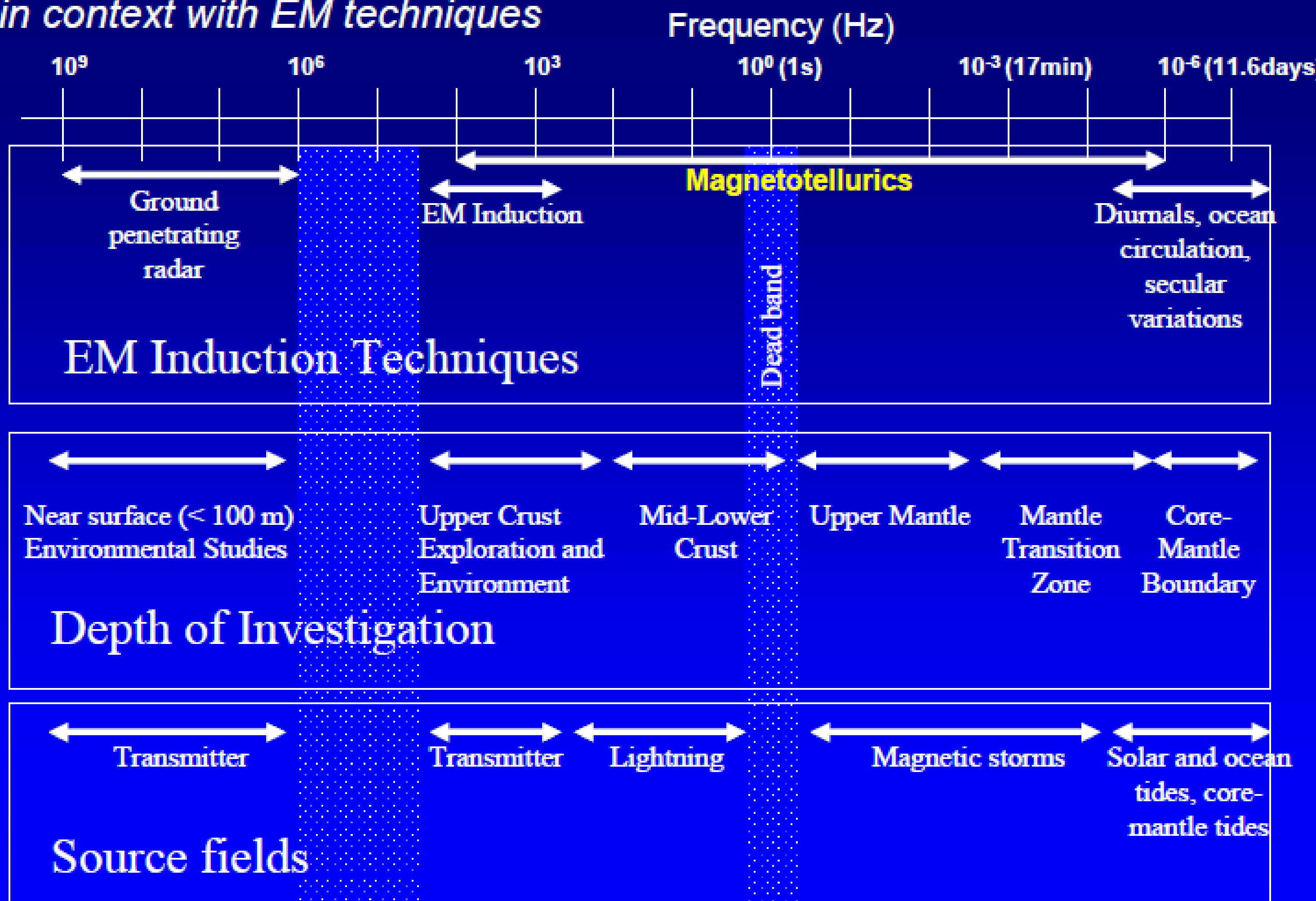

MT Theory

- Passive surface measurement of the Earth's natural electric (E) and magnetic (H) fields
- Assume planar horizontal magnetic source field (reasonable assumption in mid-latitudes, far from external source regions)
- This is a diffusive process, the physics based on Maxwell's equations of electromagnetic induction
- Measure time changes of E and H at arrays of sites
- Frequency range 10 KHz to .0001 Hz (0.0001 s to 10000 s)
- Ratio of E / H used to derive resistivity structure of sub-surface

Supported by
RawMaterials
ACADEMY
Funded by the
European Union

MT Theory

Depth of Investigation –Skin Depth

3 concepts:

- 1.Low frequencies penetrate deeper than high frequencies
- 2.High frequencies image the near-surface
- 3.Signals penetrate further in resistive material

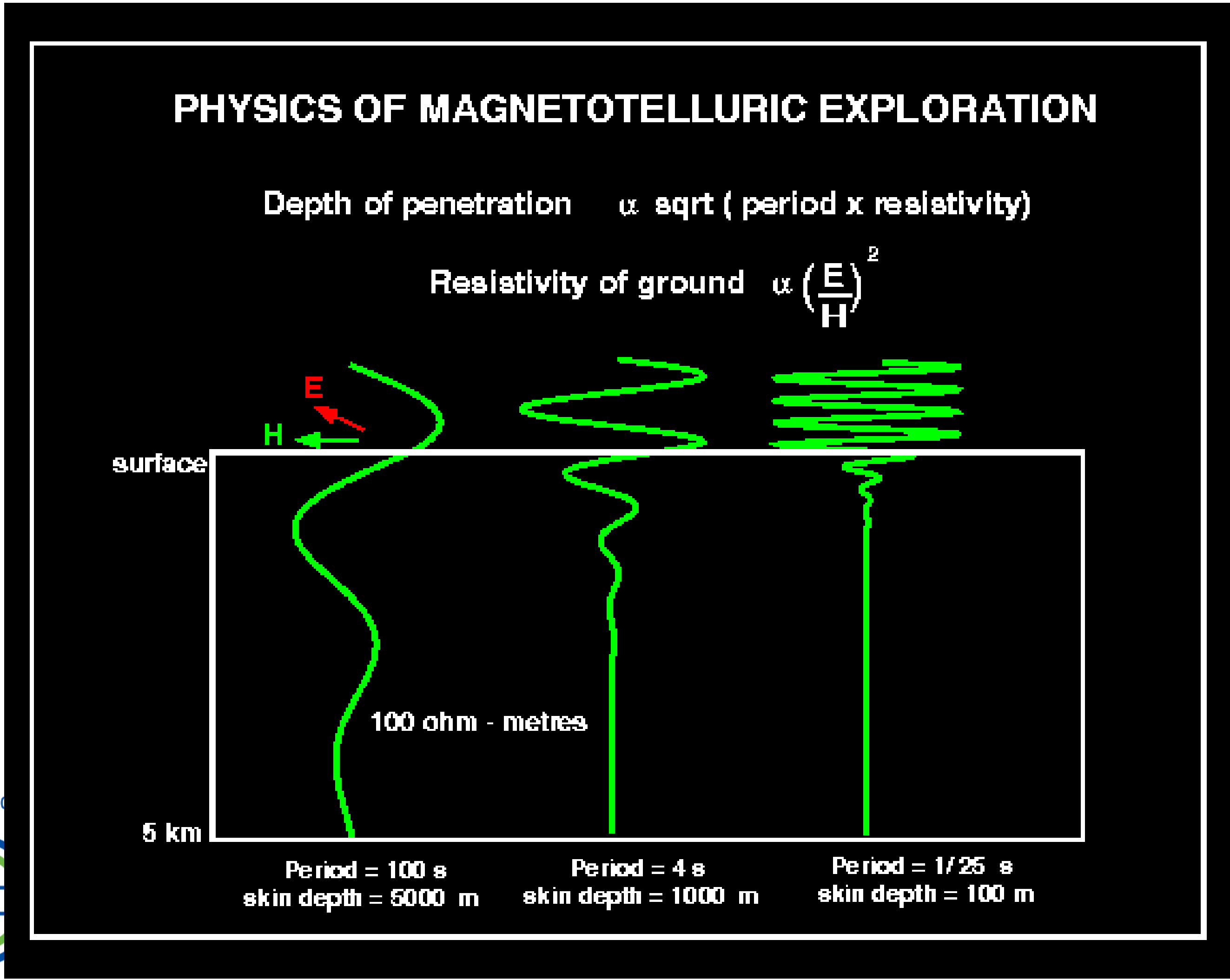

MT Theory

Source fields

- High frequencies >1 Hz from Spherics, generated by world-wide thunderstorms
- Low frequencies <1 Hz from Earth's magnetic field variations

-solar wind interactions

-variations with periods from seconds, minutes, hours, days to yearly cycles (eg. micropulsations, bays, storms)

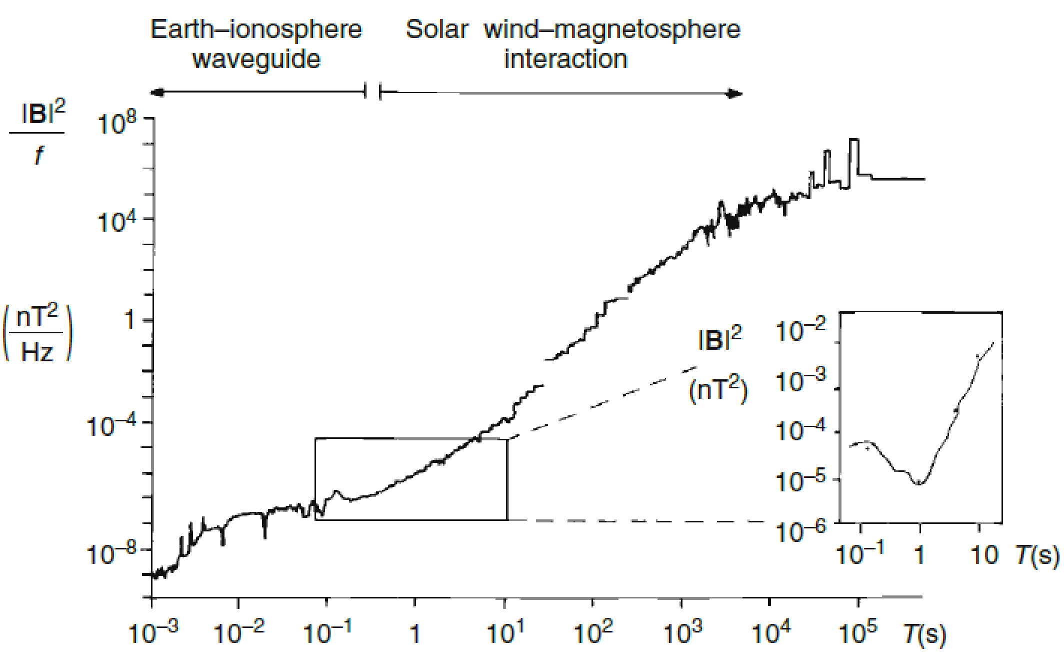

Dead Band: 10^1 Hz to 10^{-1} Hz; 0.1 to 10 s

Little energy

Skin depths 1.5 to 15 km, upper-middle crust

Funded by the European Union

MT Theory

Impedance tensor

- Measure two orthogonal components of electric field and two orthogonal components of magnetic field (usually north, x and east, y).
- Apparent resistivity is determined from their ratios. The magnetotelluric impedance tensor is defined as:

Supported by

Funded by the European Union

RawMaterials
Connecting matters
Funded by the European Union

The extent of the attenuation depends on the angular frequency (ω) and the electromagnetic properties (ε, μ, σ) of the medium.

absorbtion coefficient $$a = \sqrt{\frac{\mu\sigma\omega}{2}}$$

Skin depth $$d_s = \sqrt{\frac{2}{\mu\sigma\omega}} \cong 500\sqrt{\rho T}$$

Resistivity ρ [ohmm]	Period [s] T							
	0.0002	0.001	0.002	0.01	0.1	1	10	100
1	7	16	23	50	159	503	1592	5033
10	23	50	71	159	503	1592	5033	15915
50	50	113	159	356	1125	3559	11254	35588
100	71	159	225	503	1592	5033	15915	50329
500	159	356	503	1125	3559	11254	35588	112540
1000	225	503	712	1592	5033	15915	50329	159155
Skin depth [m]	5000	1000	500	100	10	1	0.1	0.01
	Frequency [Hz] f							

Supported by
RawMaterials ACADEMY
Funded by the European Union

Impedance tensor: $\underline{\underline{Z}}$

$$\overline{E} = \underline{\underline{Z}} \cdot \overline{H} \qquad \begin{bmatrix} E_x \\ E_y \end{bmatrix} = \begin{bmatrix} Z_{xx} & Z_{xy} \\ Z_{yx} & Z_{yy} \end{bmatrix} \cdot \begin{bmatrix} H_x \\ H_y \end{bmatrix}$$

Appatent resistivity

$$\rho_a = \frac{1}{\mu\omega} \left| Z_{ij} \right|^2$$

phase

$$\varphi_{ij}(\omega) = \operatorname{arctg}\left(\frac{\operatorname{Im}(Z_{ij}(\omega))}{\operatorname{Re}(Z_{ij}(\omega))} \right)$$

Geomagnetic induction vector („tipper”): $\overline{T}$

$$[H_z] = [T_x \; T_y] \cdot \begin{bmatrix} H_x \\ H_y \end{bmatrix}$$

Funded by the European Union

Supported by

Funded by the European Union

Field acquisition

Metronix GMS-06 MT measuring system

Supported by
eit RawMaterials ACADEMY
Funded by the European Union

Field array

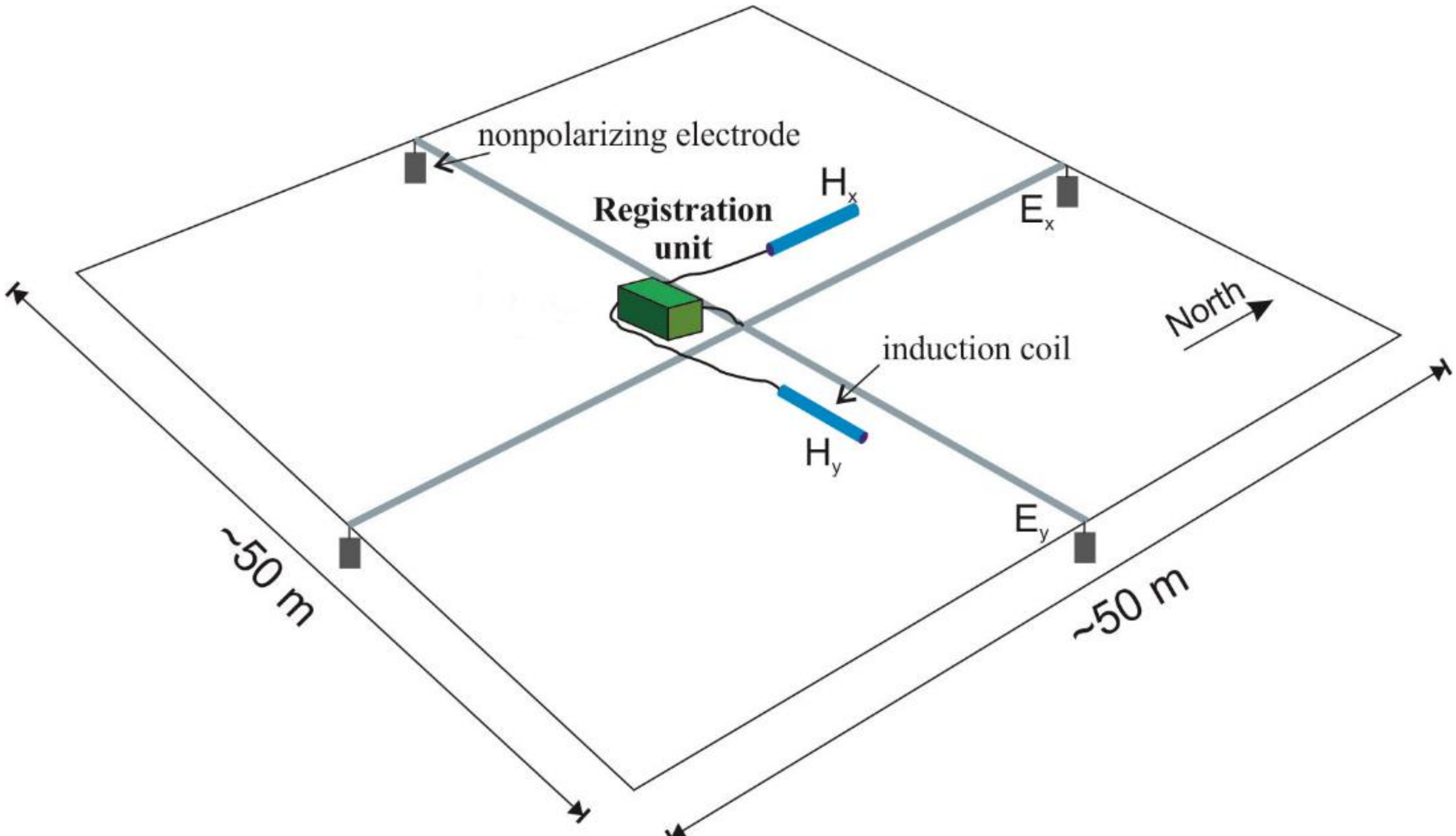

Supported by
RawMaterials ACADEMY
Funded by the European Union

Time series

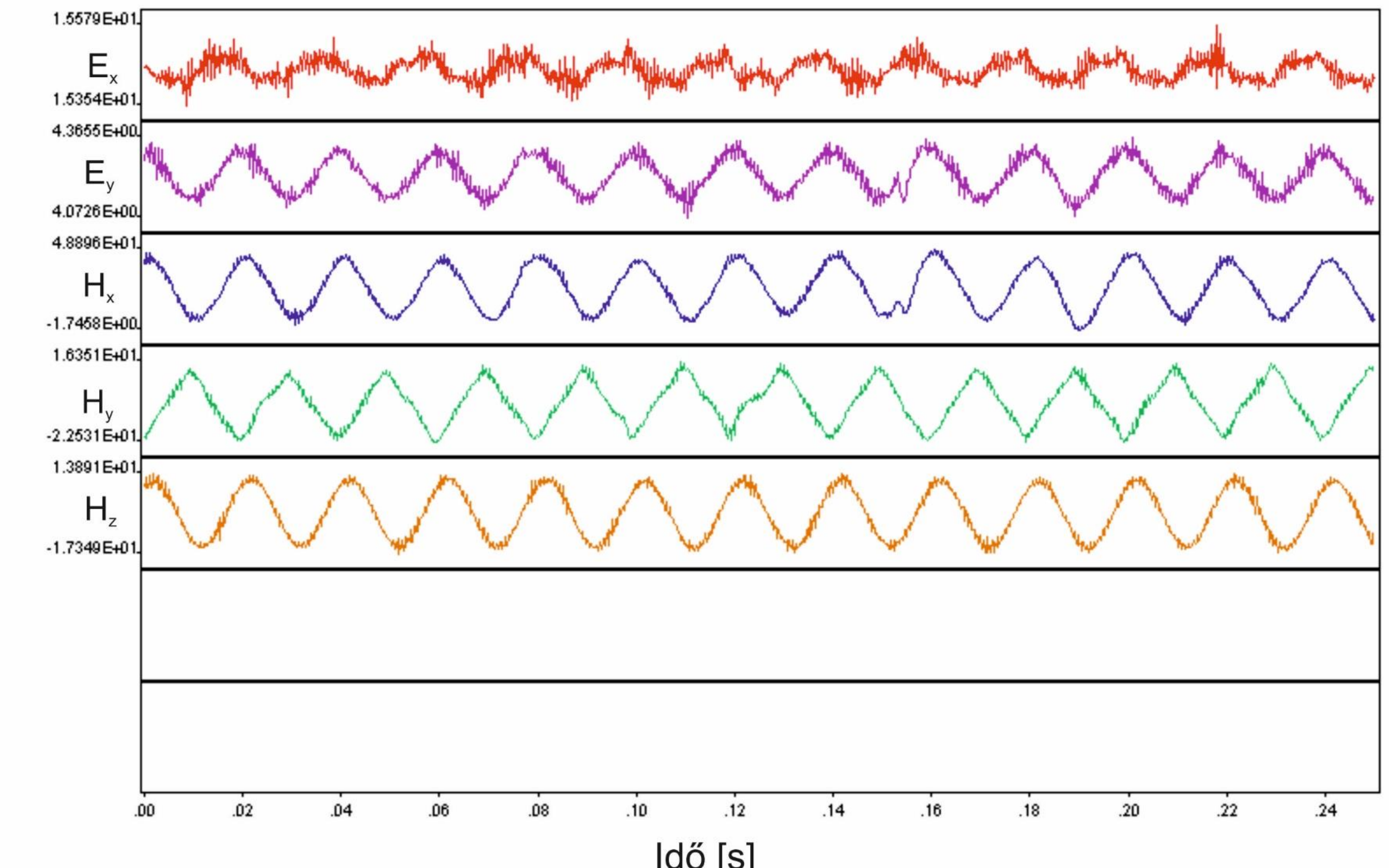

1.5579E+01
Ex
1.5354E+01
4.3655E+00
Ey
4.0726E+00
4.8896E+01
Hx
-1.7458E+00
1.6351E+01
Hy
-2.2531E+01
1.3891E+01
Hz
-1.7349E+01
.00 .02 .04 .06 .08 .10 .12 .14 .16 .18 .20 .22 .24
Idő [s]

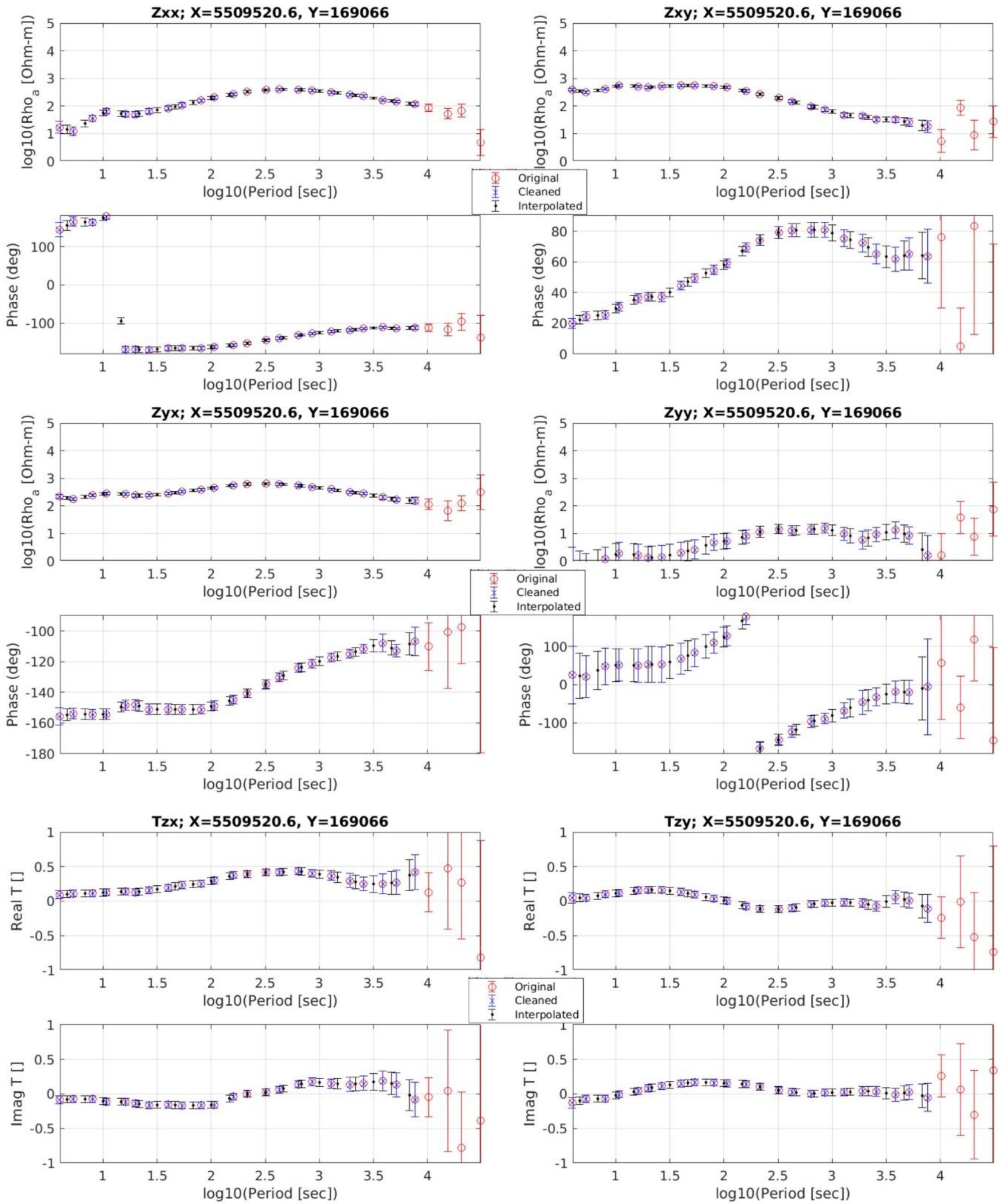
Zxx; X=5509520.6, Y=169066
Zxy; X=5509520.6, Y=169066
Zyx; X=5509520.6, Y=169066
Zyy; X=5509520.6, Y=169066
Tzx; X=5509520.6, Y=169066
Tzy; X=5509520.6, Y=169066
log10(Rho_a [Ohm-m])
Phase (deg)
Real T []
Imag T []
log10(Period [sec])
Original
Cleaned
Interpolated

MT Forward modeling problem

- $d = \begin{bmatrix} cZ^{reg} \\ W \end{bmatrix} = A(\sigma)$
- $Z = \begin{bmatrix} Z_{xx} & Z_{xy} \\ Z_{yx} & Z_{yy} \end{bmatrix}$
- $W = \begin{bmatrix} W_{zx} \\ W_{zy} \end{bmatrix}$
- $E = E^b + E^a$
- $H = H^b + H^a$
- $E^a(r_j) = G_E[\Delta\sigma(r)E] = \iiint_D \hat{G}_E(r_j|r)\Delta\sigma(r)\left(E^b(r) + E^a(r)\right)dv$
- $H^a(r_j) = G_H[\Delta\sigma(r)E] = \iiint_D \hat{G}_H(r_j|r)\Delta\sigma(r)\left(E^b(r) + E^a(r)\right)dv$

Supported by

RawMaterials ACADEMY

Funded by the European Union

Inversion techniques

- Regularized Gauss-Newton (RGN) method
- Tikhonov regularization

- $P(\sigma, c) = \|W_d(cA(\sigma) - d)\|^2 + \alpha\|S\|^2 \rightarrow min$
- $S = \begin{bmatrix} S_\sigma \\ S_c \end{bmatrix} = \begin{bmatrix} D(\sigma - \sigma_0) \\ c - c_0 \end{bmatrix}$
  - d – vector of data
  - A – forward modeling operator based on integral equations
  - W_d – diagonal matrix of data weights, based on data variance
  - α – regularization parameter
  - σ_0 - vector of a reference conductivity model
  - c_0 – 2 x 2 identity matrix, corresponding to no distortion case
  - D – matrix of the finite difference first derivative operator

Supported by
Funded by the European Union
Funded by the European Union

Case studies

Supported by

Funded by the European Union

Station map

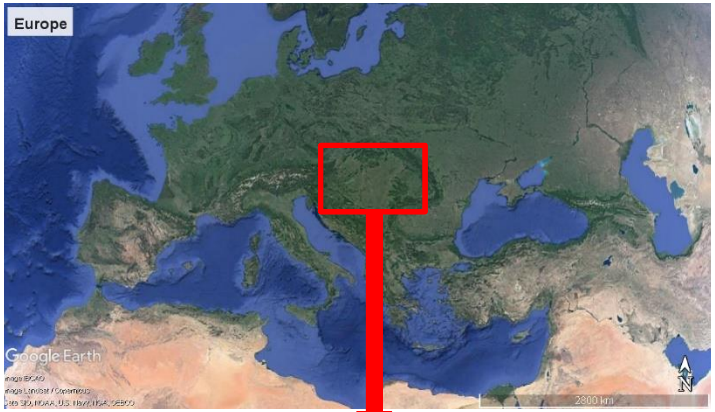

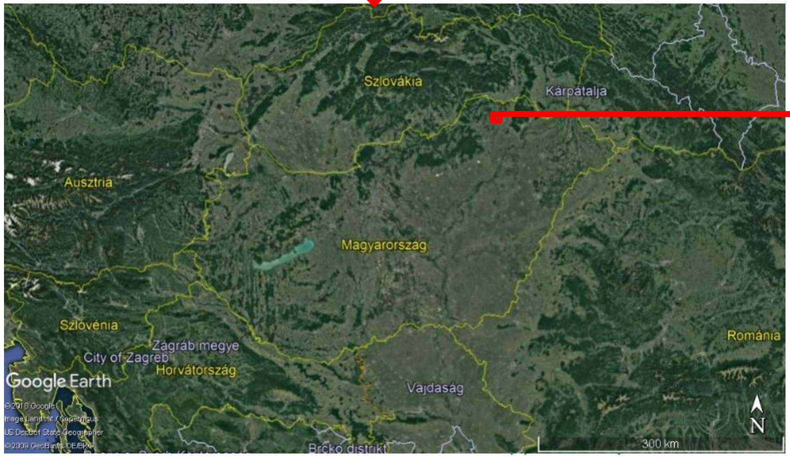

Funded by the
European Union

RawMaterials Connecting matters

RawMaterials ACADEMY

Funded by the
European Union

2D inversion

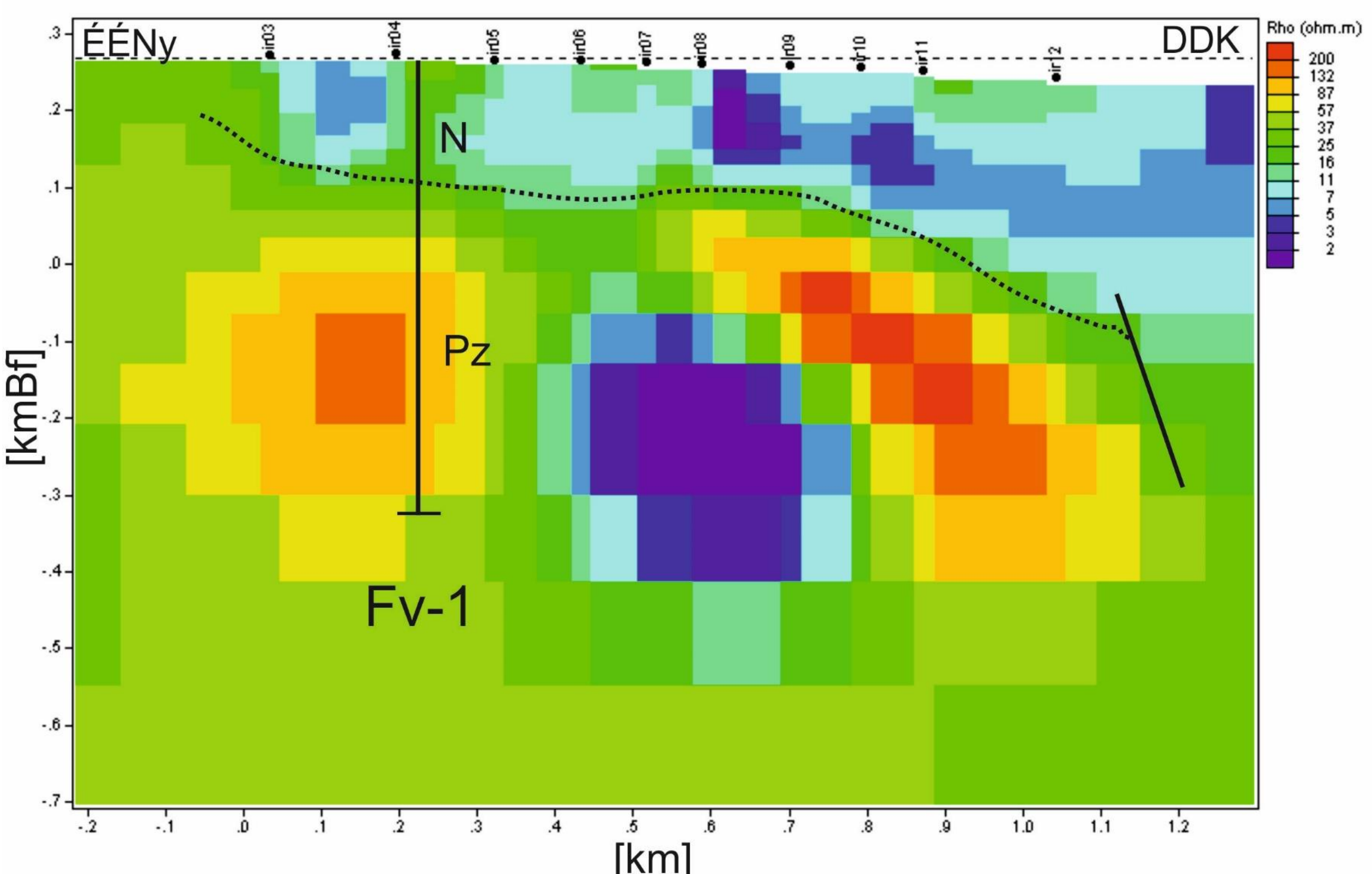

Funded by the European Union

Funded by the European Union

Geological setting

- Neogene rocks

  sedimentary hiatus (devonian, carboniferous–miocene)

- Paleozoic rocks

  Outcrop in Szendrő mountain

  Hundreds of kms lateral moving

  Greenschist facies dynamo-thermal metamorphism (Cretateous)

Supported by

Data preparation

- originally 24 MT stations
- Getting rid of 1 station (23 stations!)
- Frequency domain (0.1–100 Hz)
- At least six values in each decade
- Inverting full impedance tensor
- Number of total data values: 1514 (~23*19*4)

Supported by

EIT RawMaterials Connecting matters
Funded by the European Union
DIM 2021 ESEE

Input parameters

- Horizontal cell sizes (25*25 m)
- 84x76 cells horizontally (X*Y); 2.1x1.9 km area
- Vertical cell sizes: logarithmically increasing with depth
- 36 cells from the surface to 7090 m
- Total number of cells: 84*76*36=229824
- Average resistivity halfspace: ~15 ohmm
- Static shift: real distortion matrix

Other inversions

- Initial model: 1D layered, half space with larger resistivity values
- no shift, coarser cell sizes

Supported by
EIT RawMaterials ACADEMY
Funded by the European Union

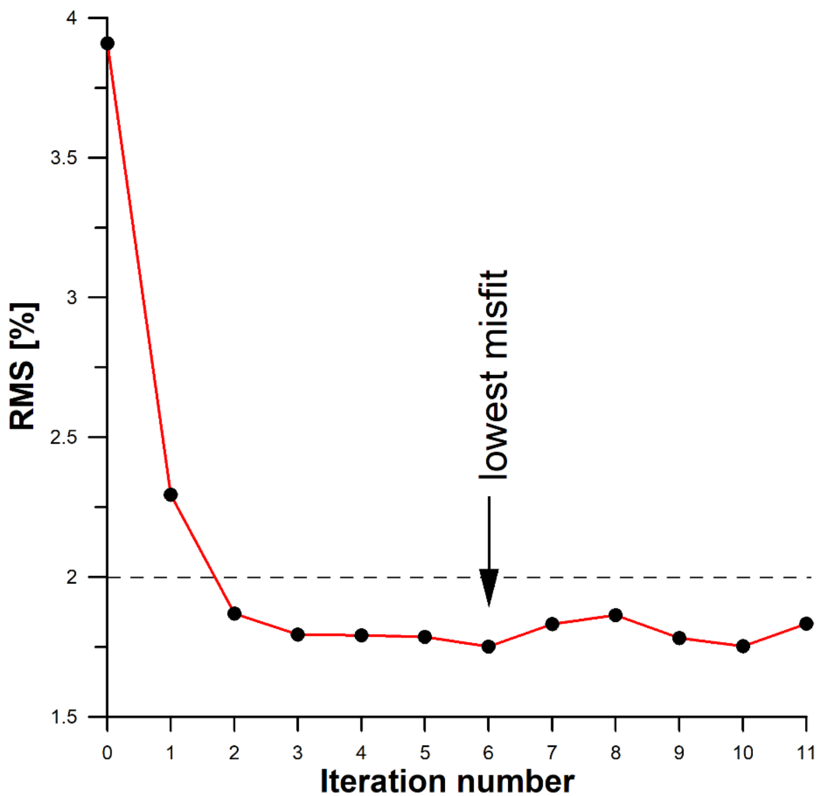

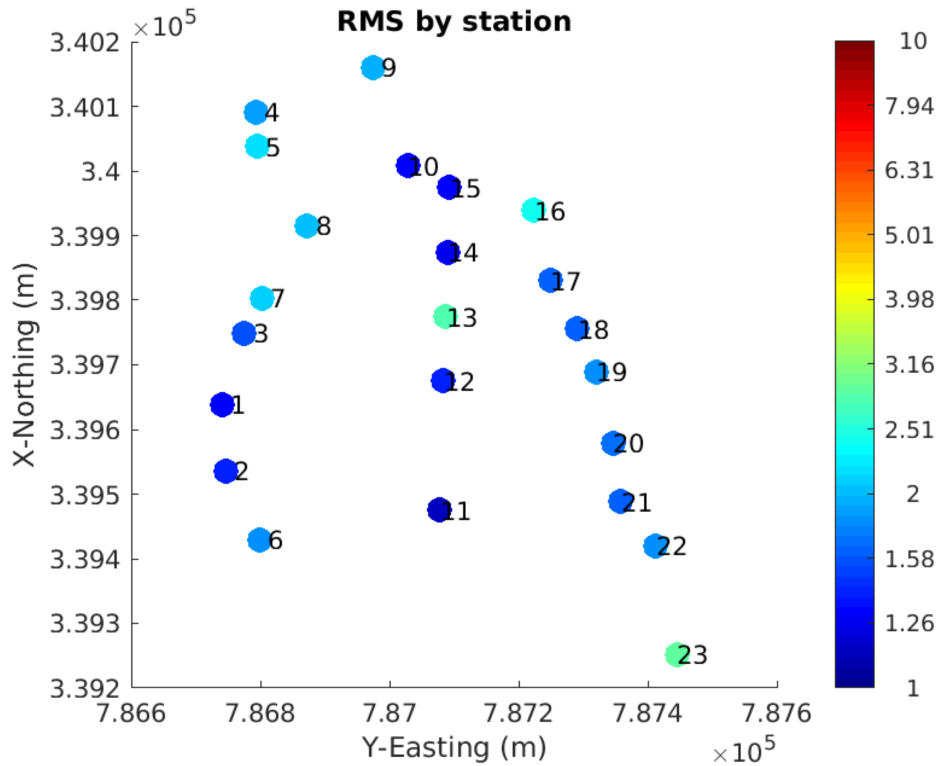

Supported by

RawMaterials
Connecting matters

Funded by the European Union

Observed, predicted data

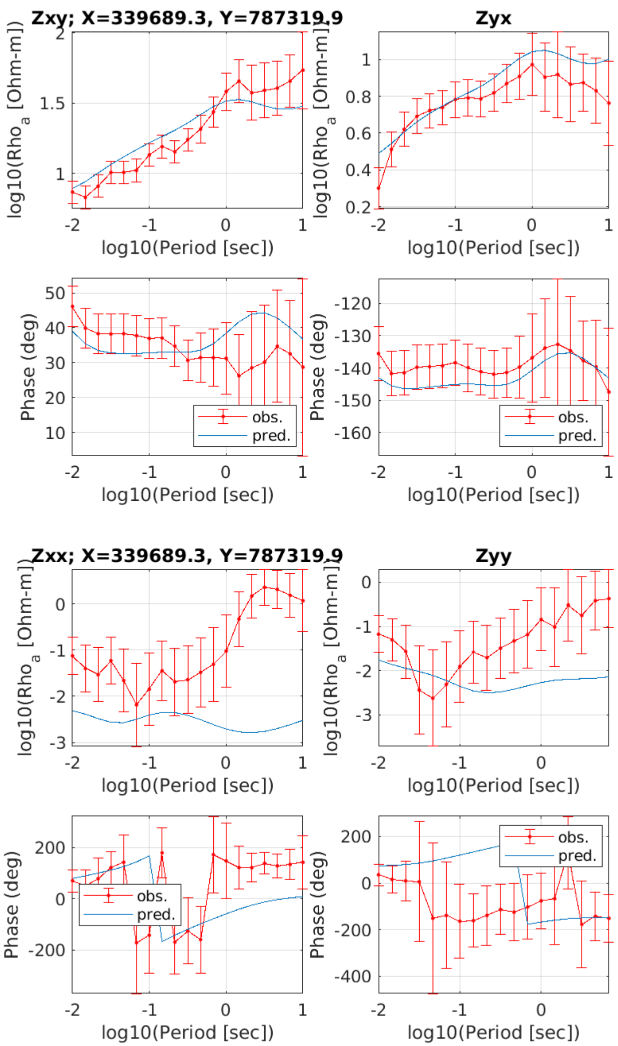

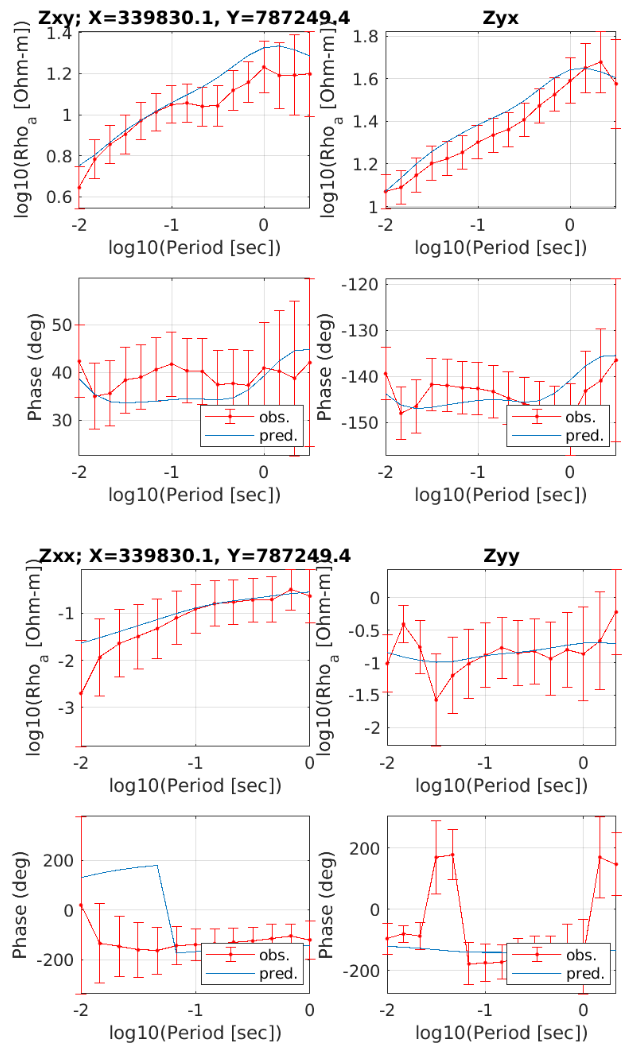

RawMaterials ACADEMY

Funded by the European Union

Vertical slices

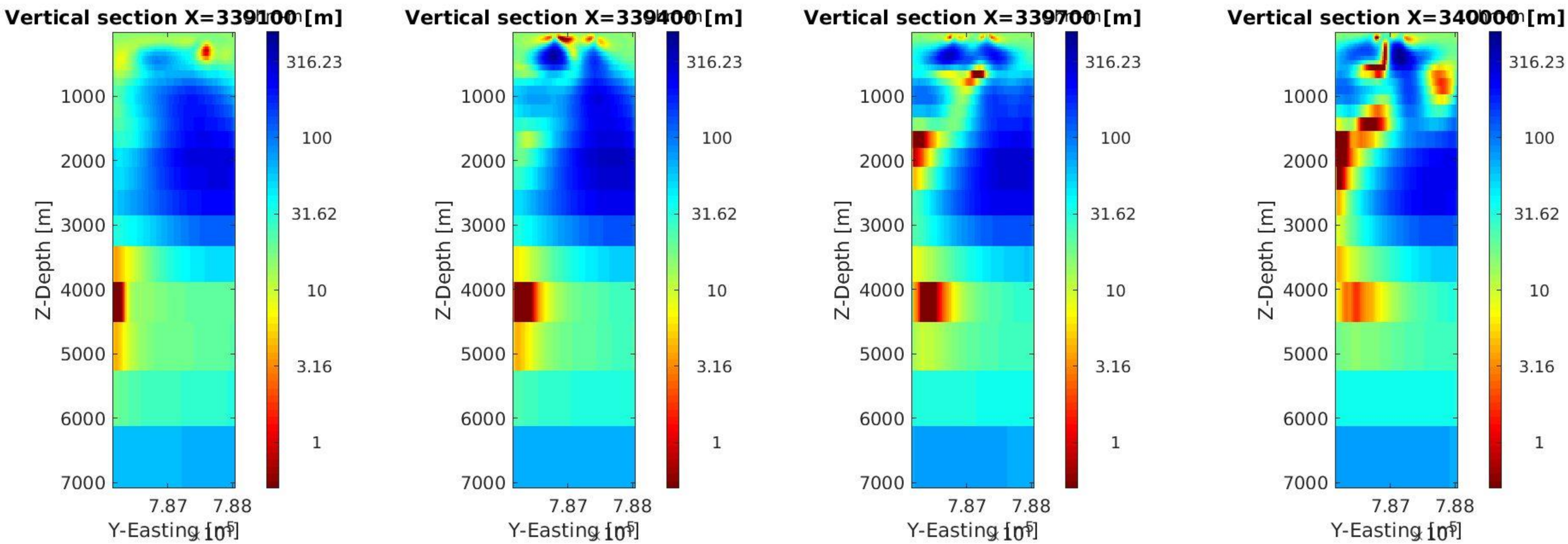

Horizontal slices (200-600 m depth)

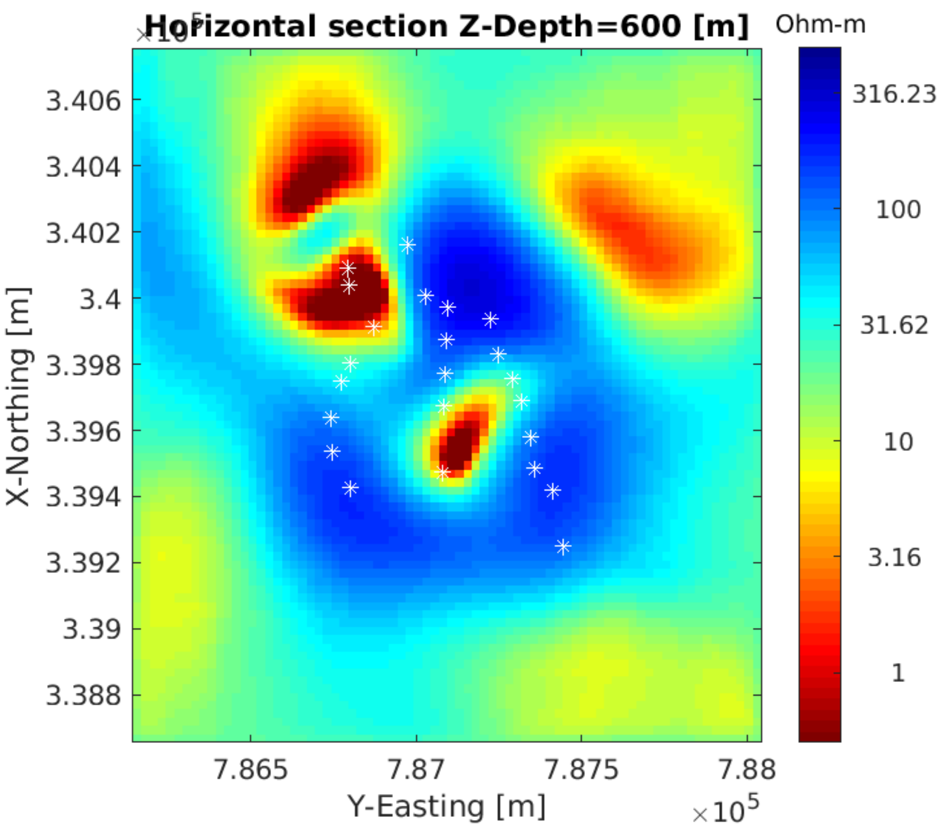

Joint interpretation of geophysical data

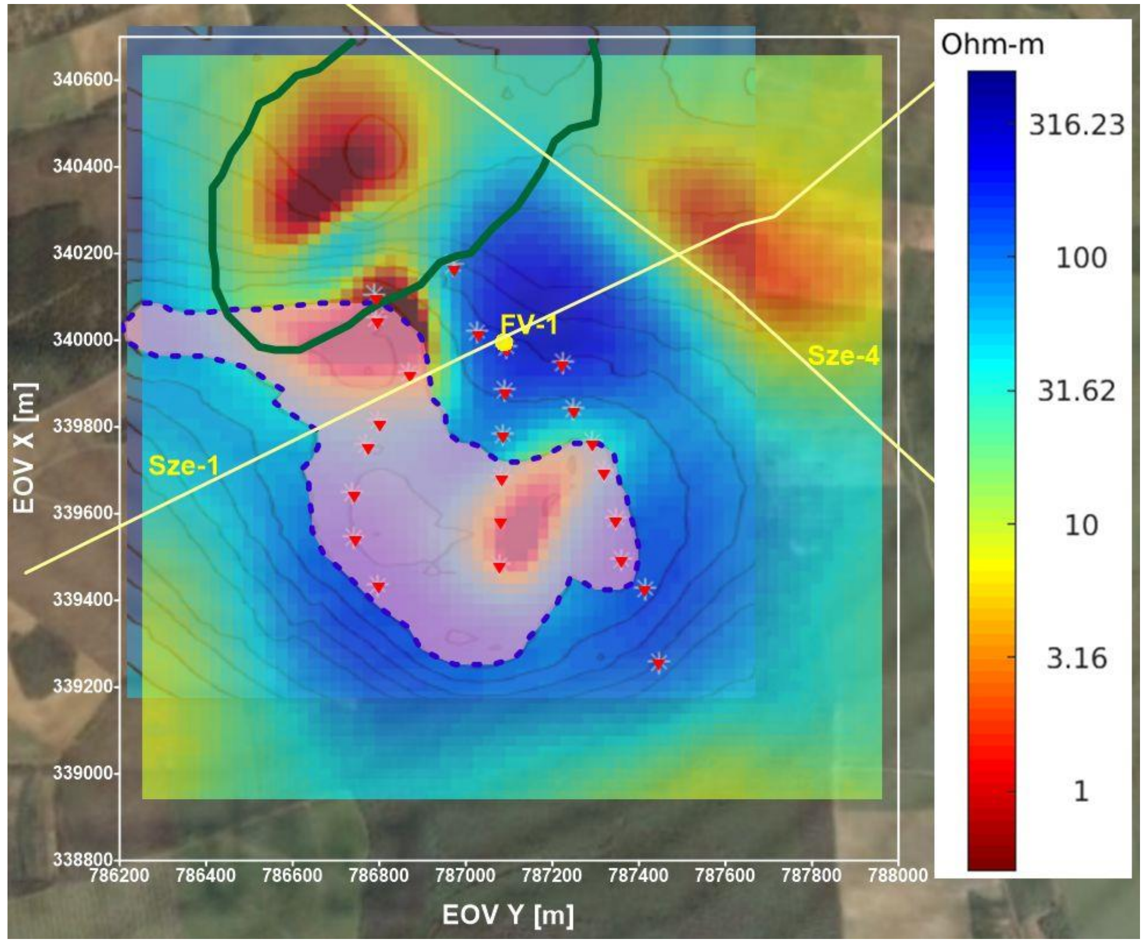

Satellite image of the Irota exploration area, with a resistivity obtained by 3D inversion in a horizontal section at a depth of 550 meters. The pink-colored area bounded by a blue dashed line on the magnetic map reduced to the pole indicates an anomaly greater than 50 nT. The green solid line delimits a gravitational anomaly greater than 26 mGal. The red triangle shows the MT stations, the yellow circle shows the FV-1 borehole, and the yellow solid lines show the Sze-1 and Sze-4 reflection seismic profiles

Supported by

Remarks

- The application of RGN method for the 3D inversion of MT data
- The inverted model shows two low resistivity anomalies, which can be interpreted in the framework of local geological setting
- The extension of inversion domain in depth (Z) can result better fit of low frequency domain
- Extension of inversion domain horizontally as well

Funded by the European Union

Supported by

RawMaterials ACADEMY

Funded by the European Union

Geophysical exploration of sea floor

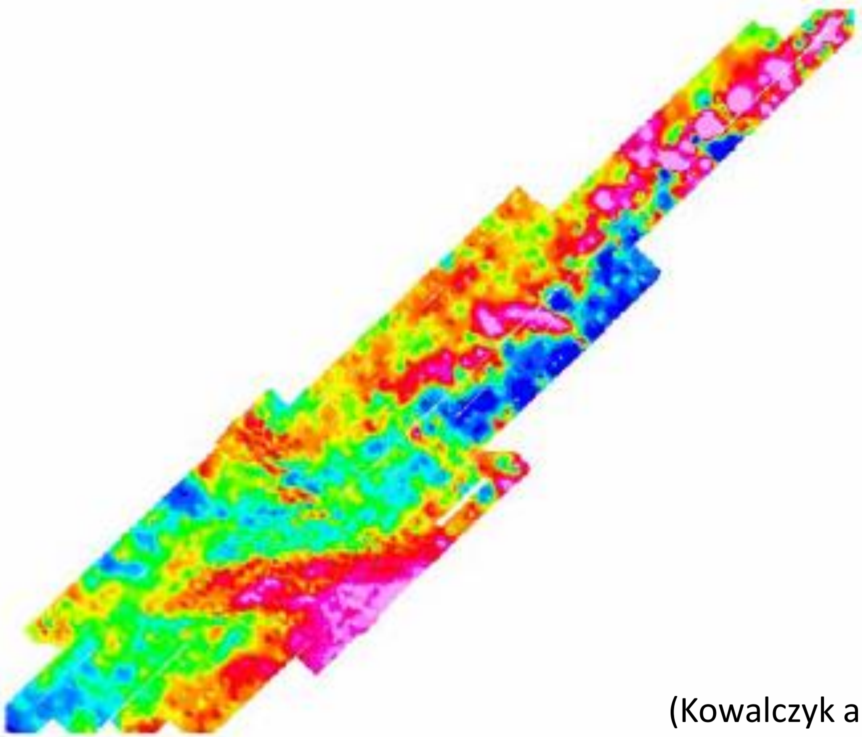

(Kowalczyk and Lum, 2018)

Supported by

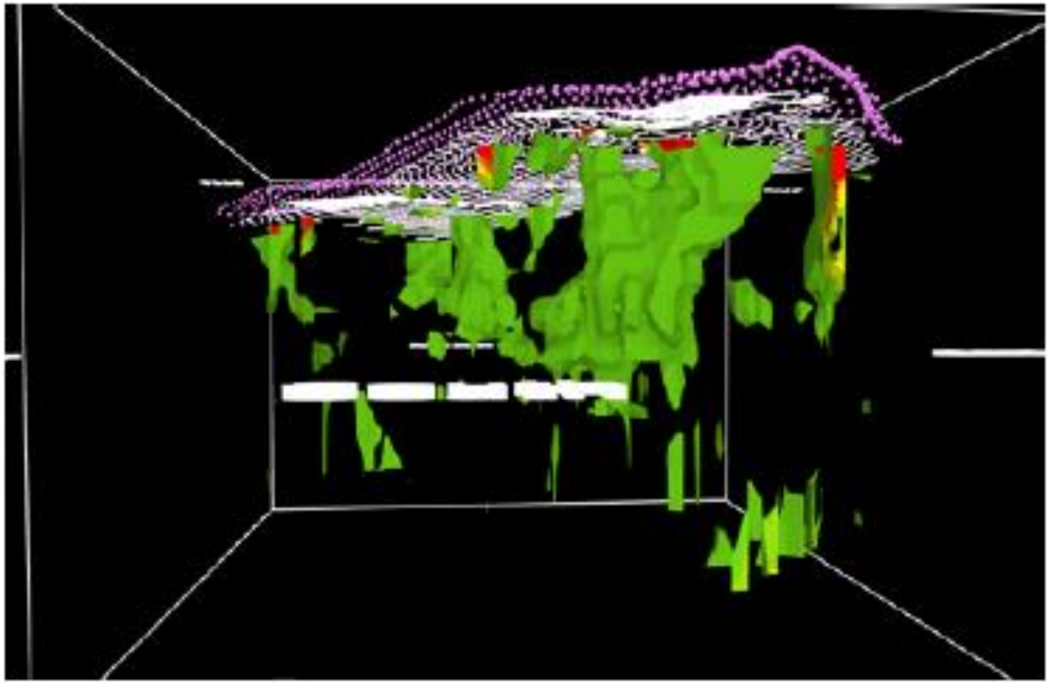

Seafloor Massive Sulfide (SMS) deposit

Magnetic inversion results of AUV magnetic data from the Solwara 1 deposit of Nautilus Minerals. Bathymetry is shown as white contours and AUV observation points as purple spheres. The green volumes are zones of reduced magnetization inferred from a 3D inversion of the magnetic data.

(Kowalczyk and Lum, 2018)

Supported by
RawMaterials ACADEMY
Funded by the European Union

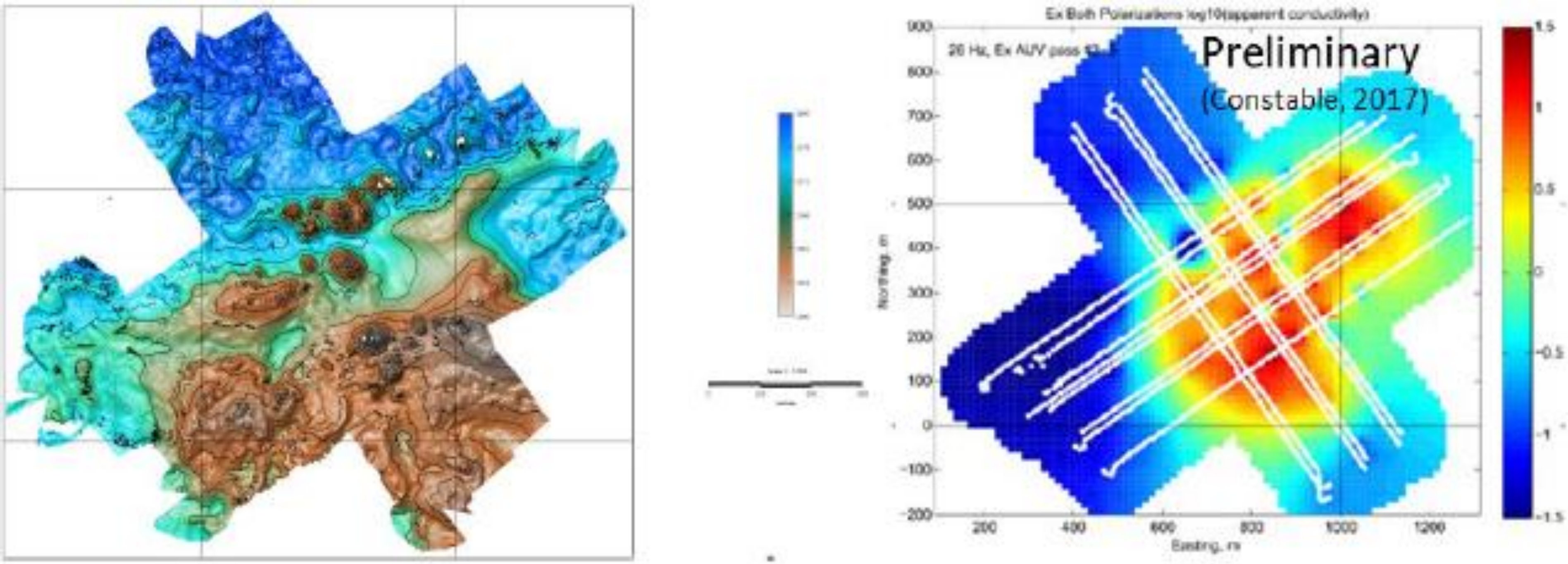

Bathymetry and apparent resistivity collected during an AUV-CSEM survey. Grid lines are every 500 m. Water depth is about 1500 m. Note the strong conductivity anomalies associated with the general zone of mineralized mounds. The multi-transmitter, multi-frequency EM survey is amenable to 3D inversion to locate the burial depth and limits of the conductive zones.

Supported by

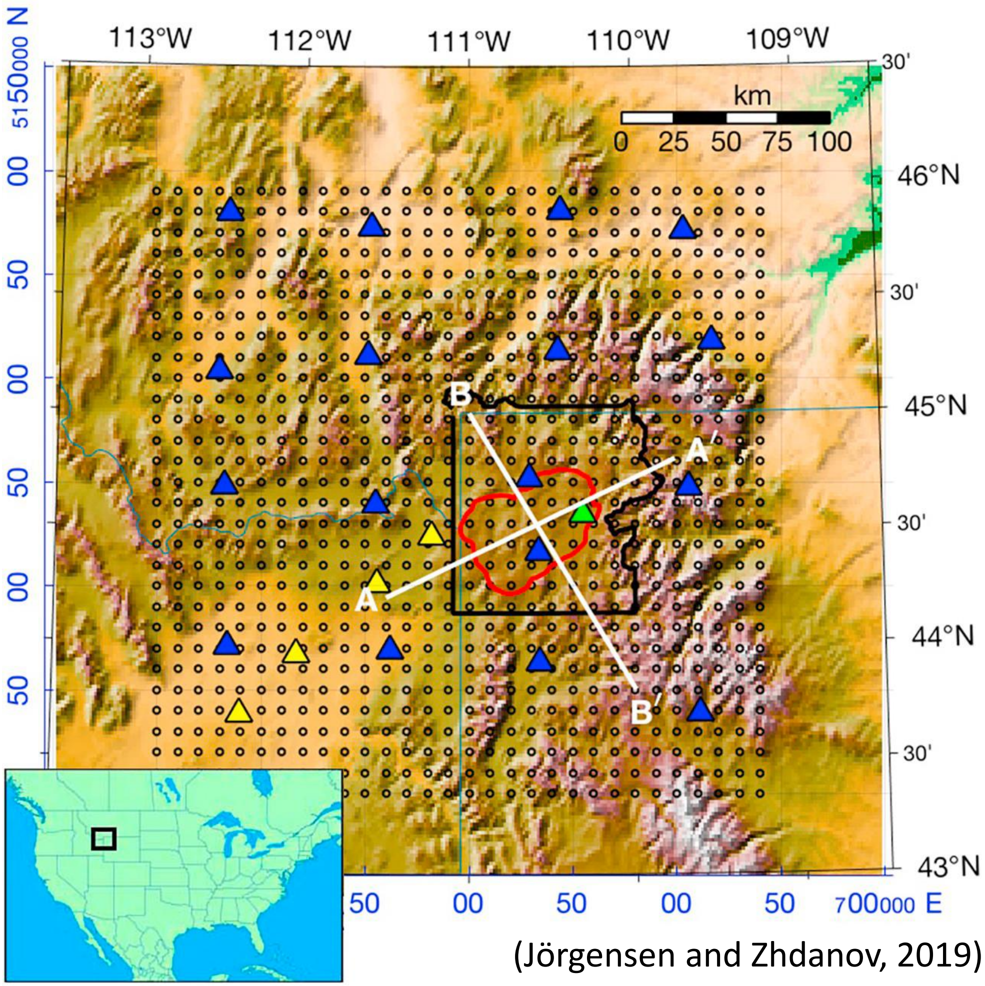

(Jörgensen and Zhdanov, 2019)

Yellowstone magmatic feeding system

Bandpass filtered gravity data (6-83 km depth)

Static shift corrected MT data

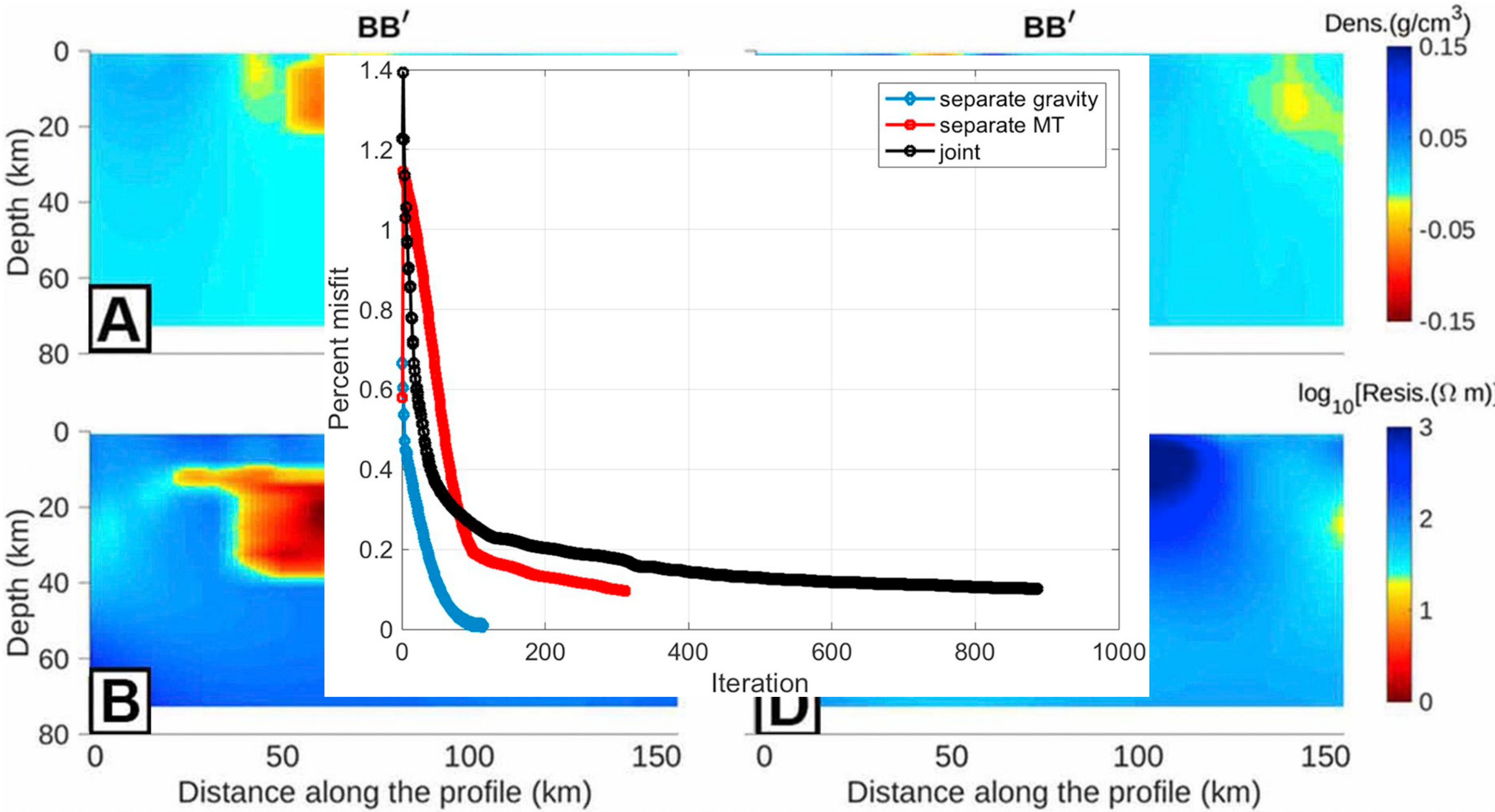

(Jörgensen and Zhdanov, 2019)

B

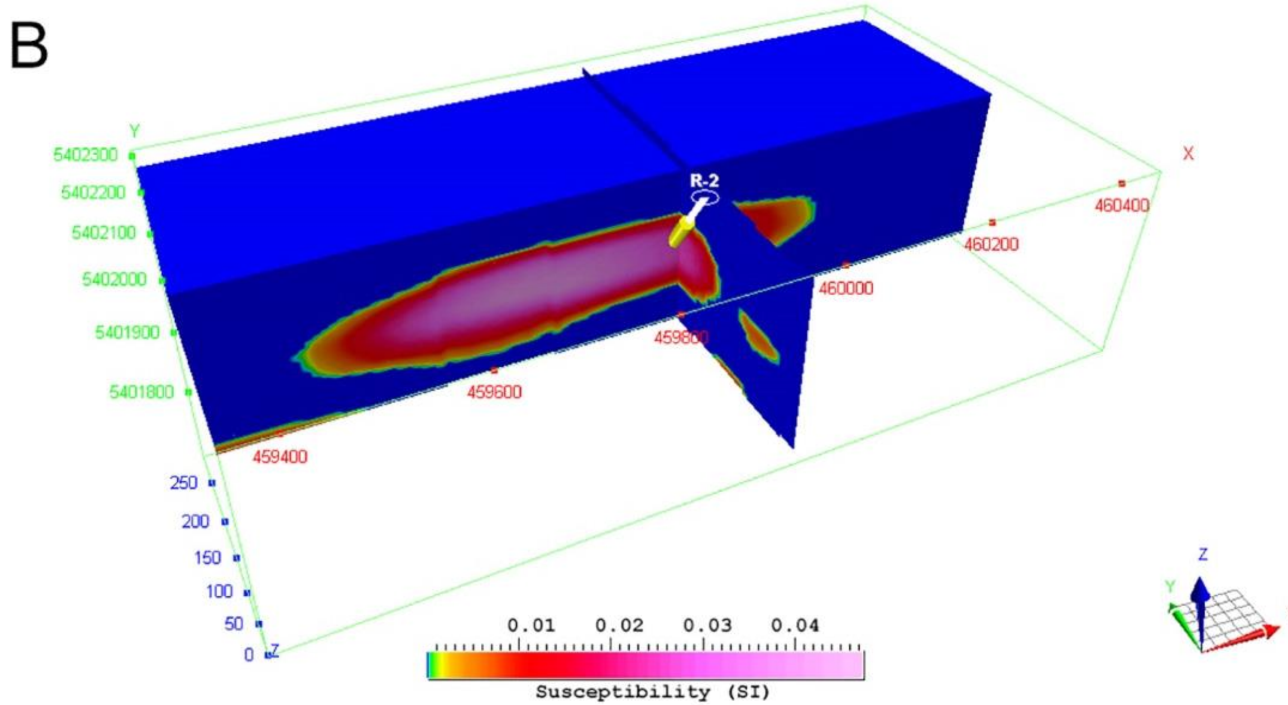

Reid-Mahaffy test site (Ontario, CAN). Joint inversion with **Gramian-based structural constraints**. The red arrow is easting, and the green arrow is northing. The location of the borehole is shown by short white line. The yellow cylinder on the borehole indicates the confirmed zone of mineralization.

(Zhdanov et al., 2021)

Standalone and joint inversion

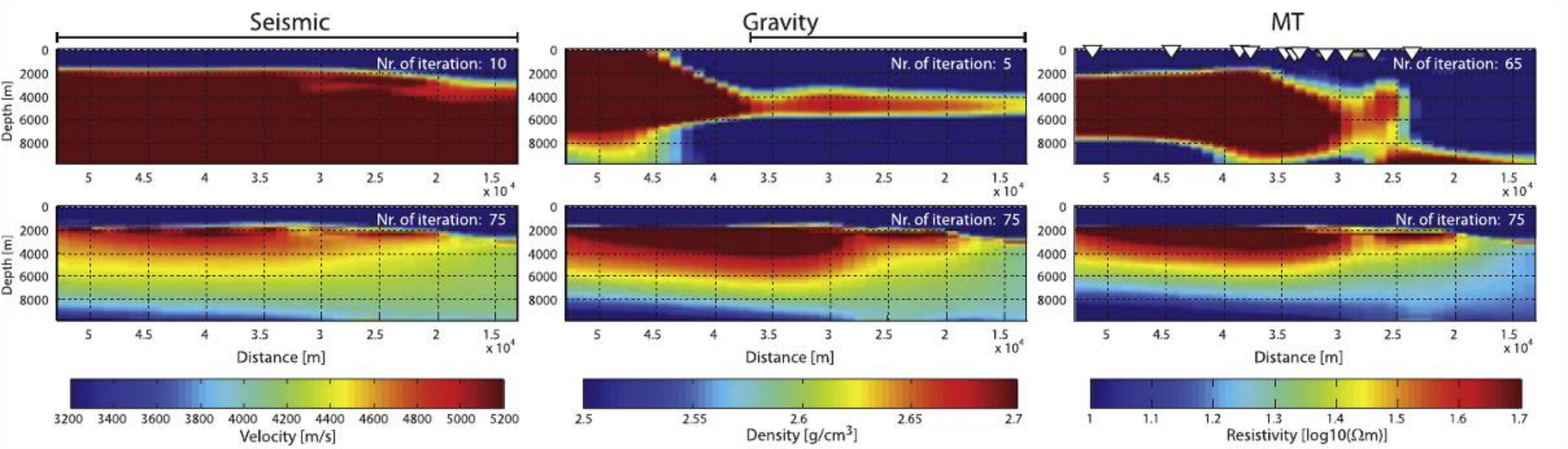

Inversion results for seismic, gravity and MT data recorded southeast of the Faroe Islands. The area is characterized by thick basaltic flows associated with continental break-up underlain by sediments accumulated during continental stretching. The two rows show the results from separate inversions and adaptive joint inversion, respectively. The individual inversion models show little resemblance, while the joint inversion result shows alternative models, fitting all three data sets at the same time.

(Heincke et al., 2017)

Supported by

RawMaterials ACADEMY

Funded by the European Union

RawMaterials Connecting matters
Funded by the European Union

Thank you for your attention!

Contact:

- info@dim-esee.eu
- *gfne@uni-miskolc.hu*

Supported by
RawMaterials ACADEMY
Funded by the European Union